THE EFFECTS OF REPLACEMENT OF FIVE HIGHLY CONSERVED AMINOACIDS OF SUBUNIT-I IN *CBB*$_3$-TYPE OXIDASE OF *RHODOBACTER CAPSULATUS*

BY

MEHMET ÖZTÜRK

THESIS SUBMITED TO
THE GRADUATE SCHOOL OF NATURAL AND APPLIED SCIENCES
OF
THE ABANT IZZET BAYSAL UNIVERSITY
IN PARTIAL FULFILMENT OF THE REQUIREMENTS FOR THE DEGREE
OF DOCTOR OF PHILOSOPHY
IN
THE DEPARTMENT OF BIOLOGY

DECEMBER, 2005

Approval of the Graduate School of Natural and Applied Sciences

_____
Prof. Dr. Davut KÖŞKER
Director

I certify that this thesis satisfies all the requirements as a thesis for the degree of Doctor of Philosophy.

_____
Prof. Dr. M. Tekin BABAÇ
Head of Department

This is to certify that we have read this thesis and that in our opinion it is fully adequate, in scope and quality, as a thesis for the degree of Doctor of Philosophy.

_____ _____
Assoc. Prof. Dr. Sevnur MANDACI Prof. Dr. Ekrem GÜREL
Co-Supervisor Supervisor

Examining Committee Members

Prof. Dr. M. Tekin BABAÇ _____

Prof. Dr. Gülay ÖZCENGİZ _____

Prof. Dr. Ekrem GÜREL _____

Prof. Dr. Sezai TÜRKEL _____

Assoc. Prof. Dr. Sevnur MANDACI _____

ABSTRACT

THE EFFECTS OF REPLACEMENT OF FIVE HIGHLY CONSERVED AMINOACIDS OF SUBUNIT-I IN *CBB*$_3$-TYPE OXIDASE OF *RHODOBACTER CAPSULATUS*

Öztürk, Mehmet
Ph.D., Department of Biology
Supervisor: Prof. Dr. Ekrem GÜREL
Co-Supervisor: Assoc. Prof. Dr. Sevnur MANDACI

December 2005, 168 pages

The heme-copper oxidases are the terminal elements of the membrane-bound respiratory chains that catalyze the reduction of molecular oxygen to water and pump protons across the membrane. Analysis of the amino acid sequences alignment of subunit I from different families of heme-copper oxidases showed that some of the amino acids, serine 333 (S333), serine 340 (S340), threonine 350 (T350), asparagine 390 (N390) and threonine 396 (T396) (*R. capsulatus* numbering) are almost strictly conserved. This work was undertaken to determine the relationships between these amino acids and the activity and assembly of the *cbb*$_3$ oxidase in *R. capsulatus*.

For this aim, 2.8 kbp fragment of the previously cloned pOX15, containing structural gene (*ccoNOQP*) of cytochrome cbb_3 oxidase of *R. capsulatus*, was subcloned into pBluescript vector. The new clone, pMOZI, was used to substitute conserved amino acids for alanine by site-directed *in vitro* mutagenesis and the integrity of each of these mutations was checked by sequencing. The mutated plasmids each of which carries one of the desired substitutions on structural gene of the cbb_3 oxidase were transferred into *R. capsulatus* strain, GK32. While the effects of the mutations on cytochrome *c* oxidase activity were evaluated by NADI plate assays, the structural integrity of the mutant oxidases were determined by separation of chromatophore membrane proteins on Schägger-type poly acrylamide gel stained with 3,3',5,5'-tetramethylbenzidine (TMBZ).

While serine and threonine mutants (S340A, T350A and T396A) had the same activity with wild-type, serine 333 mutation (S333A) decreased the enzyme activity and asparagine mutation (N390A) led to a complete loss of the cbb_3 oxidase activity. When cytochrome *c* profiles of mutants were examined, it was found that cytochrome cbb_3 profiles of S333A, S340A, T350A and T396A mutants were the same to that of the wild-type, however the c_p subunit of cbb_3 oxidase was missing and the amount of the c_o subunit was decreased in N390A mutant. The results indicated that S333 and N390 are very critical residues for activity or assembly of the cbb_3-type cytochrome oxidase in *R. capsulatus*.

Keywords: *Rhodobacter capsulatus*, respiration, cytochrome cbb_3-type oxidase activity, site-directed mutagenesis, chromatophore membrane protein isolation, SDS-PAGE and TMBZ staining.

ÖZET

RHODOBACTER CAPSULATUS'UN CBB$_3$ TİPİ SİTOKROM OKSİDAZ ENZİMİNİN I. ALT ÜNİTESİNDEKİ KORUNMUŞ BEŞ AMİNO ASİTİN DEĞİŞTİRİLMESİNİN ENZİME ETKİLERİ

Öztürk, Mehmet
Doktora, Biyoloji Bölümü
Tez Danışmanı: Prof. Dr. Ekrem GÜREL
Yardımcı Tez Danışmanı: Doç. Dr. Sevnur MANDACI

Aralık 2005, 168 sayfa

Demir-bakır oksidazlar, oksijeni suya indirgeyen, hücre zarına gömülü ve zar boyunca proton pompalayan solunum zincirinin son elemanlarıdır. Farklı türdeki Demir-bakır oksidazların I. alt ünitelerine ait amino asit dizileri eşleştirildiğinde, *R. capsulatus* ta *bulunan* cbb_3 oksidaz'a ait serine 333 (S333), serine 340 (S340), threonine 350 (T350), asparagine 390 (N390) ve threonine 396 (T396) amino asitlerinin, korunmuş olduğu görülmüştür. Bu çalışmada, *R. capsulatus'*a ait cbb_3 tipi oksidazda korunmuş olan bu amino asitlerin, enziminin yapı ve işlevine etkileri araştırılmıştır.

Bu amaçla, cbb_3 oksidazın *ccoNOQP* yapısal genini taşıyan rekombinant pOX15 DNA'sının 2.8 kbp'lik parçası pBluescript vektörüne klonlanmış ve elde edilen pMOZI klonu kullanılarak hedeflenen amino asitler yönlendirilmiş *in vitro* mutagenez ile alanine dönüştürülmüştür. Mutasyonlar DNA dizi analizi ile doğrulandıktan sonra, korunmuş amino asitler den birisini taşıyan her bir plazmid, *R. capsulatus*'un GK32 suşuna aktarılmıştır. Elde edilen mutantların enzim aktivitesine etkileri NADI boyama ile gözlemlenirken, mutasyonların enzim üzerindeki yapısal etkileri kromatofor zar proteinlerinin Schägger-tipi polyakrilamid jel de ayrıştırılması ve jelin 3,3',5,5'-tetrametilbenzidin (TMBZ) ile boyanmış ile tespit edilmiştir.

Serin ve tironin mutantları (S340A, T350A ve T396A) yaban tip ile aynı aktiviteye sahipken, serin 333 mutasyonu (S333A) enzim aktivitesini azaltmış, asparajin mutasyonu (N390A) ise enzim aktivitesini tamamen yok etmiştir. Mutantların hücre zarı proteinlerindeki sitokrom *c* profilleri incelendiğinde, S333A, S340A, T350A ve T396A mutantları yaban tip ile aynı profilleri vermiş, ancak N390A mutantında sitokrom cbb_3 oksidazın c_p alt ünitesine rastlanmamış ve c_o alt ünitesinin de azaldığı görülmüştür. Araştırma sonuçları, serine 333 ve asparagine 390 amino asitlerinin *R. capsulatus*taki cbb_3 tipi sitokrom oksidazın aktivitesi yada yapısı üzerinde kritik öneme sahip olduğunu göstermiştir.

Anahtar kelimeler: *Rhodobacter capsulatus*, solunum, cbb_3 tipi sitokrom *c* oksidaz aktivitesi, yönlendirilmiş mutagenez, kromatofor zar proteini izolasyonu, SDS-PAGE ve TMBZ boyama.

ACKNOWLEDGEMENTS

First and for most I would like to express my sincere appreciation to Dr. Sevnur MANDACI for giving me the opportunity to work in her laboratory at Research Institute for Genetic Engineering and Biotechnology. Her tremendous enthusiasm toward the basic research, and her continual willingness to discuss ideas, made my research a most rewarding and enjoyable experience.

I would like to thank Dr. Fevzi DALDAL at University of Pennsylvania, USA, for his guidance, supervision and insight through the research.

I would like to thank the other members of Dr. MANDACI's laboratory, Semra AYGUN, Yavuz ÖZTÜRK and Özlem AKKAYA not only for their technical help, but for providing such a pleasant working environment and their help and friendship.

I would also like to thank to Dr. M. Tekin BABAÇ and Dr. Ekrem GÜREL for providing me with the opportunity to make a research at Genetic Engineering and Biotechnology Research Institute, Gebze, Kocaeli and for their continual willingness to provide assistance.

I am indebted to my parent for their support during my education.

I would like to thank to my wife, Hatice and my child, A. Tarık for their love, patience and continual encouragement over the years.

Finally, I would like to thank TUBİTAK-GMBAE for research facilities.

ABBREVIATIONS

Amp^R: Ampicilline resistance

ATP: Adenosine triphosphate

bp: Base pair

BSA: Bovine serum albumin

COOH: Carboxy

CIAP: Calf intestinal alkaline phosphatase

Cyt: Cytochrome

DMSO: Dimetyl sulfoxide

ETC: Electron Transfer Chain

HEPES: N-(2-hydroxyethyl) piperazine-N'-(2-ethanesulfonic acid)

ICM: Intracytoplasmic membranes

IPTG: Isopropyl –β-D-thiogalactopyranoside

Kan^R: Kanamycin resistance

kbp: Kilo base pair

kDa: Kilo Dalton

LB: Luria Bertani Media

LHI and LHII: Light harvesting I and II complexes

MCS: Multiple cloning sites

MOPS: 3-(N-morpholino) propanesulfonic acid

NH_2: Amino

NAD: Nicotinamide adenine dinucleotide

NADH: Nicotinamide adenine dinucleotide, reduced form

NADP: Nicotinamide adenine dinucleotide phosphate

NADPH: Nicotinamide adenine dinucleotide phosphate, reduced form

ORF: Open reading frame

PAGE: Polyacrylamide–gel electrophoresis

PC: Plastocyanin

PCR: Polymerase chain reaction

PEG: Polyethylene glycol

PQ: Plastoquinone

Ps: Photosyntetic

PSI and PSII: Photosystem I and II, respectively

Q: Quinone pool

QA and QB: Primary and secondary quinine acceptors of the RC, respectively

Qo: Ubihydroquinone oxidizing site of the cytochrome bc_1 complex

Qox: Quinol oxidase

RC: Photochemical reaction center

Rc and *Rs: Rhodobacter capsulatus* and *Rhodobacter sphaeroides*, respectively

Res: Respiratory

RT: Room temperature

SDS: Sodium dodecyl sulfate

Tet^R: Tetracycline resistance

TBE: Tris/borate/EDTA (buffer)

TM: Transmembrane helix

TEMED: N,N,N',N'-tetrametyletylenediamine

TRICINE: N-tris(hydroximetyl)metylglycine

Tris: tris(hydroxymetyl)aminomethane

UV: Ultraviolet

v/v: volume/volume

w/v: weigh/volume

X-gal: 5-brome-4-chloro-3-indolyl-β-D-galactopyranoside

S: Serine (Ser)
N: Asparagine (Asn)
T: Threonine (Thr)

TABLE OF CONTENTS

LIST OF FIGURES

FIGURE

LIST OF TABLES

TABLE

INTRODUCTION

1.1 Energy Transfer, Bioenergy

All organisms require energy to survive and keep their reproduction. The energy originates either from sunlight or reduced chemical compounds. The conversion of energy occurs through the formation of an electrochemical gradient across the energy transducing membranes. Multi-subunit redox enzymes that are embedded either in the mitochondrial inner membrane, the thylakoid membrane, or in prokaryotic cell membranes cooperate to carry out energy transduction of photosynthetic and respiratory electron transport chain (ETC).

The universal cellular energy vector, ATP, is synthesized by three metabolic pathways: respiration (Res) (aerobic and anaerobic), photosynthesis (Ps) and fermentation. Contrary to fermentation, respiration and photosynthesis involve electron carrier chains formed by transmembrane complex connected by lipid (quinone) and water soluble diffusible components (cytochrome). These photosynthetic and respiratory chains catalyze electron and proton transport across the membrane and induce the formation of a transmembrane potential.

Oxidative phosphorylation and photophosphorylation are the most important forms of energy transduction in the biosphere. In both process, electrons flow through a chain of redox intermediates containing several membrane-

associated, multi subunit pigment proteins linked to each other by water soluble electron carriers and lipid. Electrons flow spontaneously from serially ordered lower oxidation potential carrier complex to higher oxidation potential carrier complexes in ETC. This downhill (exorgonic) electron transfer coupled to the uphill (endorgenic) transport of protons to cross a proton-impermeable membrane yielding a transmembrane electro-chemical potential.

The energy of the proton gradient is known as the chemiosmotic potential, or proton motive force (PMF). This potential is the sum of the concentration difference of protons across the membrane and the difference in electrical charge across the membrane. The transmembrane difference in the electrochemical potential of hydrogen ions ($\Delta\mu H^+$) is generated across the coupling membranes of bacteria, chloroplasts and mitochondria in eukaryotes by redox- or light-driven proton pumps.

1.2 General Properties of Electron Transfer Chain

Electron transfer components are involved in production of energy which is essential for cell survival. They are responsible for translocation of protons across the cellular membrane to produce a proton gradient which is then used for ATP synthesis. The energy transduction complexes contain *c*-type cytochromes (cyt) which are embedded into inner mitochondrial membrane or bacterial plasma membrane with their covalently bound heme groups facing to periplasm; catalyze respiration by using oxygen as the terminal electron acceptor. The free energy

from oxidation of hydrogen containing substances is converted into a transmembrane proton electro-chemical gradient by these respiratory enzymes.

In mitochondrial respiratory chain, NADH-1 type dehydrogenases transfer electrons from NADH to lipid soluble quinone, yielding ubiquinol. Ubiquinol is oxidized by complex III, also known as the cyt bc_1 complex, and the electrons are transferred to cyt *c*. The bc_1 is oxidized by complex IV, the cyt *c* oxidase (C_{ox}); the electrons are used to reduce molecular oxygen, and water is formed (Figure 1.1.A) [Ostermier et al., 1996].

The light reactions bring about the conversion of the light energy to chemical energy in the form of ATP. In eukaryotes, photosynthesis is associated with special intracellular organelles, the chloroplast. The chlorophyll pigments are attached to sheet like membrane structures of chloroplast. The photosynthetic membrane systems are called thlakoids. Oxygenic phototrophs such as Cyanobacteria, algae and plants contain two photo systems PSI homologous to the RC of green bacteria, and PSII, homologous to that of purple bacteria. The photosynthetic apparatus of purple bacteria consists of four membrane-bound pigment-protein complexes plus an ATPase complex that allows ATP synthesis at the expense of a proton gradient. Three of the four complexes specific to photosynthesis are the *reaction center, light harvesting I*, and *light-harvesting II* components. The fourth complex of the PS apparatus, the bc_1 complex, is common to both respiration and photosynthetic electron flow (Figure 1.1.B) [Madigan et al., 1997].

In prokaryotes, chloroplasts are not present, photosynthetic pigments are integrated into inter membrane systems that arise from invagination of the cytoplasmic membrane and it is called as an intra cytoplasmic membrane (ICM) which absorbs energy and transfer it to reaction center. Most of the anoxygenic phototrophic purple bacteria have ICM which are also described as chromatophores. The major components of the ICM are the membrane-bound energy transducing complex including the PS apparatus, and the interior of the ICM structure is equivalent to the extra-cytoplasmic or periplasmic space [Madigan et al,. 1997]. A good example of organism that exhibits such respiratory flexibility is the soil bacterium *P. denitrificans* which has gene that encode three biochemically distinct oxidases [de Gier et al., 1994]. Most microorganisms including photosynthetic bacteria posses alternate quinol oxidases which transfer electrons directly from the quinol to oxygen. On the other hand, the Res pathways are often branched at the UQ pool and contain several terminal oxidases thought to work at different oxygen tensions. *R. capsulatus* has a quinol oxidase (Q_{ox}) and C_{ox} of *cbb*$_3$- type (Figure 1.1.C) while *R. sphaeroides* also has an additional cyt *c* oxidase of *aa*$_3$-type.

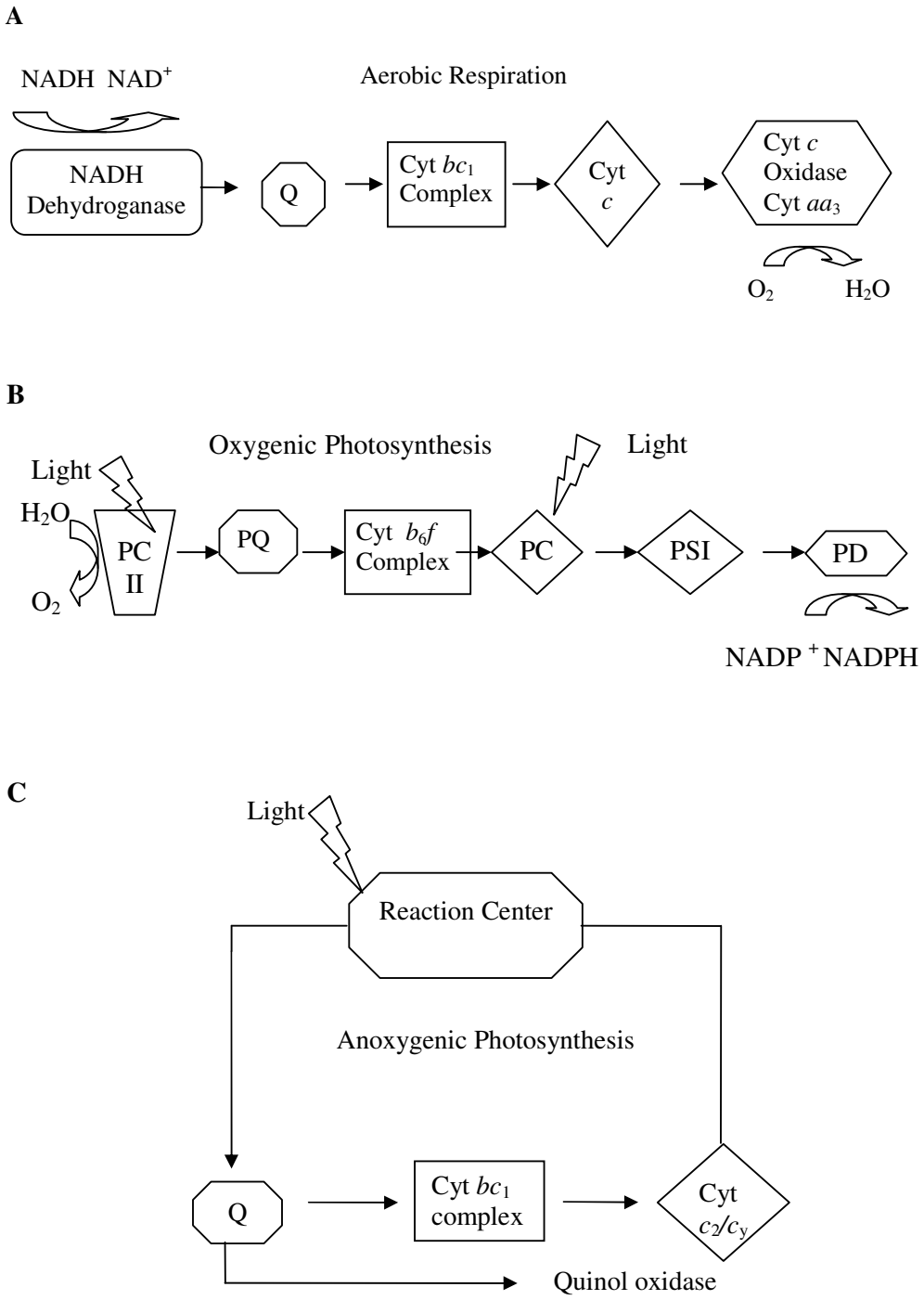

Figure 1.1: Electron transfer chains in mitochondria (A), chloroplast (B) and purple non-sulfur bacterium *R. capsulatus* (C). Arrows indicate the direction of electron flow between complexes. Cyt; cytochrome, Q; ubihydroquinone, PSI and PSII; Photo system I and II, PQ: plastoquinone, PC; plastocyanin, RC; photochemical reaction center.

1.3 *R. capsulatus* as a Model Organism to Study *cbb*$_3$-Type Cytochrome Oxidase

Structural studies and nucleotide sequence data revealed remarkable similarities between ETC complexes in higher organisms and in bacteria [Youvan et al., 1989]. Photosynthetic prokaryotes that offer several experimental advantages over eukaryotic organelles have been used as a model system for studies on biological energy transduction [Nitschke et al., 1995].

Anoxygenic phototrophic bacteria can be grouped into four categories: (1) the purple sulfur, (2) purple non-sulfur, (3) green sulfur and (4) green non-sulfur bacteria according to their phenotype. On the other hand the phylum of the purple bacteria, defined on the basis of 16S r-RNA analysis, is subdivided into five subgroups, labeled alpha to epsilon. Alpha, beta, and gamma subgroups contain photosynthetic as well as non-photosynthetic representatives [Stackebrandt et al., 1988]. The group of the purple non-sulfur bacteria (*Rhodospirillaceae*) is by far the most diverse group of the phototrophic purple bacteria. The alpha division includes species of the genera *Rhodospirillum, Rhodopila, Rhodopseudomonas*, *Rhodomicrobium* and *Rhodobacte*r [Prince et al., 1990].

R. capsulatus is a member of the *Rhodospirallaceae* family and it belongs to the genus *Rhodobacter*. *R. capsulatus* is a gram negative, purple non-sulfur and facultative phototrophic soil bacterium. It has a rod-like cell shape with a diameter of 0.5-1.2 μm. *R. capsulatus* has highly branched electron transfer pathways that allow it to sustain various growth modes. *Rhodobacter* species, *R. capsulatus* and

its close relative *R. sphaeroides*, are excellent model organisms for studying cellular energy transduction [Zannoni, 1995]. They have versatile growth modes and are capable of both unoxygenic phototrophic (Ps) and vigorous respiratory (Res) growth in the presence of oxygen. They contain a photochemical reaction center (RC) [Williams et al., 1986; Youvan et al., 1984], a ubihydroquinone: cytochrome *c* (cyt *c*) oxidoreductase (cyt bc_1 complex) [Daldal, et al., 1987; Daldal, et al., 1986], and a *c*-type cytochrome as a mobile electron carrier [Daldal, et al., 1986; Donohue, et al., 1988], but their Ps and Res electron transport chains are different [Zannoni, 1995; Donohue, et al., 1988].

Under anaerobic photosynthetic conditions, the soluble cyt c_2 and/or the membrane anchored cyt c_y mediate light driven cyclic electron transfer between the photochemical reaction center and the bc_1 complex [Zannoni and Daldal, 1993]. Under respiratory growth conditions, *R. capsulatus* can grow using a pathway reminiscent of the mitochondrial electron chain. The pathway involves the bc_1 complex, cyt c_2 or c_y, and cbb_3–type cyt *c* oxidase. This oxidase contains two *c*-type cyts, c_o and c_p, as subunits [Gray et al., 1994; Koch et al., 1998a].

Other aerobic electron transport chain called alternate respiratory pathway also exists in *R. capsulatus*. It is independent of all *c*-type cyts and uses the quinol oxidase that is thought to contain cyts *b* and *d*. *R. capsulatus* can also sustain growth under anaerobic dark conditions by using various compounds such as dimethyl sulfoxide, triethylamine oxide or nitrous oxide as terminal electron acceptors. This metabolic diversity allows cultivation of mutants with pleiotropic cyt *c* deficiency. The presence of functional *c*-type cytochromes can be readily

detected phenotypicaly by the ability of cells to sustain photosynthetic (Ps+) growth and to catalyze the reaction (ά-Naphtol + dimetylphenylene diamine + O_2 → Indophenol blue + H_2O) via an active cyt *c* oxidase ($NADI^+$). The absence of cytochromes c_1 and/or c_2/c_y abolishes photosynthetic (Ps) growth whereas absence of cytochromes c_o and/or c_p abolishes the activity of the cyt *c* oxidase (tested by the NADI reaction). Thus, *R. capsulatus* mutants, defective cbb_3-type oxidase, do not show cyt *c* oxidase activity ($NADI^-$). Yet these mutants can grow aerobically via an alternate respiratory pathway. This facilitates the isolation and detection of cbb_3-type oxidase mutants. A wide variety of growth modes allow *R. capsulatus* to survive in case of a lethal mutation that occurs in a given mode. Moreover, chromatophore vesicles, containing all of the components of energy transduction pathways in large quantities, can be easily prepared. In addition, almost all of the *R. capsulatus* genome has already been sequenced which should be helpful in identifying novel components. Therefore, these bacteria provide excellent model system to understand bioenergetics process and their components.

1.4 Respiratory and Photosynthetic Growth of *R. capsulatus*

1.4.1 Photosynthetic Electron Transfer Pathway in *R. capsulatus*

Ps electron transport pathway is cyclic in purple non-sulfur facultative phototrophs. *R. capsulatus'*s light-driven photosynthetic electron transfer pathway is a cyclic process between the photochemical reaction center and the ubihydroquinone cyt *c* oxidoreductase (cyt bc_1 complex) [Meyer, et al., 1995]. During the Ps growth of *R. capsulatus*, electrons are conveyed from the cyt bc_1

complex to the RC either by the lipid soluble quinine (Q) and well-studied mobile electron carrier cyt c_2 [Daldal, et al., 1986], or the more recently discovered membrane-anchored electron carrier cyt c_y [Jenney, et al., 1993].

The photosynthetic RC consists of several integral membrane proteins and number of pigment molecules. RC contains three polypeptides, designated L, M, and H subunits. These proteins are embedded in the photosynthetic membrane. They bind the RC photochemical complex which consists of one carotenoid molecule, two molecules of bacteriochlorophylls, one ubiquinone as primary electron acceptor Q_A, one non-heme iron, and another ubiquinone as a secondary electron acceptor Q_B. L and M subunits which are core for RC, posses five membrane spanning helices each [Debus, et al., 1985]. During the photosynthesis, light induced oxidation of RC bacteriochlorophyl dimmer (P^+) reduces a Q molecule to hydroquinone (QH_2), which is subsequently oxidized by the cty bc_1 complex [Amesz et al., 1988]. The bc_1 complex contains four metal redox centers: cytochrome b_L and cytochrome b_H, both located within the cytochrome *b* subunit, cytochrome c_1 and the riske 2Fe-2S cluster, which are each located on a separate subunit [Gennis, et al., 1993]. The bc_1 complex is similar to the cyt b_6f complex of chloroplast, but it differs in that a monomeric cyt *b* in the bc_1 complex is split into α, β dimmer in the b_6f complex [Sarıbaş, et al., 1999]. The cyt bc_1 complex directs a quinone cycle, in which the endorgonic transport of protons across the membrane is coupled to the exorgonic transport of electrons.

1.4.2 Respiratory Electron Transfer Pathway in *R. capsulatus*

The gram-negative facultative photosynthetic bacterium *R. capsulatus* has a highly branched electron transport chain, resulting in its ability to grow under a wide variety of conditions [Zannoni, 1995]. When light is unavailable, *R. capsulatus* species use alternate energy transduction pathways to ascertain their growth both in the presence or absence of molecular oxygen. Under aerobic growth conditions electrons are transferred via respiratory ETC from respiratory dehydrogenases to the Q pool, the cty bc_1 complex, and again using soluble or membrane bound electron carriers to the terminal oxidases that ultimately convert O_2 to H_2O [Koch, et al., 1998] (Figure 1.2). On the other hand, the respiratory electron transfer pathways of *R. capsulatus* are branched after the quinone pool and contain two different terminal oxidases, previously called cyt b_{410} (cyt *c* oxidase) and cyt b_{260} (quinol oxidase) [Zannoni, et al., 1976; Myllykallio, et al., 1999]. The branch involving cyt *c* oxidase is similar to the mitochondrial electron transfer chain in that it depends on the cyt bc_1 complex and a *c*-type cyt acting as an electron carrier. The quinol oxidase branch circumvents the cyt bc_1 complex and the cyt *c* oxidase by taking electrons directly from the quinone pool to reduce O_2 to H_2O (Figure 1.3). Respiratory electron transport pathways of *R. capsulatus* and *R. sphaeroides* are also similar but not identical [Baccarini-Melandri, et al., 1973]. Both species contain a respiratory electron transport pathway that is branched after the quinone pool. One of these branches contains hydroquinone oxidases (Q_{ox}) commonly found in microbes, while the other one harbors a mitochondrial-like cyt *c* oxidase(s) (C_{ox}) converting oxygen to water [Garcia-Horsman, et al., 1994]. While *R. capsulatus* contains only one cbb_3-type C_{ox} (cbb_3-

C_{ox}) [Gray, et al., 1994], both an aa_3-type C_{ox} [Hosler, et al., 1992; Sasaki, et al., 1970], and a cbb_3-C_{ox} [Garcia-Horsman, et al., 1994] are present in *R. sphaeroides*. In the latter species, the cbb_3-C_{ox} is predominant in micro aerobic or Ps-grown cells, while the aa_3-C_{ox} becomes a major component under high O_2 tension [Shapleigh, et al., 1992]. In both species, the nature of the Q_{ox} is not well known.

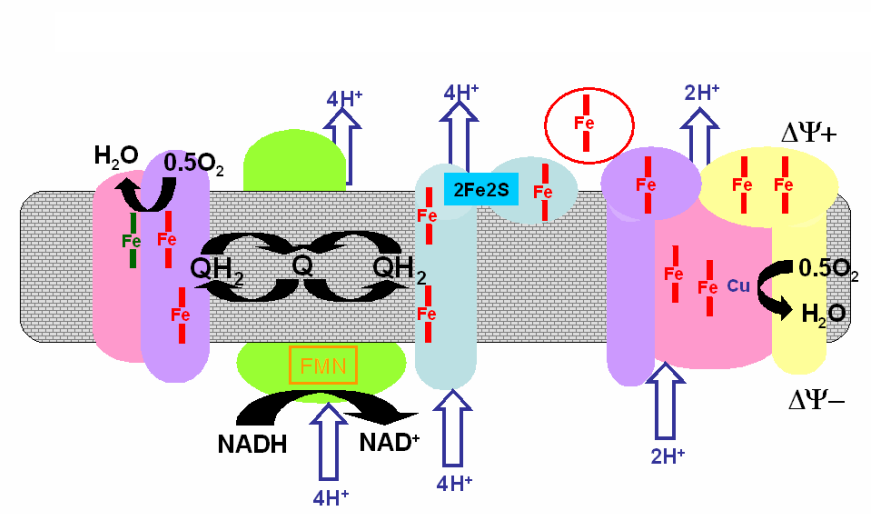

Figure 1.2: Aerobic respiration in *R. capsulatus*.

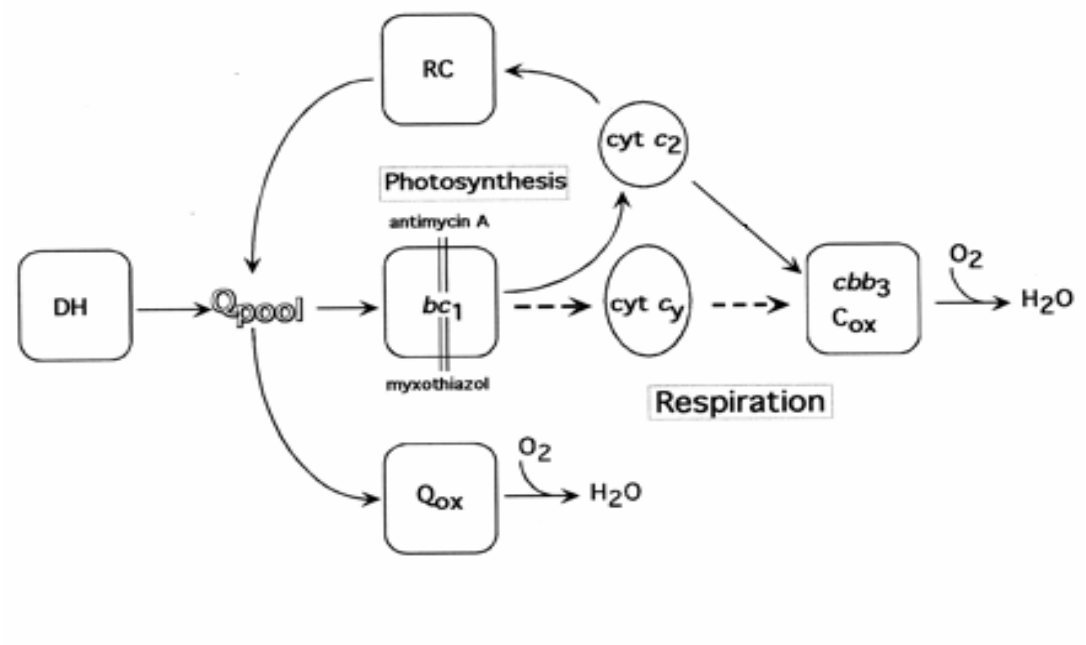

Figure 1.3: Photosynthetic and respiratory electron transport pathways of *R. capsulatus* modified from [Daldal, et al., 2001].

Figure 1.3: Photosynthetic and respiratory electron transport pathways of *R. capsulatus.* DH, Q_{pool}, bc_1, RC, Q_{ox}, cyt c_2, cyt c_y, and cbb_3-C_{ox} correspond to the respiratory NADH and succinate dehydrogenases, membrane quinone pool, cyt bc_1 complex, photochemical reaction center, hydroquinone oxidase, soluble electron carrier cyt c_2, membrane-attached electron carrier cyt c_y, and cbb_3-type cyt *c* oxidase, respectively. Dotted arrows highlight the electron transfer pathways catalyzed by cyt c_y. During the photosynthetic growth electron flow is cyclic; electrons originating from the photo-activated reaction center (RC) flow through the ubiquinone pool (Q_{pool}), the cytochrome bc_1 complex (bc_1 complex), and the electron carrying *c*-type cytochromes (soluble cytochrome c_2 and membrane-attached cytochrome c_y) and back to the RC. During respiratory growth various respiratory dehydrogenases (RDH) replenish the Q pool. From the Qpool, electrons can flow through either of the two branches. One of these is reminiscent of the mitochondrial electron transport chain and involves the bc_1 complex, cytochrome c_2 or c_y and the cbb_3-type cytochrome *c* oxidase. The second branch involves the ubihydroquinone oxidase (Qox) that does not contain any *c*-type cytochromes.

1.4.3 Other Metabolic Pathways in Non-Sulfur Purple Bacteria

Purple non-sulfur photosynthetic bacteria are probably the most versatile of all microorganisms. Besides growing photoautotrophically or photoheterophically, they can also develop chemotrophically in darkness under aerobic conditions. Moreover, some of these bacteria are capable of dark anaerobic respiration. The major of the purple non-sulfur bacteria utilize a variety of different organic carbon source. This organism can grow photoautotrophically with sulfide or hydrogen as the electron donor, chemoautotrophically with hydrogen, photohetotrophically with a variety of organic compounds as electron and carbon sources, chemohetetrophically at the expense of respiratory electron transport-driven energy generation with oxygen, nitrate, nitrous oxide, dimethylsulfoxide to TMAO as electron acceptors, and finally also by fermentation of organic substrates (Figure 1.4). The pronounced metabolic versatility, including the ability to grow under dark, anaerobic conditions [Yen, et al., 1977], makes these purple non-sulfur bacteria.

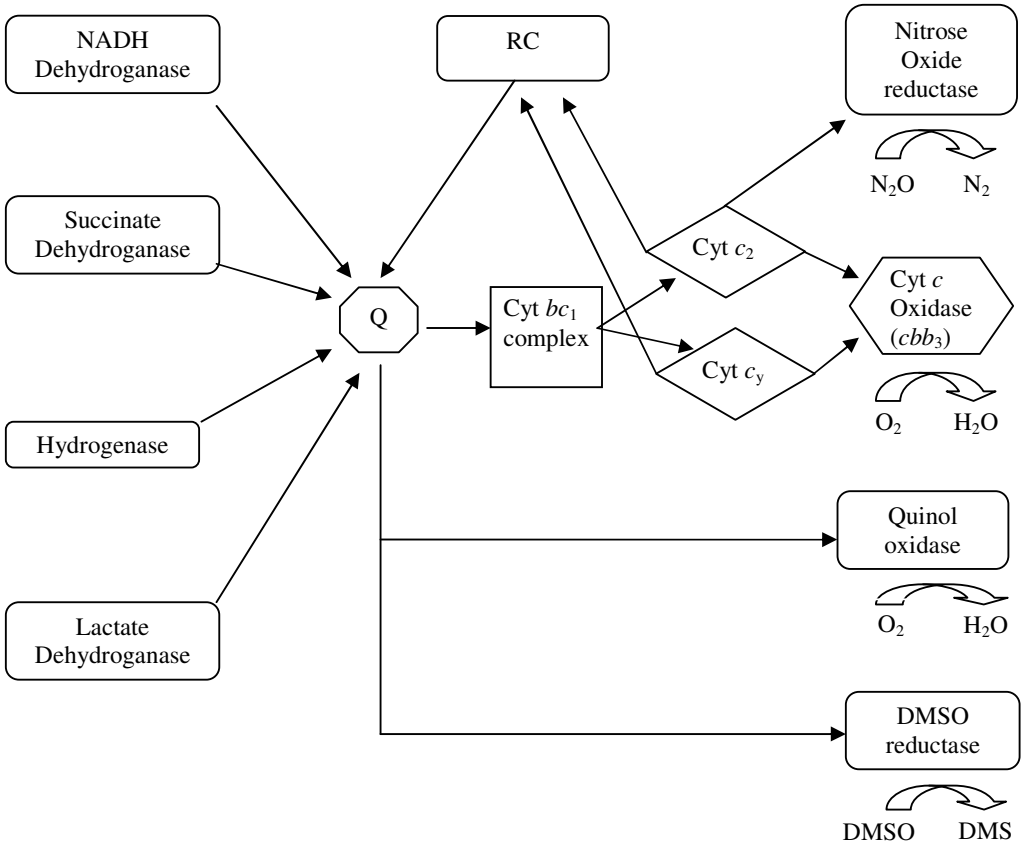

Figure 1.4: Other metabolic pathways of *R. capsulatus.* Several alternative pathways branch from the ubiquinone pool and are independent of both of the photosynthesis and aerobic respiration.

1.5 Heme-Copper Oxidase Super Family

Heme-Copper Oxidases (HCOs) are the terminal enzyme in the respiratory chains from bacteria, archaea and eukarya [Michel, et al., 1998]. The terminal oxidases are integral membrane protein complexes, which are the last components of the respiratory chains in aerobic organisms where they catalyze the reduction of molecular oxygen to water ($O_2 + 4e^- + 4H^+ \rightarrow 2H_2O$). Most members of this family of enzymes are redox-driven proton pumps, the O_2 reduction reaction is energetically coupled to proton translocation across the membrane [Namslauer, et al., 2003]. They possess a unique bimetallic active site consisting of a heme and a closely associated copper atom where O_2 is reduced. The HCO super family is therefore also called the heme-copper super family [Ferguson-Miller, et al., 1996]. Super family of the copper oxidase is divided into two major groups, the quinol oxidases and cyt *c* oxidases, which have distinct substrate specificities [Zufferey, et al., 1996].

The eubacterial HCOs can be divided into two main groups: quinol oxidases, for example *E. coli* cytochrome bo_3 oxidase and cytochrome *c* oxidases, such as the cyt aa_3 oxidase from *P. denitrificans, R. sphaeroides* and bovine mitochondria, The main difference between the two types of oxidase is the presence of a fourth metal centre, known as Cu_A or purple copper, in the hydrophilic domain of subunit II of cyt *c* oxidases. Cu_A contains two copper atoms in a mixed valence configuration [Ferrar et al., 1996] and is the primary acceptor of electrons from cyt *c* [Hill, 1993]. Quinol oxidases combine the redox chemistry mediated by both the cyt bc_1 and cytochrome c oxidase complexes; however they

do this far less efficiently than cyt *c* oxidases, with respect to overall energy transduction [Saraste, 1990].

This superfamily is quite diverse in terms of electron donors, subunit composition and heme types. Three main families of oxygen reductases are identified on the bases of common features of the core subunits, constituting three lines of evolution: (i) type A (mitochondrial-like oxidases, aa_3), (ii) type B (ba_3-like oxidases), and (iii) type C (cbb_3-type oxidases). The first group can be further divided into two subfamilies according to the helix VI residues at the hydrophobic end of one of the proton pathways (so called D-channel): (i) type A1, comprising the enzymes with a glutamate residue in the motif –XGHPEV-, and (ii) type A2, enzymes having instead a tyrosine and a serine in the alternative motif -YSHPXV- [Pareira et. al., 2001].

Eukaryotic HCO complexes contain three mitochondrially encoded subunits (I, II and III) and up to ten unclearly-encoded subunits. All prokaryotic members of the HCO super family contain homologues of subunit I and most also contain homologues of subunits II and III. The *E. coli* homologue, an ubiquinol oxidase, cytochrome b_o, has homologues of subunits I, II and III.

The most important features of the subunit I and II allow the establishment of a structural and functional classification of the oxidase families. Only subunit I is common to all heme-copper oxidases. The super family is defined by the presence, in subunit I, of a six-coordinated, low-spin heme and a unique bimetallic center composed of a high-spin heme and a copper ion, Cu_B. The low-spin heme is the immediate electron donor to the binuclear center, where the catalytic reaction

takes place. A broad subdivision of this super family was previously established, on the bases of amino acid sequence alignments more similar to the mitochondrial cytochrome oxidase, and (ii) a highly divergent group, the fixN type, also named *cbb*$_3$ oxidases [Garcia-Horsman et al., 1994]. The HCO-type oxidases have a second subunit, with one of two transmembrane helices and a peripheral domain: in cytochrome and HPIP (High potential iron-sulfur protein) oxidases this domain contains a mixed-valence binuclear copper site (Cu_A), while in quinol oxidases this center is absent. The members of the *cbb*$_3$ family, apart from subunit I, have two other subunits containing C-type hemes: a monohaemic and dihaemic cytochrome [Thöney-Mayer et al. 1994]. The prokaryotic oxidase may contain quite diverse hemes: Heme A, B, O and derivatives of the heme A and O [Lubben, et al., 1994].

Despite these conserved metal ligands and a conserved secondary structure, CcoN subunit of the *cbb*$_3$ oxidase contains neither heme O nor heme A in the active site. Several analyses of the noncovalently bound hemes present in the *cbb*$_3$ oxidase complex by high-performance liquid chromatography (HPLC) have shown that only heme b is present [Gray et al., 1994]. Consequently the dinuclear centre of cytochrome *cbb*$_3$ oxidases must consist of a *b*-type heme, heme b_3, magnetically coupled to Cu_B.

In spite of differences in their affinity of oxygen, cofactor composition and immediate electron donors, all members of the HCO super family contain a highly conserved catalytic subunit (Subunit I) [Castresana et al., 1994; van der Oast et al., 1994; Pereira et al., 2001]. Subunit I comprises at least 12 transmembrane helices

and contains the active site, a dinuclear centre formed by the iron of a high-spin, penta coordinated heme, to which substrate and other exogenous ligand can bind, and an adjacent copper ion (Cu_B) [Bobcock and Wikstrom, 1992]. This center seems to be designed to prevent the escape of partially reduced oxygen species. Also found in subunit I is the binding site for a second heme that is six coordinate, which serves to transfer electrons to the active site. Transmembrane helices II, VI, VII and X of subunit I harbor six absolutely conserved histidine residues that are diagnostic of the entire super family and which serve to ligate both heme irons and Cu_B [Saraste, 1990]

1.5.1 Proton Translocation Mechanism

The enzyme takes up eight protons from the N-site for each cyt c turnover: Four chemical protons and four pumped protons. As the electrons and protons used to form water come from opposite sites of the membrane, a total of eight charges are translocated across the membrane during the catalysis. Rich (1995) proposed that translocation is driven by the requirement for electroneuratically at the dinuclear centre. A conformational switch connects the pump site with the P-side of the membrane and opens the dinuclear centre to protonation [Wikstrom, 2000]. These protons are stored around the heme propionates and electrostatically expelled into the P-site by other protons approaching the catalytic site. It was originally thought that, to efficiently capture the energy released by the oxygen chemistry for proton translocation, the proton pumping steps occur exclusively during the oxidative phase $P \rightarrow F \rightarrow F \rightarrow O$ [Wikstrom, 1989].

The D-pathway is the only channel used during the reaction of the fully reduced enzyme with molecular oxygen molecule and there is general agreement that all of the pumped protons travel through this channel. Conserved glutamate (E286) of aa_3-type oxidase in *R. sphaeroides* has been proposed to act as proton shuttle, which can assume two different conformations, related by a 180º rotation of the carboxylate group. It has been suggested [Michel, 1999] that this switch is triggered by electric fields, and allows the delivery of the chemical and pumped protons to the dinuclear centre and heme propionate groups, which are in contact with the proton exit channel [Puistinen and Wikstrom, 1999], respectively.

1.6 *cbb*$_3$- Type Terminal Cytochrome *c* Oxidase in *R. capsulatus*

In recent years a third highly diverged group of HCO, the cytochrome cbb_3 oxidases, has been described in the Proteobacteria [Myllykallio et al., 2000]. Cytochrome cbb_3 oxidases have been purified from several species of Proteobacteria including *P. denitrificans* [de Gier et. al., 1996], *R. sphaeroides* [Garcia-Horsman et al., 1994], *R. capsulatus* [Gray et al., 1994] and *B. Japonicum* [Preisig et al., 1996a] and *P. stutzeri* [Urbani et al., 2001]. Rather poor yields and a tendency for the complex to dissociate have made detailed biochemical characterization difficult, and a structure is not yet available, although crystallization conditions have been reported [Urbani et al., 2001]. The cyt *c* oxidase of *R. capsulatus* has been purified previously and characterized as being a novel cbb_3-type cyt *c* oxidase without a Cu_A center [Gray et al., 1994]. It is composed of at least a membrane-integral *b*-type cyt (subunit I [CcoN]) with a

low-spin heme *b* and a high-spin heme b_3-Cu_B binuclear center, and two membrane-anchored *c*-type cyts (CcoO and CcoP). It has a unique active site that possibly confers a very high affinity for its substrate oxygen [Wang et al., 1995].

Cyt cbb_3 oxidases are quite distinct from other bacterial HCOs in terms of their strategy for receiving electrons, the heme prosthetic group present in the active site and their affinity for oxygen. Despite these conserved metal ligands and a conserved secondary structure, CcoN contains neither heme O nor heme A in the active site. Several analyses of the noncovalently bound hemes present in the cbb_3 oxidase complex by high-performance liquid chromatography (HPLC) have shown that only heme B is present [Gray et. al., 1994; Wang et al., 1995]. Consequently the dinuclear centre of cytochrome cbb_3 oxidases must consist of a *b*-type heme, heme b_3, magnetically coupled to Cu_B.

1.6.1 Cytochrome cbb_3 Oxidase Operon

Genes encoding a cytochrome cbb_3 oxidase were initially isolated and identified from *Rhizobium* species, *Bradyrhizobium japonicum* and designated *fixNOQP (ccoNOQP)* since their expression is required to support symbiotic N_2 fixation [Preisig et al., 1993]. More recently, homologous genes have been identified in other *Proteobacteria*, for example *R. capsulatus* [Thony-Meyer et al., 1994 and George et al., 1998], *Azorhizobium caulinodans* [Mandon et al., 1994], and five human pathogens *Campylobacter jejuni* [Parkhill et. al., 2000], *Helicobacter pylori* [Tomb et. al., 1997], *Pseudomonas aeruginosa* [Stover et al., 2000], *Vibrio cholerae* [Heidelberg et al., 2000] and *Neisseria meningitides,* in

which cytochrome cbb_3 is the only respiratory oxidase, were encoded by the genome. The structural genes of this enzyme (*ccoNOQP*) have been sequenced in last decade from *R. capsulatus* 37b4 [Thony-Meyer et al., 1994] and aligned to the partial amino acid sequence of the purified enzyme from *R. capsulatus* MT1131 [Gray et. al., 1994 and George et al., 1998].

The biogenesis of a multisubunit protein complex containing several prosthetic groups, such as cyt cbb_3 oxidase, is likely to require many accessory proteins involved in various posttranslational events, including protein translocation, assembly, cofactor insertion, and maturation [Thöny-Meyer et al., 1997]. The *ccoNOQP* operon is always found close to a second gene cluster, known as *fixGHIS* (*ccoGHIS*) whose expression is necessary for the assembly of a functional cbb_3 oxidase [Preisig et al., 1996; Koch et al., 2000] (Figure 1.5-A). The *ccoGHIS* operon comprises four tightly linked open reading frames first identified, cloned and sequenced in *Sinorhizobium meliloti* [Kahn et al., 1989]. Like the *ccoNOQP* operon, expression is strongly induced in cells grown under microaerobic or anaerobic conditions. On the basis of their derived amino acid sequences each of the four proteins encoded by the *ccoGHIS* operon are thought to be membrane-bound and it has been suggested that they may function in concert as a multisubunit complex [Preisig et al., 1996]. Biochemical and genetic characterizations of these mutants reveal that at least four additional gene products are required at some posttranslational steps for the presence of an active cyt cbb_3 oxidase in *R. capsulatus* [Aygün, 1999 and Koch et al., 2000].

In *P. denitrificans* and *R. sphaeroides*, other oxygen response regulators, the *fnr*-like genes *fnrP* and *fnrL*, respectively, are located upstream of *ccoNOQP* [de Gier et al., 1994; Zeistra el al., 1995]. In addition, *Fnr* binding consensus sequences have been identified in the intergenic region between ORF277 and *ccoN* in both organisms [de Gier et al., 1994; van Spanning et al., 1997; Zeilstra el al. 1995; Zeilstra et. al., 1996] (Figure 1.5-B). Putative *Fnr* binding sequences (TTGAT-N4-GTCAA at positions 91 to 108 and TTGAC-N4-ATCA at positions 168 to 181 from the first ATG codon of *ccoN*) are also present in the ORF277-*ccoN* intergenic region of *R. capsulatus*. However, in contrast to the other related species, an ORF containing a gene coding for a possible Fnr-like protein is absent upstream of *ccoNOQP* in *R. capsulatus*. Interestingly, no Fnr binding site is present in the *ccoP-ccoG* intergenic region of *R. capsulatus*. Considering that in many facultative aerobes an oxygen or redox-regulated switch may turn on and off various cyt *c* oxidases with different oxygen affinities [Bosna et. al., 1987; de Gier et. al., 1996; van Spanning et al., 1997], it is tempting to speculate that cyt cbb_3 oxidase in *R. capsulatus* supports aerobic growth under both high and low oxygen concentrations.

In some rhizobial species, *fixNOQP* genes are not regulated by a genuine *Fnr* but by a paralogue, called *FixK*, that also binds *Fnr* boxes [Batut et al., 1989; Fischer, 1996] but does not carry any [4Fe–4S] cluster and whose activity is not regulated by O_2 [Soupène et al., 1995]. In these cases, regulation by O_2 instead occurs at the level of *fixK* transcription, which is regulated by the *FixLJ* two-component regulatory system. Under O_2 limitation, the FixL hemoprotein kinase autophosphorylates and then transfers its phosphate group to the *FixJ*

transcriptional regulator protein. Phosphorylated FixJ then activates transcription of *fixK*. It was predicted that the primary function of the FixLJ-FixK system in these bacteria is to regulate *ccoNOQP* expression under O_2-limiting conditions. It is possible of course that FixLJ-FixK regulates additional functions in these bacteria, as it does for nitrogen fixation in some *rhizobia* [Pitcer, et. al, 2003].

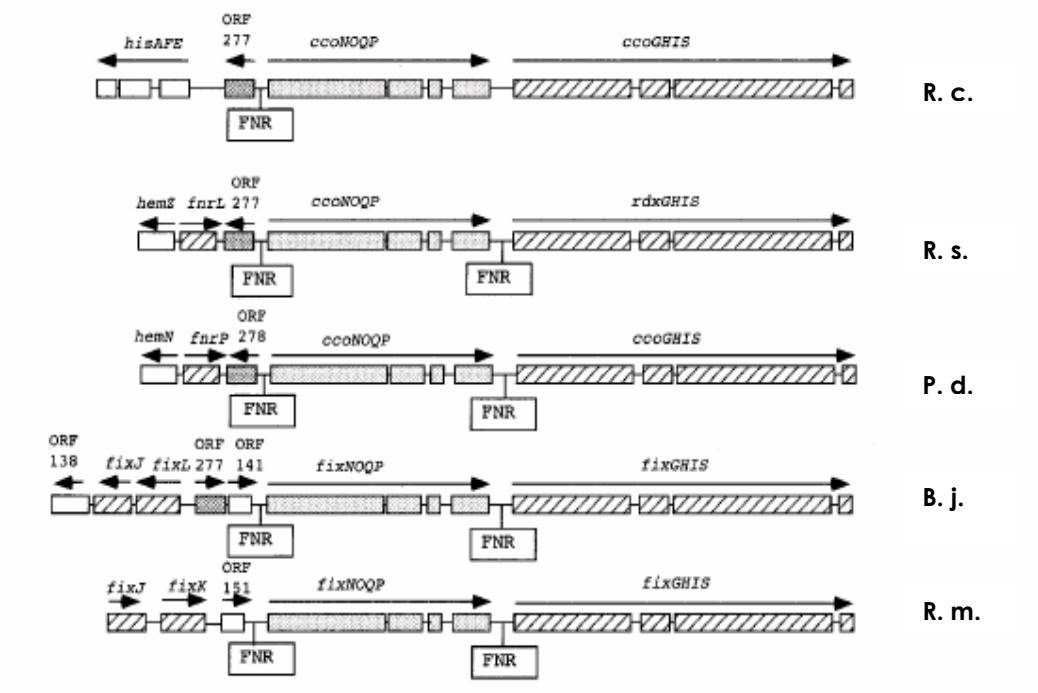

Figure 1.5: Organization of the *ccoNOQP* Operon in *R. capsulatus*. Comparison of the genetic organization of the *cco(fix)NOQP* operons and their flanking regions in different organisms [Koch et al., 1998]. FNR indicates the presence of possible Fnr-binding sites in the intergenic regions upstream and downstream of the *cco(fix)NOQP* operons. The *hisAFE* genes are involved in histidine biosynthesis, and *fnrL* and *fnrP* are *fnr*-like genes most likely involved in oxygen- or redox-regulated expression of cyt cbb_3 oxidase. *fixJ*, *fixK*, and *fixL* code for oxygen response elements in *B. japonicum. hemZ* and *hemN* correspond to the genes encoding the anaerobic coper-hydrinogen III oxidase. *R.c., R. capsulatus*; *R.s., R. sphaeroides*; *P.d., P. denitrificans*; *B.j., B. japonicum; R.m., R. meliloti.* Arrows indicate direction of the transcription

1.6.2 Organization of the Cytochrome *cbb*$_3$ Oxidase Complex in *R. capsulatus*

The *cbb*$_3$-type cyt *c* oxidase encoded by the *ccoNOQP* operon is composed of four subunits [Zufferey et al., 1998].The *ccoN* gene encodes the catalytic subunit of the oxidase, which is homologous the subunit I of *aa*$_3$ oxidase. The *ccoO* and *ccoP* genes encode two membrane anchored *c*-type cytochromes. These are the monoheme CcoO (28 kDa) and diheme CcoP (32 kDa), one or both of which may serve to transfer electrons derived from the *bc*$_1$ complex to CcoN the catalytic subunit (Figure 1.6). The cytochrome *cbb*$_3$ oxidase operon includes a fourth gene: *ccoQ* that is predicted to encode a small membrane bound polypeptide.

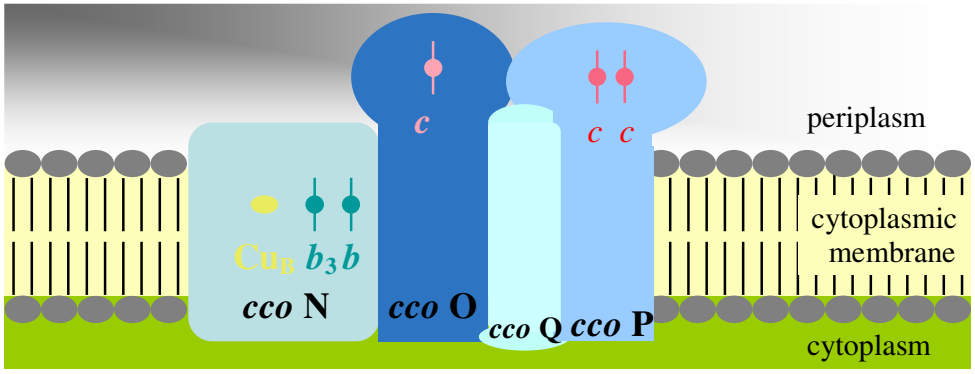

Figure 1.6: Organization of the ccoNOQP subunits of *cbb*$_3$-type oxidase in *R. capsulatus*. The *ccoNOQP* operon of *R. capsulatus* encodes the four structural proteins that comprise the cytochrome *cbb*$_3$ oxidase complex. Although CcoQ is shown as an integral part of the complex there is no evidence for its presence in the cytochrome *cbb*$_3$ oxidase purified from *R. capsulatus* which is a three subunit (CcoNOP) complex. It was modified from thesis of Aygün, S. (1999).

1.6.2.1 Subunit I of the *cbb*$_3$ Oxidase

The first gene of the *ccoN* encodes a basic membrane protein of 532 amino acid residues, with a predicted molecular mass of 45 kDa. The highly hydrophobic CcoN protein has 14 transmembrane segments with both N and C termini facing the cytoplasmic side [Gray et al., 1994]. It is a highly homologous to *fixN* gene product of *B. japonicum, R. meliloti* and *A. caulinodans* (62-77% positional amino acid identity and 79-84% similarity) This subunit is predicted to bind the low spin heme *b*, the high spin heme b_3 and the Cu_B, which have been spectroscopically detected [Thony-Meyer et al., 1994; Varotsis et al., 1995]. From 12 histidine residues (H) in the sequence, only six are conserved in all the CcoN/FixN sequences reported. By comparison with the location of the histidine ligands in cytochrome aa_3 crystal structure, it is most likely that H114 and H404 are the ligands for the low spin heme *b*, and His 402 the axial ligand for the high spin heme b_3. H264, H314 and H315 are probably ligands of Cu_B. The H394 might be equivalent to the conserved H403 (*P. denitrificans* cytochrome aa_3) which is a ligand for the magnesium ion. Otherwise, alignments of the *ccoN* sequences with subunit I of the main heme-copper oxidase family indicate that there is little homology between them. For example, residues suggested to be involved in H^+ conduction (asparagine (N124), glutamine (Q278), lysine (K354), Leucine (L393) and asparagine (N399) in *P. denitrificans* cytochrome aa_3), or in H bonding to the Cu_B histidine ligands (threonine (T344) and tyrosine and (Y280)) are missing in the cyt cbb_3 sequences, or placed in other positions. However, [Zufferey et al., 1996] showed evidence which suggests that these two helices in *B. japonicum* FixN may be peripheral facing the cytoplasm. These two helices might not have a

role in the function/structure of the oxidase since they are missing in the *Helicobacter pylori* ccoN sequence [Thony-Meyer et al., 1994].

1.6.2.2 Subunit II of the cbb_3 Oxidase

The *ccoO* gene encodes for a 242 amino acid polypeptide with a calculated molecular mass of 28 kDa, which is predicted to be a *c*-type membrane bound cytochrome. It is 61-73% identical and 77-85% similar to the corresponding Rhizobial *fixO* gene product. Hydropath analysis shows that CcoO probably has a single membrane-spanning domain near the N terminus, and a hydrophilic domain, which is most probably exposed to the periplasmic side where heme *c* is attached. A predicted totally conserved heme *c* binding site (C-Y-V-C-H- at position 68-72 and M at position 140 found in this region [Thony-Meyer et al., 1994].

1.6.2.3 Subunit III of the cbb_3 Oxidase

The *ccoQ* gene codes for a 58 amino acid residues with a calculated molecular weight of 6.5 kDa. It does not share much amino acid sequence identity (22-40%) with in the four species; however, the similarity is in the range of 53-60%. It has a high hydrophobic amino acid stretch near the N terminus, and a charged motif at the C terminus as previously suggested, in which high percentage of charged amino acid residues are present [Thony-Meyer et al., 1994]. The presence of CcoQ in purified complex has so far only been demonstrated

immunologically in *B. japonicum* (Zufferey et al., 1998) and its function remains unclear. In frame deletion mutants of ccoQ constructed in *B. japonicum* [Zufferey et al., 1996b] and *R. sphaeroides* [Oh and Kaplan, 1999] have no apparent effect upon the assembly or the activity of cytochrome cbb_3 oxidase although the cytochrome *c* quantity appeared somewhat decreased in the *ccoQ* mutant of *B. japonicum* [Zufferey et al., 1996b]. Recent evidence suggest that in *R. sphaeroides* CcoQ serves as a transporter in signal transduction pathway that controls the expression of photosynthesis-related genes in response to the flux of electrons through the cytochrome cbb_3 oxidase. It has also been suggested that this specific role for CcoQ may perhaps be related to the presence of two histidine residue that are conserved in *R. sphaeroides* and *R. capsulatus*, but which are not present in non-photosynthetic species [Oh and Kaplan, 1999; Eraso and Kaplan, 2000]. The corresponding polypeptide is apparently not present in the purified preparation [Garcia-Horsman et al., 1994], and protects the core complex, in the presence of O_2, from proteolitic degradation by a serine metalloprotease in cbb_3 oxidase of *R. sphaeroides* [Oh et al., 2002].

1.6.2.4 Subunit IV of the cbb_3 Oxidase

The last gene, *ccoP*, codes for an acidic membrane protein of 297 amino acids and calculated Mr of 32 kDa. Hydropathy profiles predict two main domains: a hydrophobic transmembrane domain near to the N terminus, and a hydrophilic domain most probably facing the periplasmic side. Two heme C binding motifs can be found in this domain (-C-A-Q-C- at position121-125, and

M at position 174; C-A-S-C-H at position 219-223 and M at position 264. CcoP shares 45-51% identical and 61-64% similar amino acid with its Fix P homologous. Considering that only CcoN, CcoO, and CcoP are part of the functional cyt cbb_3 [Thony-Meyer et al., 1994].

1.7 Proton-Conducting Pathways

1.7.1 Proton Input Channels

Three putative proton-conducting input pathways have been identified in the X-ray structures of aa_3-type oxidase [Tsukihara et al., 1998; Gennis, 1998]. These are called the K-channel, D-channel and the H-channel. The names are derived from conserved amino acid residues within each of the putative channels. The H-channel is proposed to be important for conveying pumped protons across the membrane, but only for the oxidases of animals [Tsukihara et al., 1998]. The K-channel and the D-channel, on the other hand, are observed in both the prokaryotic and eukaryotic oxidase structures [Tsukihara et al., 1996 and 1998; Ostermeier et al., 1997], and the importance of these two channels in proton input to the enzyme is supported by extensive functional analysis of mutants.

The key residue of the K-channel, found in pore B, is a highly conserved lysine (K362 in the *R. sphaeroides*) on the cytoplasmic surface of the enzyme, which is in the neutral unprotonated state in both the oxidized and reduced forms of the enzyme [Kant et al., 1998]. Equivalent mutations on the highly conserved K362 in *R. sphaeroides* [Konsatantinov et al., 1997], *P. denitrificans* [Pfitzner et

al., 1998] and *E. coli* [Thomas et al., 1993] resulted in almost complete loss of oxidase activity. Moreover analysis of K362 mutations demonstrated K channel is necessary for the reduction of the dinuclear centre prior to oxygen binding [Konstantnov et al., 1997]. This channel includes threonine (T359) and leads to the hydroxyl group of tyrosine (Y288) at the active site. Since Y288 (cross-linked to active site, it is reasonable to consider this is a proton pathway for the delivery of at least one of the substrate protons. The cbb_3-type oxidases seem to have only part of the alternative K-channel conserved with serine and tyrosine in the place of the *P. denitrificance* threonine (T351) and serine (S291). It is remarkable that an equivalent to Y288 is not present in these enzymes. None of the canonical residues of the D-channel is present for these oxidases [Michel, 1998].

In the absence of either a three-dimensional structure of a cbb_3-type oxidase or experiments that inform on the roles of conserved residues in CcoN, it is not yet possible to conclude whether cyt cbb_3 oxidases have independently evolved a distinctive method for coupling oxygen reduction to proton translocation. Alternatively, the mechanism of energy transduction might be functionally conserved in the cbb_3-type oxidases, even though key residues of the D- and K-channels are apparently missing. However, there is a further difference between the cyt cbb_3 oxidases and all other HCOs, including the enzymes found in *R. marinus* and *T. thermophilus* that might suggest that the mechanism of energy transduction evolved independently in cytochrome cbb_3 [Pitcher et al., 2003]. The cbb_3-type oxidases contain a *b*-type heme rather than *a*-type or *o* type heme in the dinuclear centre which is not only the site of oxygen reduction but is also proposed to be the site of proton-pumping in the aa_3-type oxidases. Analysis of

the bacterial [Iwata et al., 1995; Soulimane et al., 2000] and mitochondrial [Tsukihara et al., 1996] CcoO structures implicates the hydroxyl group of the heme a_3 hydroxyethylfarnesyl (hydroxyethylgeranylgeranyl in the case of cyt ba_3 oxidase of *T. thermophilus*) side chain in a pathway that may be involved in conducting protons to the dinuclear centre [Blomberg et al., 2000].

1.7.2 Proton Exit Channels

A putative water and/or proton exit channel has been suggested based on their mammalian and bacterial cyt *c* oxidase X-ray structures. It was suggested that this pathway serves as an exit for the water produced [Tsukihara et al., 1996], while Iwata (1995) preferred a role in the pathway of pumped protons from the dinuclear centre to the outside. This channel proceeds from the dinuclear centre to the outside of the membrane via a number of hydrophilic residues from both subunit I and subunit II and the Mg^{2+} binding site, located at the end of this proposed channel. Crystalographycally well-defined water molecules provide three other ligands of the Mg^{2+} site. Further more deuterium exchange between water molecules closely associated with this site and bulk solvent has been demonstrated at a rate consistent with a role for this region in product release during catalytic turnover [Florens et al., 2001]. However the route(s) to which the water and/or protons access the Mg^{2+} site and whether or not access to them are controlled remains unclear.

1.8 Site-Directed *in vitro* Mutagenesis

Site-directed *in vitro* mutagenesis is an invaluable technique for studying protein structure-function relationship, gene expression and vector modification. PCR based site-directed mutagenesis is used to amplify circler plasmid and to insert a mutation anywhere in the plasmid with no requirement for convenient restriction enzyme sites. In this technique, the initial rounds of amplification are directed by two primers located 'back-to-back' on the opposing DNA strands. One primer contains one or a few mismatches which will generate the site-directed mutation. The first cycle of PCR generates linear plasmid molecules, from one or both circular template strands. Subsequent rounds of PCR further amplify the linear plasmid sequence generated by the first PCR cycle, which is then isolated, ligated and used for transformation. This method has the advantage of introducing mutations at any desired site regardless of restriction sites are present in the surrounding sequence.

The method of site-directed *in vitro* mutagenesis, which substitutes specific amino acid residues by genetic methods, is ideal for addressing these questions of cytochrome *c* structure and function [Pielak et al., 1985; Caffrey, 1994; Caffrey et al., 1994]. *R. capsulatus* and *R. sphaeroides* have been genetically modified to allow site-directed *in vitro* mutagenesis and a number of single site mutants have been obtained in each of the three subunits. In recent years, the analysis of site directed *in vitro* mutants has led to the identification of the ligands to the metal cluster, general location of the sites of the quinone interaction and more accurate folding models of the individual subunits of the

complex [Gray et al., 1995]. It is anticipated that further application of the site-directed *in vitro* mutagenesis technique to numerous species of cyt c will better define the roles of conserved and non-conserved residues in the structure and function of cyt *c*.

The *cyt* cbb_3 structural genes have been cloned in a broad host range plasmid, pOX15/HB101. The mutations are often generated by *in vitro* mutagenesis techniques. Any desired mutation can therefore be efficiently constructed and introduced into *R. capsulatus* using the system. We used the plasmid pBluescript II SK+ as a template DNA for site-directed mutagenesis.

1.9 Conjugation (Triparental Mating)

Plasmid DNA can be introduced into *Rhodospirillacea* by conjugation [Simon et al., 1988]; transformation [Fornari et al., 1982] and electroporation [Timothy et al., 1991]. Transformation system may be difficult to obtain in photosynthetic bacteria owing to intrinsic properties of their membranes, restriction endonucleases or other unknown factors. Electroporation with pRK404 or pRK415 has not been successful in *Rhodobacter* genera. The most efficient and generally applicable system for introducing plasmid DNA into purple bacteria is conjugation.

Plasmids pRK404 [Dita et al., 1985] and pRK415 [Keen et al., 1988] were initially used for such purposes in *R. sphaeroides* and other RK2 derivatives are known to be used in *R. capsulatus*. RK2 plasmids and its derivatives are stable in

R. sphaeroides as long as selective pressure is maintained [Davis et al., 1988; Brander et al., 1989]. Another conjugative plasmid, RP1::Tn501, was derived from RP1 via the insertion of the mercury-resistance transposon Tn501. Chromosome mobilization activity has been demonstrated in *R. capsulatus* with the conjugative plasmid pBLM2 and pTH10 which appear to initiate chromosome transfer from multiple sites of origin.

Transfer can take place both between *E. coli* and the purple bacteria and among various purple species. Mating are performed by mixing the donor and recipient cells and plating on a solid surface, such as an agar plate or a membrane filter, incubating for several hours to overnight, and then replica plating, replating or overlaying onto a selection medium [Donohue et al., 1991]. Selection for the recipient over the donor strain is usually accomplished by antibiotic resistance markers in the recipient or auxotrophic markers in the donor.

Most engineered plasmid systems utilize a mobilizable but not self-transmissible plasmid vector, with the transfer functions provided in *trans* either from a helper plasmid such as pRK2013, a derivative of RK2, in a triparental mating [Ditta et al., 1980]. In this work, the mobilizable site-directed mutant of pOX15 amplified in HB101 *E. coli* HB101 was transferred to GK32 strain Δ(*ccoNO*::kan) of *R. capsulatus* in the presence of pRK2013 helper cells by triparental mating.

1.10 Aim of the Study

Amino acid sequences are known for cyt *c* oxidase subunit I of many prokaryotic and eukaryotic organisms. Alignments of these sequences among 26 different species revealed that they possess sixteen highly conserved amino acids in all subunit I of heme copper oxidases (HCO) although subunit I of the ccb_3-type oxidase has a lower degree of similarity at the amino acid sequence level being less than 20% [Pereira, et al., 2001]. Six of these sixteen highly conserved amino acids in subunit I of the HCO*s* are histidines. They are predicted to serve as the cofactor ligands. Besides these histidines, ten conserved amino acids are strictly conserved (Table 1). The residues valine (V279), tryptophane (W272) and arginine (R474) (*P. denitrificans* numberin*g*) have been pointed out to be critical for the key process of oxygen diffusion, proton pumping and electron transfer. A few other residues, serine (S333), serine (S340), threonine (T350) in helix VIII, asparagine (N390) and threonine (T396) amino acids located the loop between helix IX and X (*R. capsulatus* numbering) are almost strictly conserved in all oxidases reported so far (Figure 1.7 and Figure 1.8).

Substitutions on these amino acids indicate that most of these amino acids are important for integrity, assembly and activity of cyt *c* oxidases. For example, three substitutions examined for threonine amino acids, threonine (T352) and threonine (T359), on subunit I of the bo_3 quinol oxidase in *E. coli* and it was pointed out that T352 and T359 residues appeared to be strictly important for catalytic function of the oxidase [Thomas et al., 1993]. Several mutations on asparagine at N399 position of *P. denitrificans* of aa_3-type cyt *c* oxidase led to

complete inhibition of proton pumping [Pfitzner et al., 2000]. However, in the position of T350 and T396 in *R. capsulatus,* there is no mutagenesis data, reported so far, for any type of the cyt *c* oxidases. It is not known why they had been conserved during evolutionary period for almost all types of cyt *c* oxidase, thus it has not been possible to infer their possible functions from the structural data. This work conducted to determine the possible involvements of the amino acids, serine (S333), serine (S340), threonine (T350), asparagine (N390) and threonine (T396) respectively, in terms of the activity and the assembly of the cbb_3-type oxidase in *R. capsulatus*.

Table 1: Conserved residues in heme-copper oxidase subunit I, besides the metal ligands.

Residue	Function
Valine (ValI-279)	O_2-chanel
Tryptophane (TrpI-272)	interaction with HisI-326
Arginine (ArgI-474)[a]	H-bond to x-propionate of the low-spin heme
Arginine (ArgI-54)	H-bond to formyl group of heme a
Aromatic (TrpI-87)	H-bond to one of the propionates of the low-spin heme
Threonine/Serine (ThrI-344)	H-bond to HisI-325
Aspartate/Asparagine(AspI-399)	H-bond to one of the propionates of the high-spin heme
Phenylalanine (PheI-412)[b]	Possible electron transfer between the hemes
Threonine/Serine (ThrI-361)	Unknown
Threonine/Serine (ThrI-405)	Unknown

[a]Only in heme *a* low spin-containing oxidases. [b]Absent in cbb_3 oxidase and in the oxidase from *Anaboena* sp. form Pereira et al; 2001.

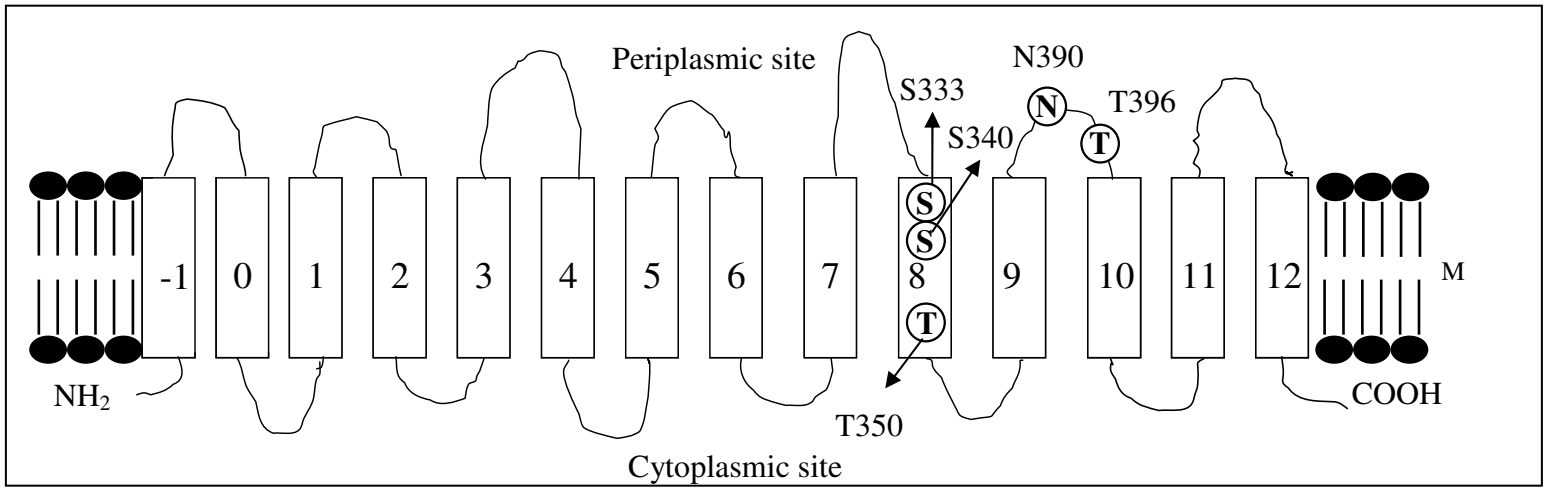

Figure 1.7: Topological model of subunit I (ccoN) of *cbb*$_3$-type oxidase in *R. capsulatus*. Circles represent conserved and mutated amino acids present in subunit of all heme-copper oxidase. S: Serine. T: Threonine, N: Asparagine, M: Membrane.

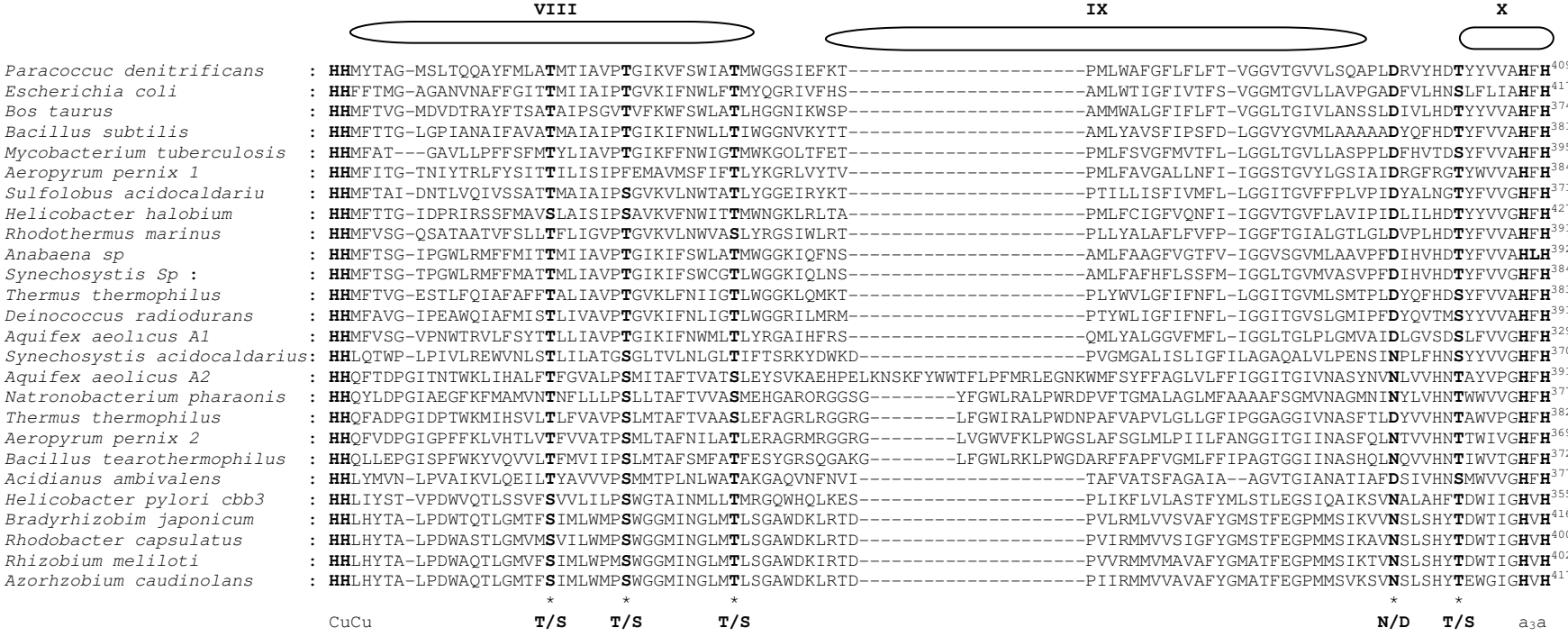

Figure 2: Some part of the amino acid sequence alignment of subunit I of heme-copper oxidase. *P., Paracoccus* (P082837), *E., Escherichia* (P18400), Bo., Bos (P00396), B., *Bacillus* (*subtilis* caa_3, P24010, *stearothermophilus* ba_3, 082837), M., *Mycobacterium* (O53290), *A., Aeropyrum* (1,Q9YDX6, 2, BAA80883), *S., Sulfolobus* (SoxM, p39481, SoxB, S21042), *R., Rhodothermus* (CACO8532), *A., Anabaena* (*Anabaena sp.* Strain PCC 7937, Z 98264), *Sy., Synechosystis* (*Synecosystis sp*. Strain PCC 6803, Q06473/P73261), *T., Thermus* (caa_3, P98005, ba_3, CAB06339), *D., Deinococcus* (G75251), *Aq., Aquifex* (A1, C70488, A2, E70488), *N., Natronobacterium* (CAA71525), *A., Acidianus* (CAA69980), *H., Helicobacter* (AAD0571), *Br., Bradyrhizobim* (Q0373), *Rhd., Rhodobacter* (AAC46108), *Rh, Rhizobium* (A39988), *Az., Azorhzobium* (CAA52429). Strictly and almost strictly conserved amino acid residues are shaded in black. The histidine ligands to low- and high-spin hemes and to Cu_B are indicated by *a*, a_3 and Cu, respectively. It was modified from Pereira et al., 2001.

MATERIALS AND METHODS

2.1. Bacterial strains and growth conditions

The bacterial strains and plasmids used in this work are listed in Table 2.1. *Escherichia coli* strains were grown in Luria-Broth (LB) medium supplemented with appropriate antibiotics (ampicillin, 100µg/ml; kanamycin, 50µg/ml; tetracycline, 12.5 µg/ml per ml, respectively) for plasmid selection and maintenance as described previously [Daldal et al., 1986; Jenney and Daldal, 1993] (Appendix C).

R. capsulatus strains were grown on Sistrom's minimal medium A (Med A) [Sistrom, 1960] or MPYE enriched growth medium [Daldal et al., 1986] supplemented with appropriate antibiotics (supplemented with tetracycline, 2.5µg/ml; kanamycin, 10 µg/ml; or ampicillin, 10 µg/ml as needed) [Daldal et al., 1986] at 35 °C chemoheterotrophically under aerobic conditions in the dark on plates or liquid cultures (shaken at 40-50 rpm).

Table 2.1: Bacterial strains and plasmids used in this study

Strains	Genotype	Phenotype	Reference
E. coli			
XL1-Blue	rec A end A 1 gyr A986 thi-1hsdr17supE44 rel A1 lac [F' proAB lacIq ΔM15 Tn 10(Tetr)]		Stratagene
XL1-Blue/pMOZI	2.8 kbp *Xho*I *ccoNO'* fragment in pBluescript SK+ DNA	Amp^r	This work
XL1-Blue/pMOZIS333A		Amp^r	This work
XL1-Blue/pMOZIA340A		Amp^r	This work
XL1-Blue/pMOZIT350A		Amp^r	This work
XL1-Blue/pMOZIN390A		Amp^r	This work
XL1-Blue/pMOZIT396A		Amp^r	This work
HB101	F-proA2 hsdS20 (Rb-, mB-) recA13 ara14 lac Y1		Sambrook et. al., (1989)
HB101/pACYC177	xy15 galK2 rpsL20 supE44 rpsL20 supE44 proA2 mtl-1	Amp^r, Kan^r	Biolabs
HB101/pMOZII	2.8 kbp *Xho*I *ccoNO'* fragment in pACYC177 DNA	Amp^r	This work

Strains	**Genotype**	**Phenotype**	**Reference**
HB101/pMOZIIS333A		Amp^r	This work
HB101/pMOZIIS340A		Amp^r	This work
HB101/pMOZIIT350A		Amp^r	This work
HB101/pMOZIIN390A		Amp^r	This work
HB101/pMOZIIT396A		Amp^r	This work
HB101/pOX15	4.7 kbp *Bam*HI *ccoNOQP* fragment in pRK404	Tet^r	Koch et al. (1998)
HB101/pOX15S333A		Tet^r	This work
HB101/pOX15S340A		Tet^r	This work
HB101/pOX15T350A		Tet^r	This work
HB101/pOX15N390A		Tet^r	This work
HB101/pOX15T396A		Tet^r	This work

Strains	**Genotype**	**Phenotype**	**Reference**
R.capsulatus			
MT1131	*crtD121 Rif*r	Wild-type	Daldal et al., (1986)
MT1131/pOX15		Tet^r	Koch et. al., (1998)
GK32	Δ(cco*NO*::kan)	Kan^r	Koch et. al., (1998)
GK32/pOX15S333A	GK32, complemented with pOX15S333A	Tet^r	This work
GK32/pOX15S340A	GK32, complemented with pOX15S340A	Tet^r	This work
GK32/pOX15T350A	GK32, complemented with pOX15T350A	Tet^r	This work
GK32/pOX15N390A	GK32, complemented with pOX15N390A	Tet^r	This work
GK32/pOX15T396A	GK32, complemented with pOX15T396A	Tet^r	This work

Plasmids	**Genotype**	**Phenotype**	**Reference**
pBluescript	SKII+	Amp^r	Stratagene
pMOZI	pBlue Script SK+ with a 2.8-kbp *Xho*I insert	Amp^r	This work
pMOZIS333A	Substitution of serine 333 by alanine	Amp^r	This work

Plasmids	Genotype	Phenotype	Reference
pMOZIS340A	Substitution of serine 340 by alanine	Amp^r	This work
pMOZIT350A	Substitution of threonine 350 by alanine	Amp^r	This work
pMOZIN390A	Substitution of asparagine 390 by alanine	Amp^r	This work
pMOZIT396A	Substitution of threonine 396 by alanine	Amp^r	This work
pACYC177		Amp^r, Kan^r	New Englend Biolabs
pMOZII	pACYC177 with a 2.6-kbp *Xho*I insert	Amp^r	This work
pMOZIIS333A	pMOZII replaced 0.6-kbp *BsaA*I fragment of pMOZIS333A	Amp^r	This work
pMOZIIS340A	pMOZII replaced 0.6-kbp *BsaA*I fragment of pMOZIS340A	Amp^r	This work
pMOZIIT350A	pMOZII replaced 0.6-kbp *BsaA*I fragment of pMOZIT350A	Amp^r	This work
pMOZIIN390A	pMOZII replaced 0.6-kbp *BsaA*I fragment of pMOZIN390A	Amp^r	This study
pMOZIIT396A	pMOZII replaced 0.6-kbp *BsaA*I fragment of pMOZIT396A	Amp^r	This work
pOX15	pRK404 with 4.7-kbp *BamH*I-*EcoR*I fragment	Tet^r	Koch et. al., (1998)

Plasmids	**Genotype**	**Phenotype**	**Reference**
pOX15S333A	pOX15 replaced 2.8-kbp *Xho*I fargment of pMOZIIS333A	Tet^r	This work
pOX15S340A	pOX15 replaced 2.8-kbp *Xho*I fargment of pMOZIIS340A	Tet^r	This work
pOX15T350A	pOX15 replaced 2.8-kbp *Xho*I fargment of pMOZIIT350A	Tet^r	This work
pOX15N390A	pOX15 replaced 2.8-kbp *Xho*I fargment of pMOZIIN390A	Tet^r	This work
pOX15T396A	pOX15 replaced 2.8-kbp *Xho*I fargment of pMOZIIT396A	Tet^r	This work
pRK2013		Kan^r, helper	Ditta et al.(1985)

2.2. Molecular Genetic Techniques

2.2.1. Plasmid DNA Isolation

5-10 ml culture of each sample was prepared and grown at 37 ºC, with shaking at 200-225 rpm for 12-16 hs. 5 ml cultures were prepared for the strains containing high copy and 10 ml cultures were used for low-copy number of plasmids. DNAs were isolated using Wizard SV Minipreps DNA Purification Kit and the protocol of manufacturer was followed (Promega cat. #: A1330).

2.2.2. Enzyme Digestion

Insert and plasmid DNAs were cut using the appropriate endonucleases (Fermantase) according to the Manufacturers' instruction. For cloning, 2 µg plasmid DNA was digested with 1 µl of restriction enzymes (10 U/µl) in 50-60 µl final volume at 37 ºC for 1-2 h. For double digestion, 5 µg plasmid DNA was digested with 2 µl of restriction enzyme in 100 µl of final volume at required temperature for 2 hours or more. The name and catalog number of restriction endonucleases are listed at Appendix E. The pOX15 was digested at 37 ºC for 30 minutes and dephosphorylated at 37 ºC for 45 minutes because pRK derivative vectors are sensitive to heating. For the insert control 200 ng of plasmid DNA was digested with 0.5 µl of restriction enzymes (5 U/µl) in 20 µl of final volume at 37 ºC for 1 h.

2.2.3. Purification of Digested DNA Samples

Plasmid DNAs isolated from the transformants and to be used for sequencing were purified and concentrated by Promega SV Minipreps DNA purification System (cat. #: A1330). Final volume of the sample was adjusted according to the concentration of the DNA.

2.2.4. Isolation of DNA Fragments from Agarose Gel

The QIAGEN QIAquick^{R} Gel Extraction Kits (cat. #: 28704) was used and the protocol of the Manufacturer was followed to isolate DNA fragments from the agarose gel. Digested DNA solution was loaded on 1% agarose gel and the gel was run to separate reaction products. Agarose gel bands containing the desired DNA was excised (minimization of UV exposure was taken care to protect DNA). The approximate volume of gel slice was determined by its weight (1 g equals approximately 1 ml) and placed into 1.5 ml eppendorf tube. 3 volumes of buffer QG to one volume of the gel (100 mg ≈ 100 µl) was added and incubated at 50 ºC for 10 minutes to dissolve agarose. To help dissolve gel, it was mixed by vortexing the tube every 2-3 min during the incubation. After silica gel was dissolved completely, one gel volume of isopropanol was added to the sample and mixed. (This step increase the yield of DNA fragments ≤500 bp and ≥ 4 kbp). To bind DNA was transferred to the QIAquick column, and centrifuged for 1 minute. Liquid was discarded flow through and QIAquick column was placed back in the same collection tube. To wash the QIAquick column, 750 ml PE buffer was added which was then centrifuged for 1 min. After liquid was discarded, the QIAquick

column was centrifuged for an additional 1 min at 13.000 g. Finally to elute DNA, 50 µl EB buffer (10 mM Tris-HCl, pH 8.5) or H_2O was added to center of the QIAquick membrane and centrifuged for 1 min at maximum spread. (Sometimes to increase DNA concentration, it was occasionally eluted in 30 µl of the buffer).

2.2.5. Ligation Reaction

MBI Fermentas T4 ligase (cat. # EL0331) was used for ligation reaction. Concentration of vector and insert are determined by either OD_{260} measurement or comparing visually for its value with 1 kbp marker on agarose gel. Amount of the vector and insert as a pmol were calculated by pmol =1.52 pmol × µg of DNA/kbp of DNA equation. Ligation reaction mixture should contain an equal or higher (generally 4-fold was used) concentration of foreign DNA termini than that of vector DNA. In micro centrifuge tube: X pmol vector, 2 µl 10x ligation buffer, 4x pmol insert and 2U-4U T4 Ligase are combined and final volume are completed to 20 µl with ddH_2O. The ligation mixture was incubated at 22 ºC for 1-2 h when working with pBluesicript and pACYC177 derivative vectors, but ligation mixture was incubated on ice overnight and then at 22 ºC for 30 minutes while working with pOX15 DNA. T4 DNA ligase was inactivated by heating reaction mixture at 65 ºC for 10 minutes.

2.2.6. Competent Cell Preparation and $CaCl_2$ Transformation

For *E. coli* HB101 and XL1-Blue competent cells, 50 ml LB in a 500 ml flask were inoculated with 500 µl overnight culture of *E. coli* HB101 and XL-Blue strains respectively. The inoculated cultures were incubated at 37 ºC with shaking until OD_{600}= 0.4-0.5 (it takes nearly 2 h) and then cells were taken on ice. From this point, the cells must be on ice until heat shock step. Cells were centrifuged for 10 minutes at 5000 rpm at 4 ºC. Supernatant was discarded and pellet was resuspended in 25 ml (1/2 of the culture volume) of ice-cold 100 mM $CaCl_2$ and incubated on ice for 30 minutes. Cells were centrifuged for 10 minutes at 5000 rpm at 4 ºC. Supernatant was discarded and pellet was resuspended in 2.5 ml (1/20 of the culture volume) of ice cold 100 mM $CaCl_2$. Competent cells were aliquoted 100 µl into Eppendorf tubes. For stock competent cells, glycerol was added (10% of final conc.). DNA was added to 100 µl competent cells which were then incubated on ice for 45 min. Heat shock was applied to the sample for 5 minutes at 37 ºC. 1 ml LB was added and cells were incubated for 1 h at 37 ºC with shaking. Cells were centrifuged for 1 minute at 5000 rpm at RT and resuspend in 100 µl LB. Cells were plated on a selection plate and incubated overnight [Davis et al., 1986].

2.2.7. Construction of pMOZI

The 15.3 kbp pOX15 plasmid DNA, constructed by Koch et al., 1998 containing 4.7 kbp *ccoNOQP* operon of the cbb_3-type oxidase (Figure 2.1), was digested with *Xho*I. Resulting fragments, 12.5 kbp and 2.8 kbp, were separated on a 1% agarose gel by electrophoresis (Figure 2.2). The 2.8 kbp fragment was isolated from the agarose gel using the QIAGEN QIAquick^R Gel Extraction Kits (cat. #: 28704) and were kept at -20 ºC. Then 2.9 kbp pBluescript vector digested with *Xho*I at 37 ºC for two hours (Figure 2.3). After two hours Calf intestine alkaline phosphatase (CIAP) was added for 1 hour to dephosphorylate both ends to prevent self ligation of the vector during the ligation reaction. Digested samples were loaded and electrophoresed on agarose gel to separate digested and undigested DNAs. Then linear vector DNA was isolated from the gel using a QIAGEN QIAquick^R Gel Extraction Kit (cat. #: 28704). 2.8 kbp *NO'* fragment was inserted into *Xho*I site of dephosphorylated 2.9 kbp pBluescript vector (Affix G), (Figure 2.4). 5 µl ligation reaction was transformed into $CaCl_2$ treated XL1-Blue cells. Transformants were selected in the presence of ampicillin (100µg/ml). The clone, 5 kbp in size, was also tested with *Sac*I which cuts the plasmid once resulting in a 5.7 kbp fragment. The new subclone obtained was designated as pMOZ1.

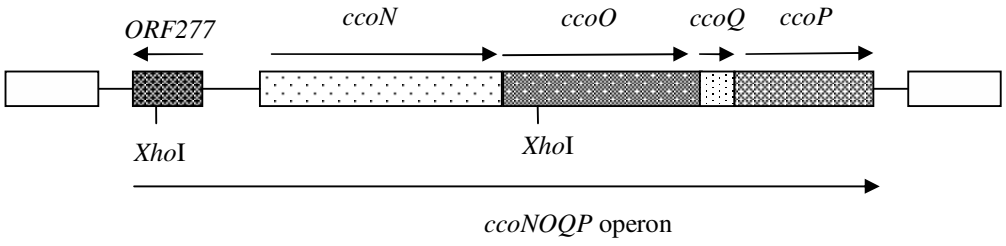

Figure 2.1: The map of the pOX15 DNA carrying c*coNOQP,* 4.7 kbp.

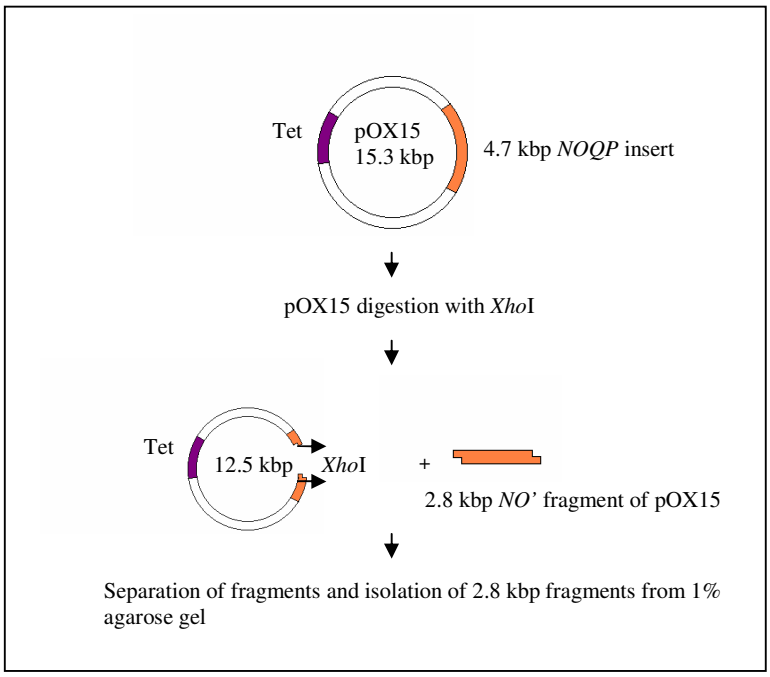

Figure 2.2: Isolation of 2.8 kbp and 12.5 kbp fragments of *Xho*I digested pOX15.

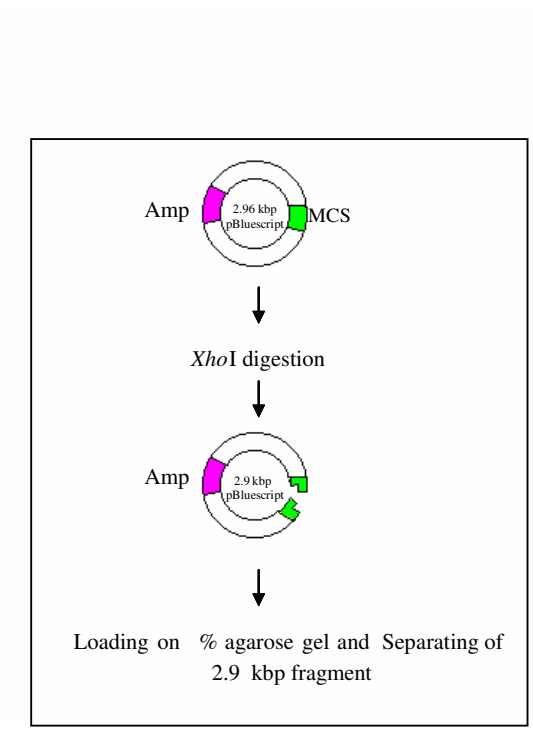

Figure 2.3: Linearization of pBluescript DNA.

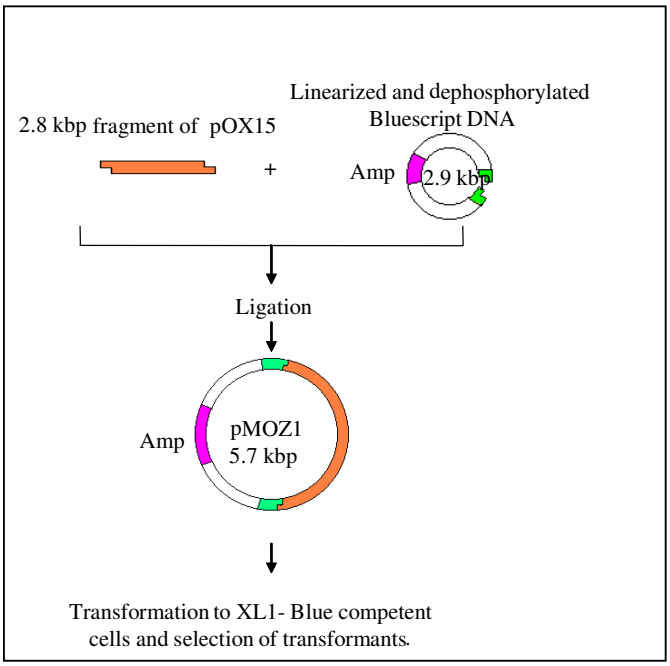

Figure 2.4: Strategy for construction of the pMOZI.

2.2.8 PCR-Based Site-Directed Mutagenesis

The Quick Change Site-Directed Mutagenesis (Stratagene) protocol was used to make mutations. This method was performed using *Pfu* DNA polymerase (MBE Fermantas) and a thermal temperature cycler (Appendıx F). *Pfu* DNA polymerase replicates both plasmid strands with high fidelity and without displacing the mutant oligonucleotide primers. The basic procedure utilizes a supercoiled double-stranded DNA vector with an insert and two synthetic oligonucleotide primers containing the desired mutation. The oligonucleotide primers each of which complementary to opposite strands of the vector are extended during temperature cycling by using *Pfu* DNA polymerase.

The pMOZI DNA was used as the template to substitute five target amino acids, serine (S333), serine (S340), threonine (T350), asparagine (N390) and threonine (T396), respectively, for alanine by Quick Change™ Site Directed Mutagenesis protocol using forward and reverse primers for each mutations. Forward and reverse mutagenic primers, designed based on nucleotide sequence (Table 2.2a) of subunit I of cbb_3 oxidase in *R. capsulatus*, were listed on Table 2.2b. Two types of PCR reactions defined on Table 2.3 were prepared for each mutation, the sample reaction as well as the control reaction which does not contain *Pfu* DNA polymerase. All reaction mixtures were incubated at the conditions defined Table 2.4. Following temperature cycling, 10 µl of PCR products from sample and control reaction to replace five amino acids, S333A, S340, T350, N390 and T396, were loaded on 1% agarose gel and electrophoresed for 1 h to visualize the PCR product.

The PCR products were treated with *Dpn*I, specific for methylated and hemimetylated DNAs, to digest the parental template DNA and to select the PCR synthesized DNA. Following PCR product digestion, The *Dpn*I treated PCR product was transformed into XL-1 blue cells. Finally, to find transformants that had desired mutations, DNA was isolated from four transformants for each mutation to be sequenced. The strategy used to select transformants was summarized in (Figure 2.5).

Table 2.2: Nucleotide sequence of the subunit I of the *cbb*$_3$ type oxidase and primers.

a) Nucleotide sequence of subunit I of the *cbb*$_3$-type oxidase in *R. capsulatus*[a].

>RRC04162 1D09-1F02_110436_112031

ATGTGGGATTACGTCAAGCTTGTCGCGCTTGGCGTCGTGGTGGCTATTGCCGCTTACGCC
GCCAGTCAGGCGCGAGATTTGCCGTATATGGTGAACATGGTCGAGGTCGCGCTGGCGGCC
GTGATCGCGTTCATCTGGGTGCTGCGCACCATGGGGGACGCCAAACCCTCGAAAGACGAG
TATTTCGACGGCGTGATCCGCGCCGGCGTGATCGCAACCACCTTCTGGGGGATCGTCGGC
TTTCTCGTGGCCGTCATCATCGCCTTCCAGCTTGCCTTCCCCGCGCTGAACCTTGAATTC
GGCAACGGGATGCTGAACTTCGGGCGCCTGCGTCCGCTGCACACCTCGGCGGTGATCTTC
GCCTTTGGCGGCAACGCCCTGATCGCCTCGGCCTTCTATGTCGTGCAGCGCACCTCGGCG
GCGCGTCTCTTCGGGGGCACGGCGCTTGGCTGGTTCGTGTTCTGGGGCTGGCAGCTGATC
ATCGTCACCGCCGCGACCTCCTATCTGCTGGGCGGCTCGCAGGGCAAGGAATATGCCGAG
CTGAACTGGCATCTCGACATCCTCGTCGCGATCGTCTGGGTGGCCTATCTGATCGCCTTC
CTCGGCACGATCTTCAAGCGCAAGGAACCCCACATCTACGTGGCGAACTGGTTCTACCTG
TCCTTCATCGTGACGATCGCCATGTTGCACATCGTCAACAACCTGGCCGTTCCGGTCTCG
ATCTTCGGCACCAAATCGGTGCAGCTGATGGCGGGCGTGCAGGATGCGATGACGCAATGG
TGGTACGGCCACAACGCCGTGGGCTTCTTCCTCACCGCGGGCTTTCTGGGCATGATGTAT
TACTTCGTGCCGAAACAGGCCGAGCGTCCCGTCTATTCCTACAAGCTCTCGATCGTCCAC
TTCTGGGCGCTGATCTTCCTCTACATCTGGGCCGGTCCGCACCACCTGCATTATACCGCG
CTGCCCGACTGGGCCTCGACGCTGGGCATGGTGATG**TCG**GTGATCCTGTGGATGCCG**TCC**
TGGGGCGGCATGATCAACGGCCTGATG**ACG**CTTTCGGGCGCCTGGGACAAGCTGCGCACC
GATCCGGTGATCCGGATGATGGTGGTTTCGATCGGCTTTTACGGCATGTCGACCTTTGAA
GGCCCGATGATGTCGATCAAGGCGGTC**AAC**TCGCTCTCGCACTAC**ACG**GACTGGACCATC
GGTCACGTGCATTCGGGCGCGCTGGGCTGGAACGGCATGATCACCTTCGGCATGCTCTAC
TTCCTGACGCCGCGCCTGTGGGGCCGTTCGGGGCTTTACTCGCTGAAACTGGTCAGCTGG
CACTTCTGGCTCGCCACCATCGGGATCGTGCTTTACGCCTCCTCGATGTGGGTGTCGGGC
ATCATGGAAGGCCTGATGTGGCGTGAAGTCGATGCGCAGGGCTTCCTGGTGAACGGTTTC
GCCGACACCGTGGGCGCCAAGTTCCCGATGAACGTCGTGCGTGGCGTCGGGGGTGTGCTG
TATCTGACCGGCGGTCTGATCATGGCCTACAACCTTTGGGCCACGGTCGCGAAACAACCG
AAGACGGCCAATCTCGCCGTTGCGGTTCCGGCGGAA

[a] Codons of the target conserved amino acids, S333, S340, T350, N390 and T396, respectively were highlighted.

Table 2.2: b) Forward and reverse primers used for substituting desired amino acids for alanine.

Primers	Sequence of the primers
S333AF	5'-CTG GGC ATG GTG ATG **GCC** GTG ATC CTG TGG ATG-3'
S333AR	5'-CAT CCA CAG GAT CAC **GGC** CAT CAC CAT GCC CAG-3'
S340AF	5'-G ATC CTG TGG ATG CCG **GCC** TGG GGC GGC ATG-3'
S340AR	5'-C ATG CCG CCC CAG GCC **GGC** ATC CAC AGG ATC 3'
T350AF	5'-G ATC AAC GGC CTG ATG **GCG** CTT TCG GGC GCC TGG G-3'
T350AR	5'-C CCA GGC GCC CGA AAG **CGC** CAT CAG GCC GTT GAT C-3'
N390AF	5'-G TCG ATC AAG GCG GTC **GCC** TCG CTC TCG CAC TAC-3'
N390AR	5'-G TAG TGC GAG AGC GAG **GCG** ACC GCC TTG ATC GAC-3'
T396AF	5'-CG CTC TCG CAC TAC **GCG** GAC TGG ACC ATC GG-3'
T396AR	5'-CC GAT GGT CCA GTC **CGC** GTA GTG CGA GAG CG-3'

Table 2.3: Reaction condition's of site-directed *in vitro* mutagenesis.

Reactants	Sample Reaction	Control Reaction
Template DNA (50 ng/	1µl	1µl
Buffer (10X *Pfu* pol. buffer)	5µl	5µl
Primers (Forward, 125 ng/µl)	1µl	1µl
Primers (Reverse, 125 ng/µl	1µl	1µl
ddH_2O	40µl	41µ
dNTP mix (10 mM)	1µl	1µl
Enzyme (*Pfu* DNA pol. 5 u/µl)	1µl	-
Total reaction volume	50µl	50µl

Table 2.4: Cycling parameter's for the Quick Change site-directed *in vitro* mutagenesis method.

Reactant	Temperature and cycle numbers	Time
Initial denaturation	95 °C	1 min.
Denaturation	95 °C	30 sec
Annealing	60 °C	1 min.
Extension	72 °C	14 min.
Go to cycle	2	
Cycle number	16	
Hold at	4 °C	

Pfu synthesizes 2 kbp DNA/min.

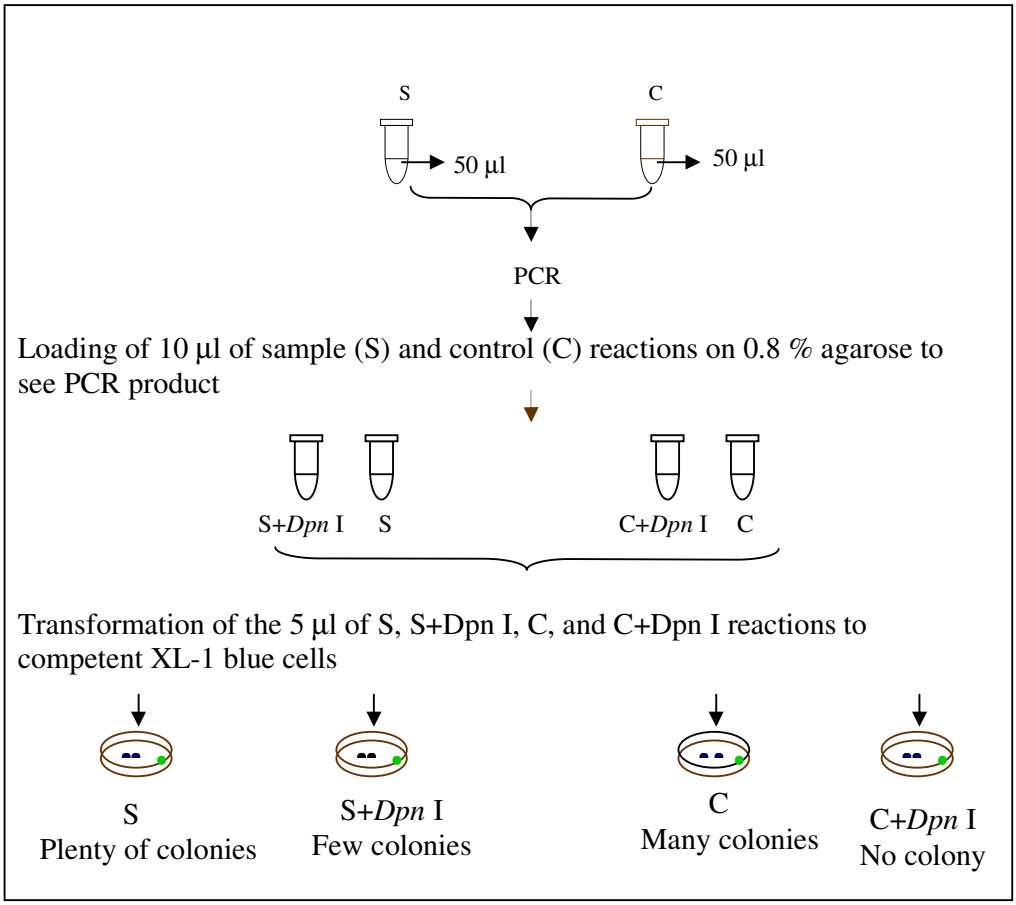

Figure 2.5: Strategy for selecting mutagenized transformants.

2.2.9 DNA Sequencing

To ensure that unintended mutations are not responsible for the observed phenotypes and to see desired mutations, pMOZIS333A, pMOZIS340A, pMOZIT350A, pMOZIN390A and pMOZIT396A DNAs were partially sequenced (0.6 kbp part of the 2.8 kbp *NO'* insert DNA fragment of pOX15) using the primer 578-F (5'- GGT GGGC CTA TCT GAT CG- 3') by MWG-BIOTECH AG (Germany) and Iontek (Istanbul).

2.2.10 Construction of pMOZII

Because sequencing of the five 2.8 kbp *NO*' fragment as a whole will be expensive and time consuming, first the 2.8 kbp *NO'* insert was checked by DNA strider program to find suitable restriction enzyme sites with the aim of producing smaller fragments. It was found that *BsaA*I RE cuts 2.8 kbp insert two times, resulting in a 0.6 kbp smaller and convenient fragment, while cutting the vector once. In this situation, to replace 0.6 kbp fragment of pMOZI with that of pMOZI* (containing mutation) would be impossible, therefore the 2.8 kbp *NO'* fragment needed to be cloned into the vector having restriction site for *Xho*I. It was found that pACYC177 vector DNA, 4.0 kbp, is a good vector for this purpose (Affix G).

To clone 2.8 kbp *NO*' fragment into *Xho*I site of pACYC177 vector, pACYC177 DNA was digested with *Xho*I at 37 ºC for two hours (Figure 2.6). *Xho*I digested sample DNA was dephosphorylated with calf intestine alkaline phosphatase (CIAP, MBI Fermantase) to prevent self ligation of linear vector during the ligation reaction for 1 hour at 37 ºC. Digested and undigested DNAs were separated on 1% agarose gel. The 4.0 kbp linear vector was isolated from the agarose gel by QIAquick gel extraction kit. The *NO*' fragment was inserted into *Xho*I site of pACYC177 vector at 22 ºC overnight (ON) (Figure 2.7). 5 µl of ligation mix was transferred into $CaCl_2$ treated HB101 cells. Transformants were selected based on ampicillin resistance and kanamycin sensitivity. The new clone was named as pMOZII/HB101, 6.8 kbp in size.

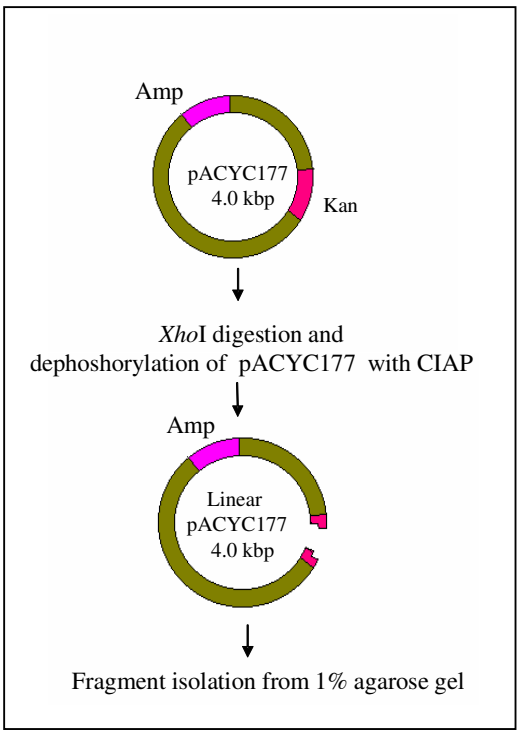

Figure 2.6: Linearization of pACYC177 vector.

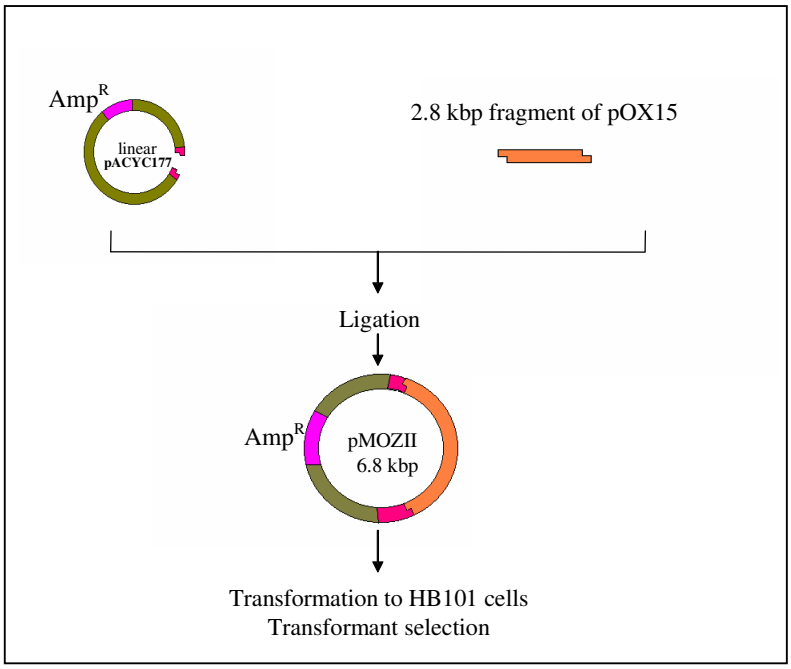

Figure 2.7: Preparation of pMOZII vector for subcloning.

2.2.11 Replacement of the 0.6 kbp *N*' Fragment with the mutated one

To replace the 0.6 kbp fragment of pMOZII with that of the mutant (pMOZI*, corresponding one of the five mutants), pMOZI* and pMOZII DNAs were digested with *Bsa*AI (Figure 2.8 and 2.9) respectively. Before separation of fragments on the agarose gel, *Bsa*AI digested sample was dephosphorylated by CIAP to prevent self ligation of vector. Then fragments obtained from both of the digested samples were separated on a 1 % agarose gel. The 0.6 kbp mutated fragment from pMOZI*s and the 6.2 kbp fragment from pMOZII were isolated from agarose gel by QIAquick gel extraction kit. The 0.6 kbp mutated fragment was inserted into *Bsa*AI site of the 6.2 kbp vector at 22 ºC for two hours (Figure 2.10). Finally 5 µl of the ligation mixture was transformed into HB101 cells. Transformants were selected as based on the size of the clone, 6.8 kbp, and ampicillin resistance and kanamycin sensitivity phenotypes.

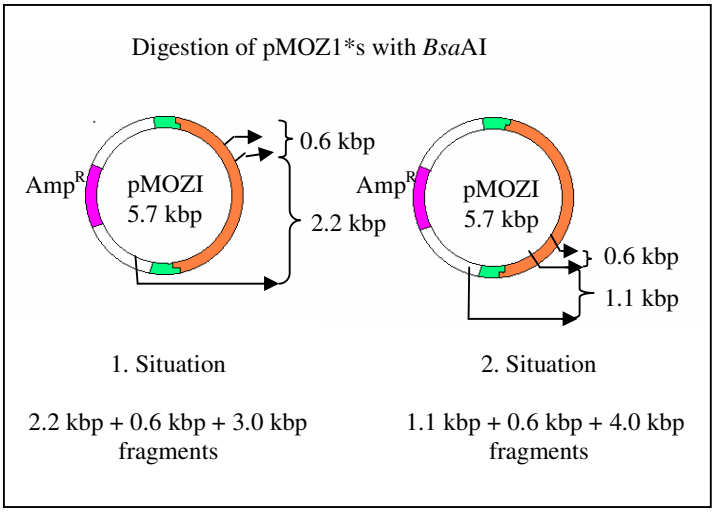

Figure 2.8: Digestion of pMOZI* DNA with *Bsa*AI.

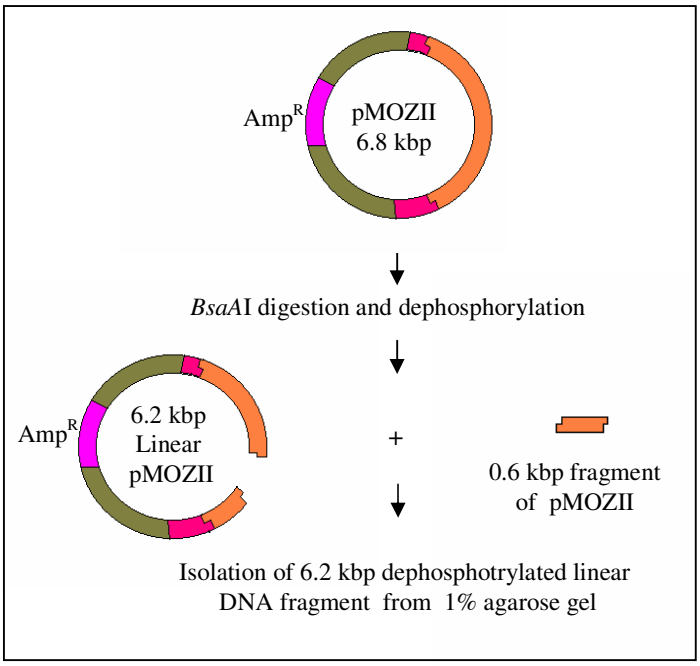

Figure 2.9: Digestion of pMOZII with *Bsa*AI.

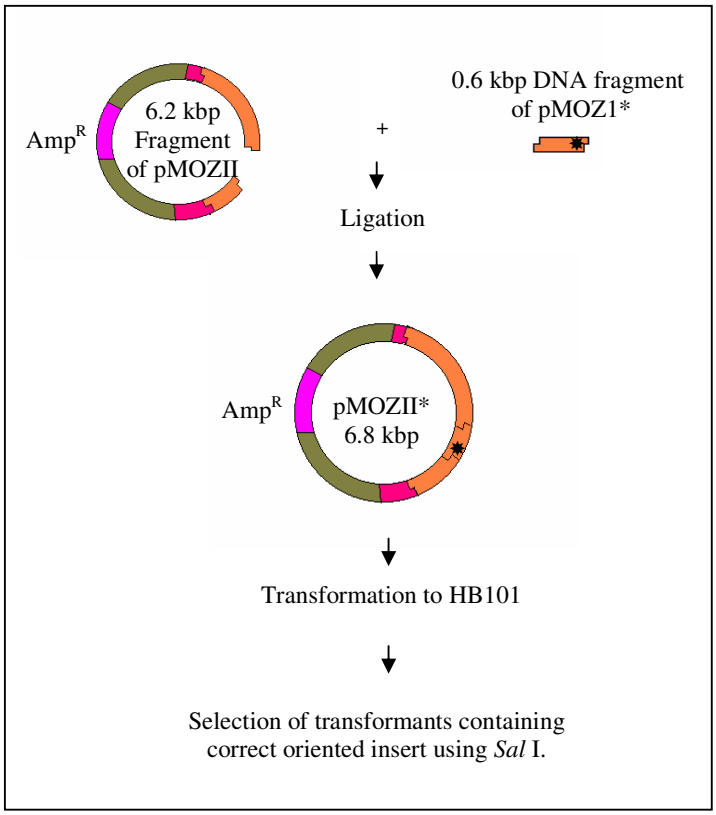

Figure 2.10: Replacement of the 0.6 kbp pMOZII fragment with that of pMOZI*. Sign "*" corresponds to one of the target mutations, S333A, S340A, T350A, N390A and T396A.

2.12 Control of the 0.6 kbp Insert Orientation

Since insert and vector were digested with *Bsa*AI, 0.6 kbp fragment could be inserted into vector in two orientations. To select the clone that have correct oriented insert, plasmid DNAs were isolated from three transformants and digested with *Sal*I at 37 C for 2 hours. *Sal*I cuts once vector and once insert resulting 1.5 kbp and 5.3 kbp fragments if insert is correct oriented and 1.1 and 5.7 kbp fragments if insert is wrong oriented (Figure 2.11). The new clones each of

which contains one of the five desired mutations were saved and designated as HB101/pMOZIIS333A, HB101/pMOZIIS340A, HB101/pMOZIIT350A, HB101/ pMOZIIN390A and HB101/pMOZII T396A at -80 ºC.

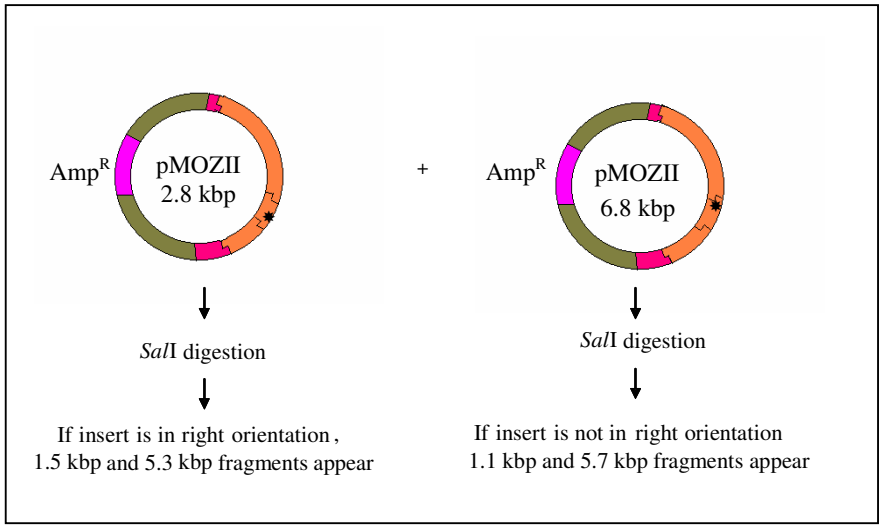

Figure 2.11: Control of the 0.6 kbp insert orientation. The pMOZII* DNA was digested with *Sal*I to select transformant having correct oriented insert.

2.2.13 Replacement of the 2.8 kbp *NO*' Fragment with the Mutated One

To replace 2.8 kbp fragment of pOX15 with the 2.8 kbp mutated insert that contains one of the five desired mutations, pMOZII*s plasmid DNA containing one of the desired mutations were digested with *Xho*I restriction enzyme. Resulting fragments, 2.8 kbp and 4.0 kbp fragments were separated on 1 % agarose gel by electrophoresis (Figure 2.12). Then 2.8 kbp fragment was isolated from the agarose gel using QIAquick gel extraction kit and also amount of the DNA was determined by loading of 1 µl DNA on 1% agarose gel. On the other

hand, 15.3 kbp pOX15 DNA that contains 4.7 kbp structural gene of cbb_3 oxidase was also digested with *Xho*I restriction enzyme at 37 ºC for two hours and then *Xho*I digested vector was also dephosphorylated with CIAP to prevent self ligation of vector. *Xho*I digested and dephosphorylated DNA sample was loaded on 1 % agarose gel to separate 12.5 kbp and 2.8 kbp fragments. 12.5 kbp fragments were isolated from agarose gel and amount of the 12.5 kbp fragment was determined. Gel purified 2.8 kbp fragment was inserted in 12.5 kbp dephosphorylated vector in 20 µl volume on ice overnight and at 22 ºC for 30 minutes (Figure 2.13). Then half of the ligation mixes were transformed into 100 µl HB101 cells to increase transformation efficiency. Transformants were selected based on clone size, 15.3

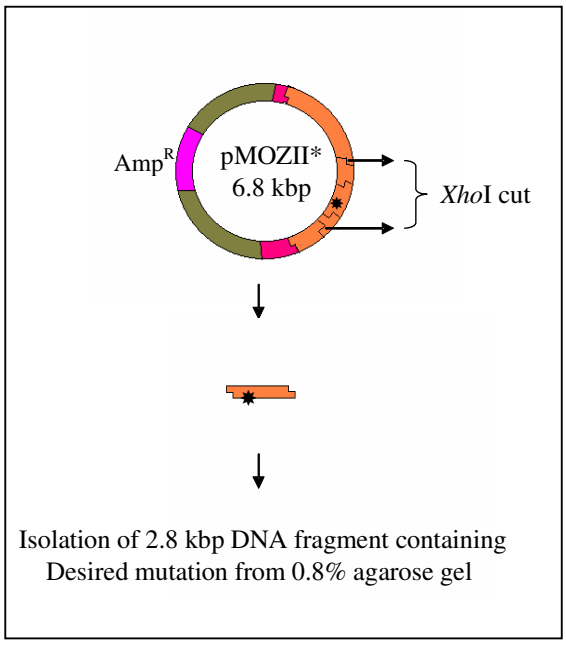

Figure 2.12: Digestion of pMOZII* with *Xho*I.

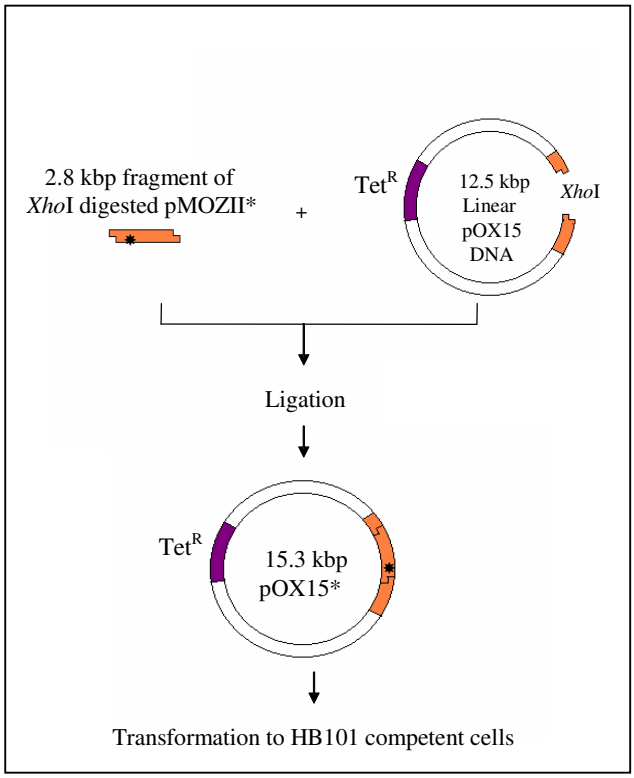

Figure 2.13: Replacement of the 2.8 kbp parental fragment of pOX15 with that of the pMOZII*.

2.2.14 Control of the 2.8 kbp Insert Orientation

To select the pOX15*clones that have correct oriented insert, plasmid DNAs were isolated from three transformants then they were digested with *Hind*III RE at 37 ºC for 1 hour. *Hind*III cuts once vector and once insert resulting 3.6 kbp and 11.7 kbp fragments if insert is correct oriented but 2.8 kbp and 12.5 kbp fragments if the insert is wrong oriented (Figure 2.14). The new clones each of which contains one of the five desired mutations were saved and named as HB101/pOX15S333A, HB101/pOX15S340A, HB101/pOX15T350A, HB101p/OX15N390A and HB101/pOX15T396A at -80 ºC.

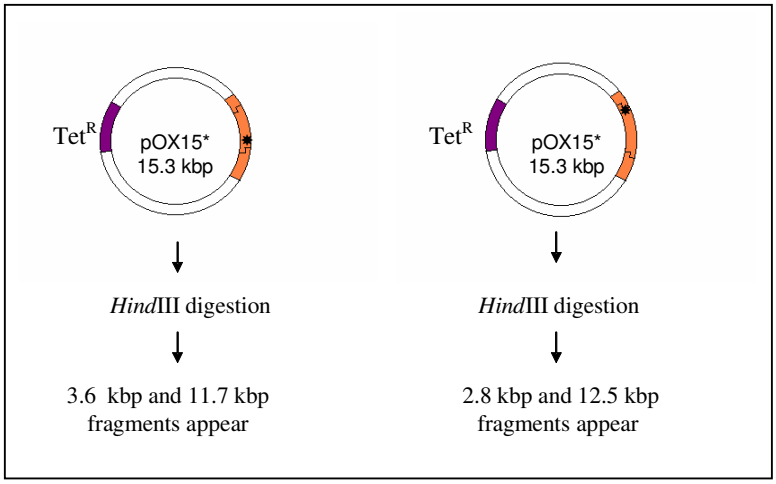

Figure 2.14: Digestion of pOX15* with *Hind*III.

2.2.15 Conjugation (Triparental Mating)

The most efficient and generally applicable system for introducing plasmid DNA into *R. capsulatus* is conjugation. The *E. coli* donors contain chromosomal copies of the trans-acting elements that mobilize *oriT*-containing plasmids. The most commonly used vector system for complementation is those based on the RK2 replication. Plasmid pRK404 and pRK415 are used for such purposes in both *R. sphaeroides and R. capsulatus*. RK2 plasmids are stable in *R. capsulatus* as long as selective pressure is maintained (Figure 2.15).

R. capsulatus GK32 strain, lacking *ccoNOQP* gene, complemented with five recombinant plasmids in *E. coli* strain, HB101, and each of which containing desired mutation by using Triparental Mating procedure as described in [Ditta et al., 1980]. Two days before the cross, 1 ml Med A + kanamycin was inoculated with single colony of the recipient *R. capsulatus* GK32 strain, which lacks *ccoNO'*

(ccoNO'::kan), from a fresh plate and incubated overnight (18-24 hs) at 35 ºC with shaking. The day before the cross 1 ml culture was added to 10 ml Med A + kanamycin and incubated overnight (16-18 hs) at 35 ºC. At the same day, 2 ml LB + kanamycin culture was inoculated directly from the glycerol stock of the helper strain pRK2013/HB101. 2 ml LB+ tetracycline or kanamycin, depending on the vector, was inoculated with the donor strain pOX15*/HB101 from single colony on a fresh stock plate and grown overnight (12-16 hs) at 37 ºC with shaking. The required numbers of MedA plates (number of crosses plus a control) were dried in the incubator for 30 min. The cell density of each culture was determined by using the following conditions [Ditta et al., 1980].

R. capsulatus: $7.5x10^8$ cells/ml at $OD_{630}= 1$

E. coli : $5.0X10^8$ cells/ml at $OD_{600}= 1$

It is best to take OD at 1/10 dilution so that the value is well below 1. The cells were centrifuged for 10 min at 5000 rpm at RT. The cells were washed twice with 1 ml Med A to remove all antibiotics. The cells were resuspended in a volume of Med A that the final density was 10^{10}/ml. In the middle of Med A plate, 100 µl of recipient *R. capsulatus* was pipetted; to the spot 20 µl of each and donor *E. coli* were added and mixed well. Plates were waited for absorption of the spot into the agar completely before placing it in the incubator for overnight. The control plates made with just the recipient/helper and recipient/donor in the spot as the control. Approximately 24 hs later, the cells were collected from each spot in 1 ml MedA and transferred to eppendorf tubes. The cells were centrifuged for 1 min at 13000 rpm at RT. The supernatant was discarded, and the cells were washed in

1 ml Med A. Washed cells were resuspended in 400 µl Med A. 10 µl and 100 µl of the cell suspension were plated on Med A plates with appropriate antibiotics; as for the control, 100 µl of the recipient/helper and recipient/donor were plated on a selection plate were incubated for 2-3 nights (Figure 2.16). At least 4 transconjugants from each cross were purified by picking from the center of well-separated colonies and streaked on MPYE or Med A plate with appropriate selection.

Thus the pOX15* plasmid DNA, which is in HB101 strains, was transferred into GK32 strain of *R. capsulatus* that lacks *ccoNOQP* structural gene of cbb_3 oxidase by three parental mating in the presence of HB101/pRK2013 cells. Transconjugants were selected based on tetracycline resistance. Transconjugants were selected and kept for further analysis such as cbb_3 oxidase respiratory phenotype by NADI staining.

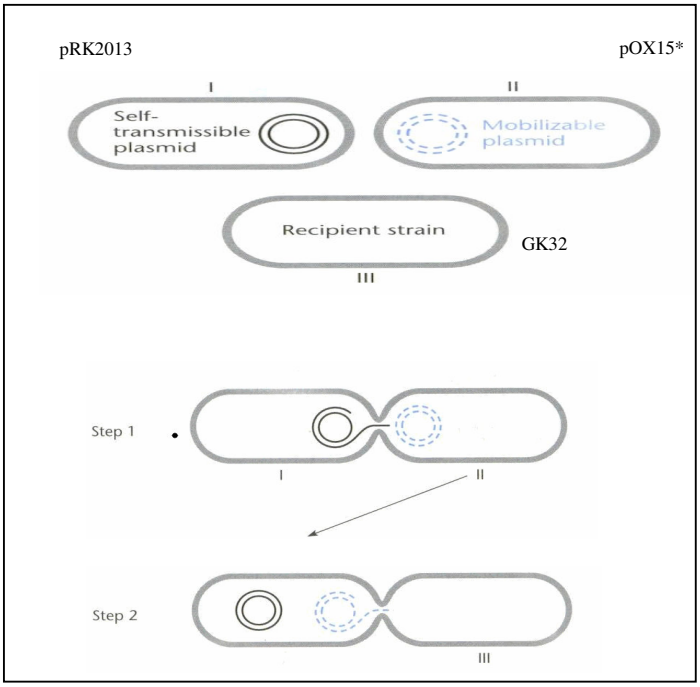

Figure 2.15: Triparental mating among the pRK2013, pOX15* and GK32.

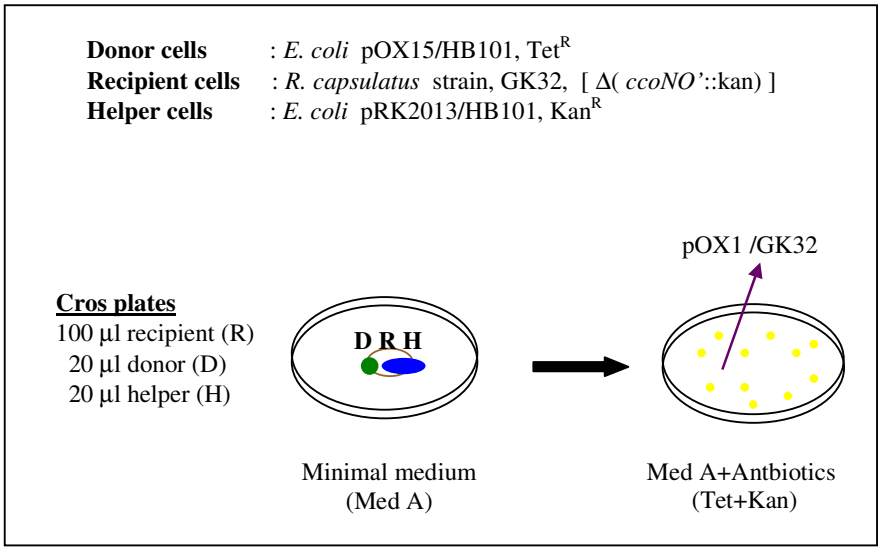

Figure 2.16: Complementation of the GK32 strains of *R. capsulatus* with pOX15* Mutants: pOX15S333, pOX15S340, pOX15ST350, pOX15N390 and pOX15T396.

2.3 Analysis of the Cytochrome *cbb*$_3$ Oxidase Activity and Assembly

2.3.1 NADI Test

The presence of only one-type of cyt *c* oxidase in *R. capsulatus* allows efficient utilization of the NADI (α-Naphthol + DMPD + O_2 → Indophenol Blue + H_2O) reaction [Keilin, 1966] for identification of mutation affecting cyt *cbb*$_3$ oxidase activity. pOX15S333A, pOX15S340A, pOX15T350A, pOX15N390A and pOX15T396A plasmids were introduced into GK32 mutants *cbb*$_3$ type oxidase of which was inactivated, Δ(*ccoNO'*::kan) by triparental mating. Transconjugants were tested for their cyt *c* oxidase activity by being overlaid with a 1:1 (v/v) mixture of 35 mM α-naphthol in ethanol and 30 mM *N*,*N*-dimethyl-*p*-phenylene diamine in H_2O [Keilin, 1966]. Colonies grown on MedA medium turn blue within 30 seconds if they contain an active cyt *cbb*$_3$ oxidase.

2.3.2 Chromatophore Membrane Protein Preparation

Three days before the chromatophore isolation, 1 ml MPYE+ tetracycline is inoculated with a single colony of the MT1131, GK32, GK32/pOX15, GK32/pOX15S333A, GK32/pOX15S340A, GK32/pOX15T350A, GK32/pOX15-N390A and GK32/pOX15T396A strains of *R. capsulatus* from a freshly streaked plate and incubated over night (18-24 hs) at 34 °C with shaking at 150 rpm. Next day, 1 ml culture is added to 10 ml MPYE+ tetracycline and incubated overnight (16-18 hs) at 34 °C. The day before starting chromatophore isolation, 10 ml cultures were transferred to 250 ml MPYE + tetracycline medium in 1lt flasks

shaking at 150 rpm and incubated overnight (16-18 hs) at 34 °C. Streaking from cultures was made appropriate control to check their NADI phenotypes. Optic density of the cultures at 630 nm was checked periodically. When growth of cultures was appeared to expected value, ≥ 0.6 at $OD_{600,}$ all cultures were kept on ice until chromatophores to be isolated.

The cells were centrifuged at 5000 rpm and at 4 °C for 15 minutes. The supernatants were discarded, and cells were resuspended in 10 ml 50 mM MOPS/ 1 mM KCl buffer (pH: 7). Resuspended solutions centrifuged again at 5000 rpm and 4 ºC for 15 minutes and supernatants were discarded. Washing process was repeated twice. Before breaking the cells, pellets were resuspended in 10 ml 50 mM MOPS/1 mM KCl solution containing, RNAse, DNAse (10 mg/ml), 1 mM $MgCl_2$ and 1 mM PMSF (Phenylmethanosulphonyl Floride) which was added just before breaking the cells and mixed well. Then cells were broken by passing through a French press at 18000 psi (approximately 1100 on high ratio). This process repeated two times. The broken cells were centrifuged to remove the cells membrane debris at 15 000 rpm for 45 minutes. Supernatats were transferred to ultracentrifuje tubes and pellets were discarded. The membrane fraction was obtained by ultra-centrifuging at 45 000 rpm (100 000 g) and 4 ºC for two hours and supernatans were kept at -20 ºC. To distingush cytoplasmic and integral membrane proteins, membrane fragments were then washed and resuspended gently in 10 ml 50 mM MOPS/ 1 mM KCl buffer with help of the paint brush and then centrifuged at 45 000 rpm and 4 °C for two hours. Finally, pellet was dissolved in 400 µl 50 mM MOPS/1 mM KCl buffer contaning 1 mM PMSF and kept at -80 °C.

2.3.3 Determination of Amount of the Membrane Protein by Lowry Assay

Protein concentration was determined by Lowry method with BSA as the standard protein [Lowry et al., 1951]. To prepare standart BSA protein solution, 1 g solid BSA (Bovin Serun Albumin) dissolved in 1 ml ddH_2O and, 20, 40, 60, 80, 100 µl protein solutions from 1µg/µl stock BSA were added into five appendorf tubes, respectivelly and final volume completed to 200 µl by adding required amount of 1% SDS/0.1 N NaOH. 10 µl chromatophore samples from each mutant was dissolved in 990 µl MOPS. Then 50 µl and 100 µl diluted chromatophore samples from each mutants were mixed with 150 µl and 100 µl 1 % SDS/0.1 N NaOH solution respectively and than reagent E (appendix) was added to BSA standart proteins and chromatophore memebrane proteins and they incubated at RT for 10 minutes.

Then 100 µl 1 N Folin and Ciocalteu's Phenol reagent was added to all protein samples and they were incubated at RT for 30 minutes. The curve was made by the mesurement of the OD (Optic Density) of the standart BSA samples concentration of which are different at 660 nm (Figure 2.17). The OD of the chromatophore samples were determined at OD_{660} nm and amout of the chromatophore vesicles vere determined by the following formula: y =0.0026x +0.0444, (y is absorbance and x is amont of the protein as a µg/ml).

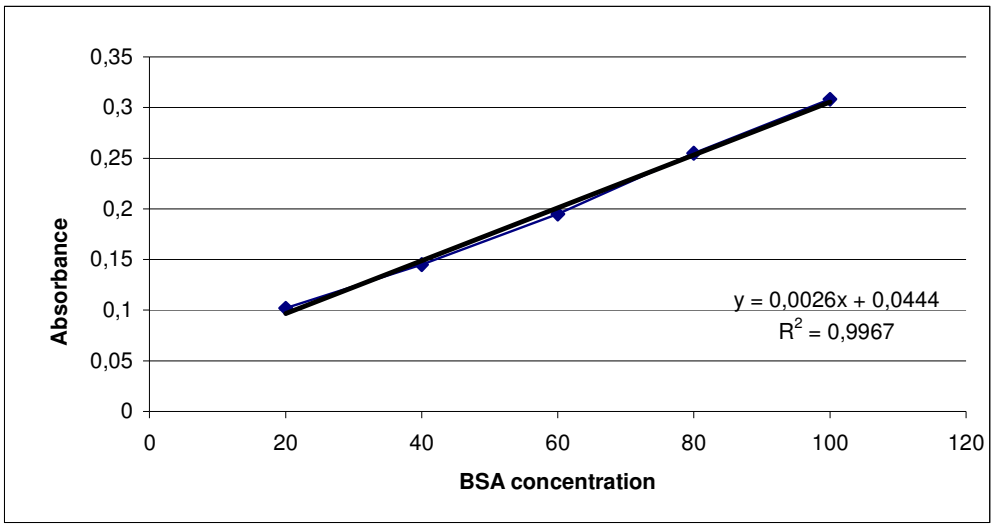

Figure 2.17: Determination of amount of the chromatophore membrane protein by Lowry method. The concentrations of the chromatophore from mutants were determined by using this curve and equation, y =0.0026x+0.0444.

2.3.4. The 16.5 % Schägger Type SDS-PAGE Gel

Schägger-type sodium dodecyl sulfate SDS-PAGE were performed using 16.5% acrylamide Tris-Tricine gel as described in [Schägger et al., 1987]. Gel was prepared by using fallowing solutions; Acrylamide-Bis Acrylamide mixture (49.5% T, 3%C), Gel buffer (3M Tris, 0.3% SDS, pH 8.45), Glyserol, H_2O, Ammonium persulphate (APS, 10%) and TEMED, Tetrametylethylendiamine (Table 2.5). First separating, running gel, was prepared then after 45 minutes staking gel was poured in gel apparatus. After polymerization of the gel, it takes at least two hours, samples were loaded. Before loading the chromatophore samples on SDS-PAGE, equal volume of the loading dye (Appendix C) was added to samples and β-Mercaptoethanol (MBE) was added just prior to use and they are incubated at 37 °C for five minutes. Usually 100 µg chromatophore protein from

MT1131 (wild type), GK32 (negative control mutant), GK32/pOX15 (positive control mutant) and pOX15*s (generated mutant) were loaded on 16.5 % Schagger type SDS-PAGE and runed first at 30V for 1 hour than at 90-120V for 20-24 hs. To indicate mobility of the proteins on SDS-PAGE, Kaleidoscope Prestained Standarts (BIO-RAD, # 161-0324) was used.

Table 2.5. The preparation of the 16.5 % Schägger type SDS-PAGE.

Gel content	**Separating Gel**	**Staking Gel**
Glycerol	5.3 g	-
Acrylamide/Bis Acrylamide	13.3 ml	1.0 ml
Gel Buffer	13,3 ml	3.1 ml
dH_2O	9.0 ml	8.4 ml
10% APS	130 µl	100 µl
TEMED	20 µl	10 µl
Total Volme	40 ml	12.5 ml

2.3.5 Staining of the SDS-PAGE Gel with TMBZ

Schägger type SDS-PAGE gel was washed with 0.25 M Na- acetate buffer, pH 5 for 20 minutes. Washing of the gel was repeated three times. Mean time 45 mg TMBZ, 3, 3', 5, 5' Tetrametyl Benzidine, was dissolved in 30 ml methanol (6.3 M) and mixed with 70 ml 0.25 M Na-Acetate (dissolving takes place 20- 30 minutes, covered with alimunium foil) Then gel was placed in TMBZ solution and washed it by shaking gently for 1 h in dark (TMBZ percipiates on the gel as white powder). Finally, 1240 µl 30% Hydrogen peroxide, H_2O_2, was added (to 30 mM) and gel was incubated for more 10-30 minutes at RT. After bands were appered, the solution was poured off and gel was covered with Isoproponol and 0.25 M sodium acetate mix (3:7 ratio). Photograph of the gel was taken. Gels are stained to determine the peroxidase activity of heme and heme proteins by a 6.3 mM TMBZ (3, 3'5, 5'-tetramethylbenzidine) as described in [Thomas et al., 1976]. Heme staining of the membrane bound *c*-type cyts indicates that whenever ccoO and ccoP were present.

RESULTS

3.1. Construction of a pMOZI as Template DNA

The structural gene of cbb_3-type oxidase, *ccoNOQP*, is 4.7 kbp long [See Figure 2.1]. The *ccoNOQP* gene has been cloned into 10.6 kbp pRK404 vector and it was designated as a pOX15, 15.3 kbp [Koch et. al., 1998]. Since pOX15 DNA is very sensitive to heat, it is degraded during the PCR process. Moreover, the size of the pOX15 DNA is too large to be used as a template DNA in PCR based site-directed mutagenesis procedure. Therefore pOX15 DNA is not suitable to mutagenize desired amino acids by PCR-based site-directed mutagenesis.

To create convenient template DNA containing target genes of cbb_3 type oxidase, 50 µl (5µg) pOX15 DNA and pBluescript plasmid DNA were digested with *Xho*I restriction enzyme and resulting fragments, 2.8 kbp and 12.5 kbp from pOX15 and 2.9 kbp linear vector from pBluescript, were separated by loading all of the digested samples on 1% agarose gel (Figure 3.1 A and B). 2.8 kbp fragments from pOX15 DNA as an insert and 2.9 kbp pBluescript fragments as vector were isolated and purified from gel using Qiagen DNA Purification Kit. Amount of the purified fragments was determined by loading and electrophoresing them on 1% agarose gel (Figure 3.1 C). 2.8 kbp fragment was inserted into *Xho*I restriction site of the pBluescript vector, 2.9 kbp (Affix G). 5 µl ligation reaction was transformed into $CaCl_2$ treated XL1-Blue cells.

Transformants were selected based on ampicillin resistance, also by X-gal and IPTG. The clone was also tested with *Sac*I, *Xho*I and *Bsa*AI. After digestion of 5.7 kbp pMOZI DNA with *Sac*I, *Xho*I and *Bsa*AI REs, 5.7 kbp pMOZI linear DNA fragment; 2.8 and 2.9 kbp fragments; and 0.6 kbp, 1.1 kbp and 4 kbp fragments were generated, respectively (Figure 3.2). Thus, the new clone was called as pMOZ1, 5.7 kbp in size (Figure 3.3).

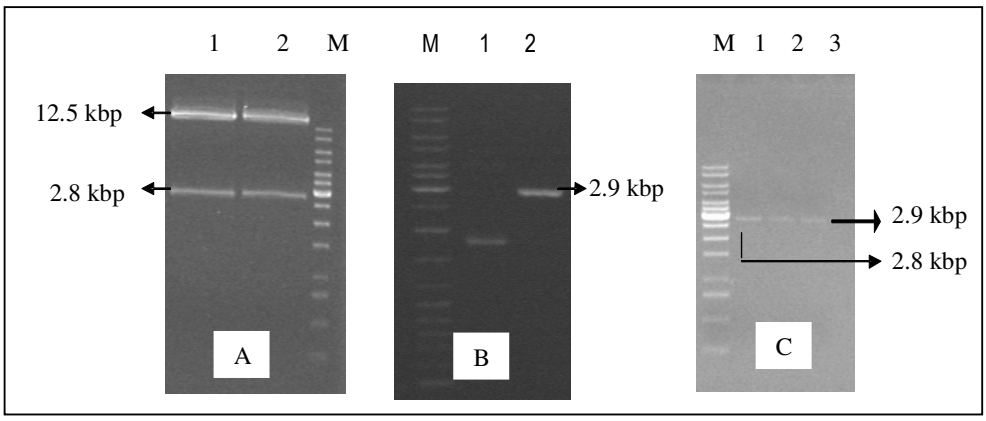

Figure 3.1: Isolation and purification of *Xho*I digested pBluescript DNA on 1% agarose gel. **A**. Digestion of pOX15 with *Xho*I and separation of 12.5 kbp and 2.8 kbp fragments. **B**. Digestion of pBluescript plasmid with *Xho*I RE and separation of 2.9 kbp linear fragments. **C**. Determination of the gel purified 2.9 kbp pBluescript vector and 2.8 kbp insert fragments. Line 1 contains 20 ng/µl dephosphorylated 2.9 kbp vector. Line 2 and line 3 have 15 ng/µl 2.8 kbp inserts.

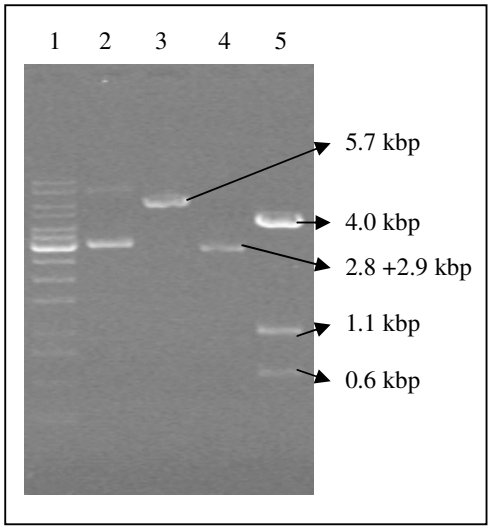

Figure 3.2: Testing the pMOZI clone with *Sac*I, *Xho*I and *BsaA*I. Line 1 has a marker; line 2 contains uncut pMOZI DNA; line 3 contains *Sac*I digested 5.7 kbp linear pMOZI DNA; line 4 has *Xho*I digested 2.9 and 2.8 kbp fragments. Line 5 has a 4.0 kbp, 1.1 kbp and 0.6 kbp *BsaA*I digested pMOZI fragments.

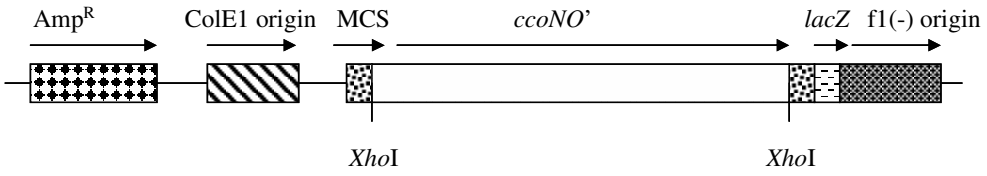

Figure 3.3: Map of pMOZI, 5.7 kbp. The pMOZI was constructed by ligation of the 2.8-kbp *Xho*I fragment of pOX15 into the *Xho*I site of pBluescript SK+ DNA, 2.9 kbp.

3.2. Substitution of Target Amino Acids by Alanine

The pMOZI DNA was used as template DNA to substitute five target amino acids, serine (S333), serine (S340), threonine (T350), asparagine (N390) and threonine (T396) for alanine by Quick Change^{TM} site-directed mutagenesis protocol. Two types of PCR reactions were prepared for each mutation, sample reaction and control reaction which does not contain *Pfu* polymerase enzyme. Following temperature cycling, 10 µl PCR products from sample and control reaction for five amino acids, S333, S340, T350, N390 and T396, were loaded on 1% agarose gel and electrophorased for 1 h to see PCR product. The PCR products of the S333 (Figure 3.4), S340 (Figure 3.5), T350, N390 and T396 (Figure 3.6) sample reactions were visible on agarose gel. PCR products were treated with *Dpn*I, specific for methylated and hemimetylated DNAs, to digest the parental template DNA and to select mutated and PCR synthesized DNA. Following PCR product digestion, the *Dpn*I treated PCR product was transformed into XL1-Blue cells. It was found that there was no transformant for S340 mutation although there were many transformants for other mutations. Sample and control reactions before and after *Dpn*I incubation were loaded on agarose gel (Figure 3.6). After digestion of PCR products with *Dpn*I, 5 µl samples and control PCR reactions from S340 were transformed into XL-1 blue cells. Finally, DNAs were isolated from at least four transformants for each mutation, S333, S340, T350, N390 and T396, to determine desired mutation by sequencing (Table 3.1).

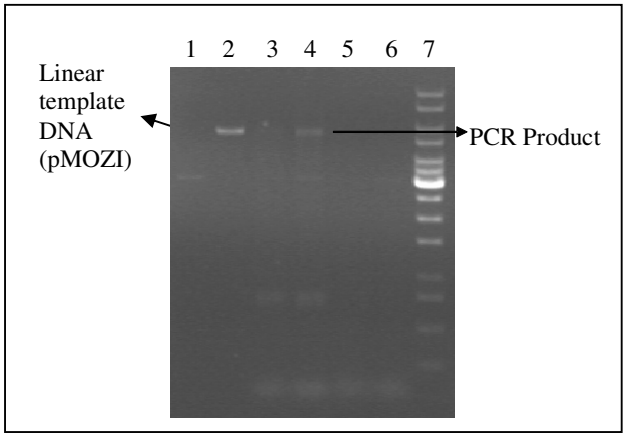

Figure 3.4: pMOZIS333 and pMOZIS340 PCR products (10 µl) loaded on 1 % agarose gel. Line 1: circler pMOZI DNA; line 2: linear pMOZI DNA; line 3: pMOZIS340 sample reaction; line 4: pMOZIS333 sample reaction; line 5: pMOZIS340 control reaction; line 6: pMOZIS333 control reaction.

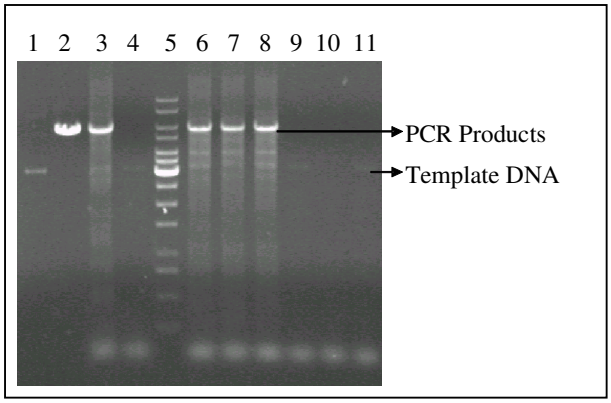

Figure 3.5: pMOZIS340 PCR product (10 µl) loaded on 1 % agarose gel. Line 1: circler pMOZI DNA; line 2: linear pMOZI template DNA; Line 3: pMOZIS340 sample reaction; Line 4: pMOZIS340 control reaction; line 5: marker; line 6: pMOZIS340 sample reaction; line 7: *Dpn*I added S340 sample reaction; line 8: pMOZIS340 sample reaction without *DpnI*. Line 9: pMOZIS340 control reaction; line 10: *Dpn*I added pMOZIS340 control reaction; line 11: pMOZIS340 control reaction without *Dpn*I.

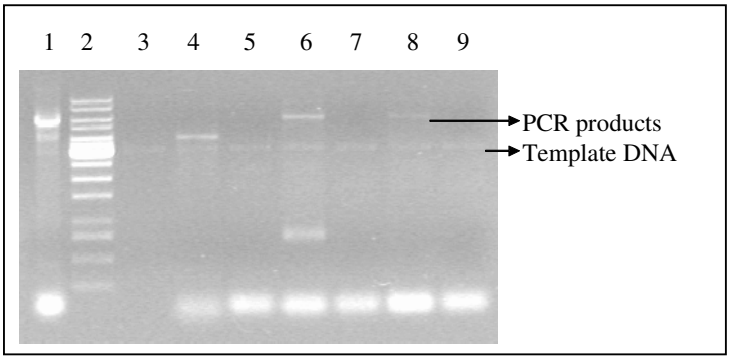

Figure 3.6: pMOZIT350, pMOZIN390 and pMOZIT396 PCR product (10 µl) loaded on 1 % agarose gel. Line 1: pMOZIT396 sample reaction; line 2: marker; line 3: pMOZI template DNA; Line 4: pMOZIS340 sample reaction; Line 5: pMOZIS340 control reaction; line 6: pMOZIT350 sample reaction; line 7: pMOZIT350 control reaction; line 8: pMOZIN390 sample reaction; line 9: pMOZIN390 control reaction. M: Marker, R: sample reaction, C: control reaction.

Table 3.1: DNAs prepared from different transformants for sequencing.

S333		S340	T350	N390	T396
pMOZIS333-1	**pMOZIS333-5**	**pMOZIS340-1**	pMOZIT350-1	pMOZIN390-1	pMOZIT396-1
pMOZIS333-2	pMOZIS333-6	pMOZIS340-2	**pMOZIT350-2**	pMOZIN390-2	pMOZIT396-2
pMOZIS333-3	pMOZIS333-7	pMOZIS340-3	pMOZIT350-3	**pMOZIN390-3**	**pMOZIT396-3**
pMOZIS333-4	pMOZIS333-8	pMOZIS340-4	pMOZIT350-4	pMOZIN390-4	pMOZIT396-4

The plasmids with desired mutation were bolded

3.3 Construction of pMOZII Vector to Replace Mutated Fragments

Since sequencing of the five 2.8 kbp *NO*' fragment would be expensive and time consuming, before starting to sequencing, the 2.8 kbp *NO'* insert was checked by DNA strider program to find restriction site(s) that produce smaller suitable fragment from 2.8 kbp NO' structural gene. It was found that *Bsa*AI cut 2.8 kbp insert two times, resulting 0.6 kbp smaller and convenient fragment, but *BsaA*I also cut vector once. In this situation to replace 0.6 kbp fragment of pMOZI with that of pMOZI* (containing one of the desired five mutations) would be impossible, so *NO'* fragment was subcloned into the 4.0 kbp pACYC177 DNA vector that has restriction site for *Xho*I and not for *Bsa*AI (Affix G). To clone 2.8 kbp *NO*' fragment of pOX15 into pACYC177 vector, pACYC177 plasmid DNA was digested with *Xho*I. Digested DNA samples were loaded on a 1% agarose gel and resulting 4.0 kbp linear fragments were separated (Figure 3.7.A) and 4.0 kbp linear vector DNA was isolated from 1% agarose gel. Then amount of the vector DNA was determined by loading 1µl of vector DNA, 40ng/µl (Figure 3.7 B). The 2.8 kbp *NO*' fragment was inserted into *Xho*I site of pACYC177 vector by ligation reaction at 22 ºC for overnight (ON) and 5 µl of ligation mix was transferred into $CaCl_2$ treated HB101 cells, *E. coli* strain. Transformants were selected based on kanamycin sensitivity. DNA from clone was also digested with *Sac*I and *Sal*I enzymes and expected fragments, 6.8 kbp pMOZII linear DNA and 5.3 kbp and 2.5 kbp fragments were determined (Figure 3.8). The new subclone was named as HB101/pMOZII, 6.8 kbp in size (Figure 3.9).

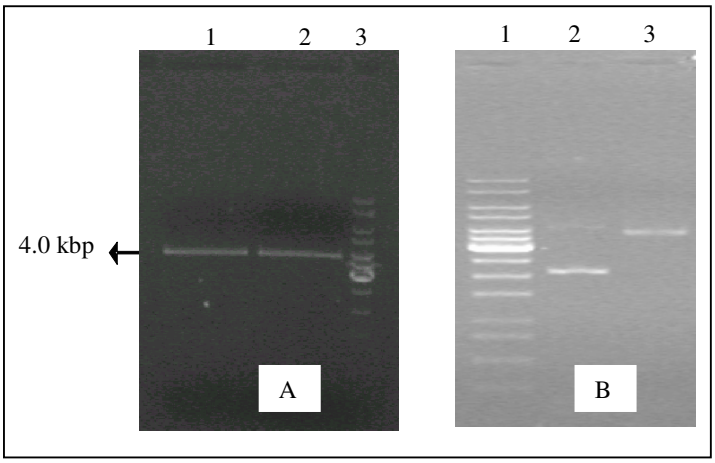

Figure 3.7: Purification of the *Xho*I digested linear 4.0 kbp pACYC177. **A**. Separation of linear 4.0 kbp vector on 1% agarose gel. Line 1 and line 2: *Xho*I digested 4.0 kbp linear pACYC177 DNA; line 3: marker. **B**. Determination of the amount of the gel purified pACYC177 vector. Line 1: marker; line 2: uncut pACYC177 DNA; line 3: linear pACYC177 DNA (40 ng/µl).

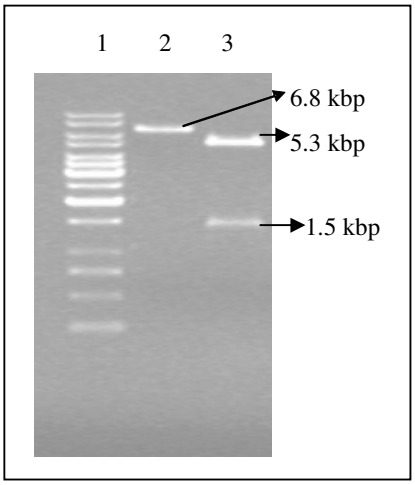

Figure 3.8: Digestion test of pMOZII DNA with *Cla*I and *Xho*I. Line 1: marker; Line 2: *Cla*I digested 6.8 kbp pMOZII DNA. Line 3: *Bsa*AI digested pMOZII DNA containing 5.3 kbp and 1.5 kbp fragments.

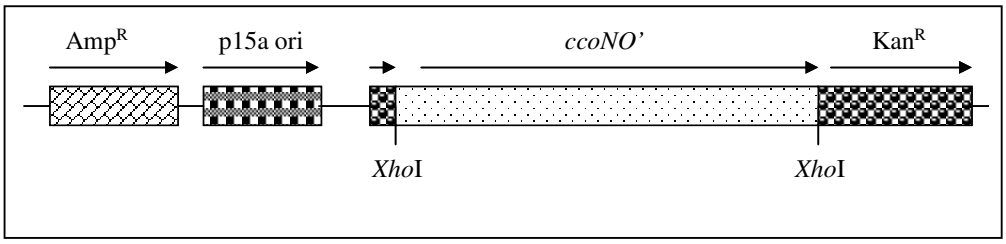

Figure 3.9: Map of pMOZII. The pMOZI DNA was constructed by ligation of the 2.8-kbp *Xho*I fragment of pOX15 into the *Xho*I site of 4.0 kbp pACYC177 DNA. Arrows shows the direction of the transcription.

3.4 Construction and Analysis of GK32/pOX15S333A Mutant

3.4.1 Sequencing of pMOZI333-5 Mutant

Plasmid DNA from pMOZ1S333-5 transformants was sequenced using primer named 578F 5' GGTGGCCTATCTGATCG 3' at Iontek Company, Istanbul. Sequence obtained from pMOZ1S333-5 plasmid DNA was compared with the sequence of the cbb_3 oxidase from gene data bank. It was found that the sequence has a desired mutation (GCC), it is long enough to see cloning site of *Bsa*AI (ACGT) and there is no mutation other than desired one. The mutated codon and restriction sites for *Bsa*AI are underlined (Figure 3.10 row 4, 1 and 5 respectively). The pMOZ1S333-5 clone was named as pMOZIS333A.

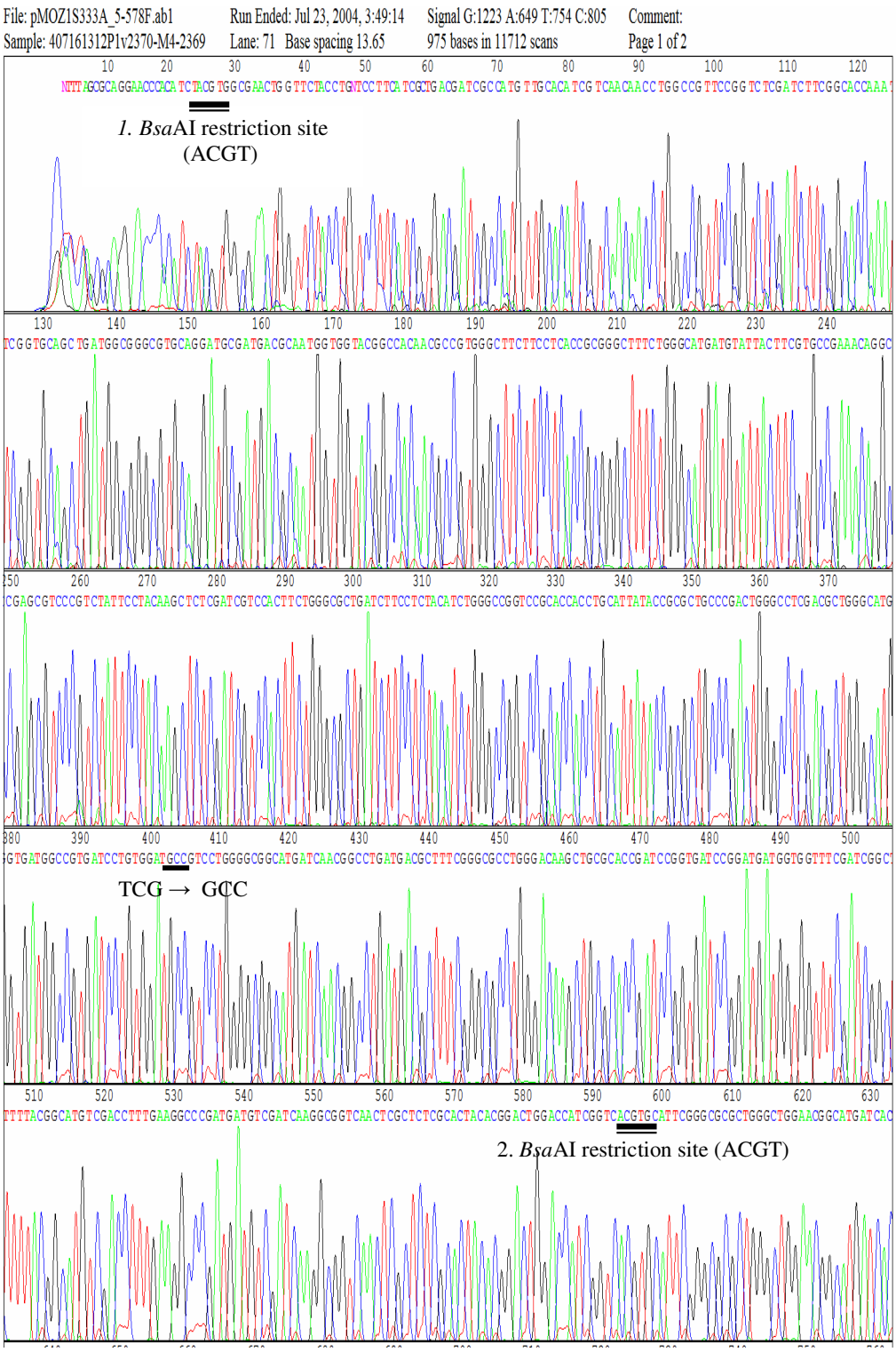

Figure 3.10: The partial sequence of pMOZIS333-5 transformant. The **TCG** codon was converted to **GCC** codon which is underlined.

3.4.2 Replacement of the 0.6 kbp Fragment of pMOZII with that of the pMOZIS333A

To replace 0.6 kbp fragment of pMOZII with that of pMOZI333A, pMOZII and pMOZIS333A DNAs were digested with *Xho*I. The *Xho*I digested pMOZII DNA sample was dephosphorylated with calf intestine alkaline phosphatase enzyme, CIAP, to prevent self ligation of the vector. *Xho*I digested pMOZII and pMOZIS333A DNA samples were loaded on 1% agarose gel and resulting fragments, 0.6 kbp, 1.1 kbp and 4.0 kbp fragments from pMOZIS333A (Figure 3.11.A-B) and 0.6 kbp and 6.2 kbp from pMOZII were separated (Figure 3.12.A-B). Then 6.2 kbp from pMOZII vector and 0.6 kbp insert fragments from pMOZIS333A were isolated from 1% agarose gel (Figure 3.12.C) and then 0.6 kbp mutated fragment was inserted into 6.2 kbp vector by incubating at 22 ºC for two hours. Finally 5 µl ligation mix was transformed into HB101 cells. Transformants were selected based on the size of the clone, 6.8 kbp in size.

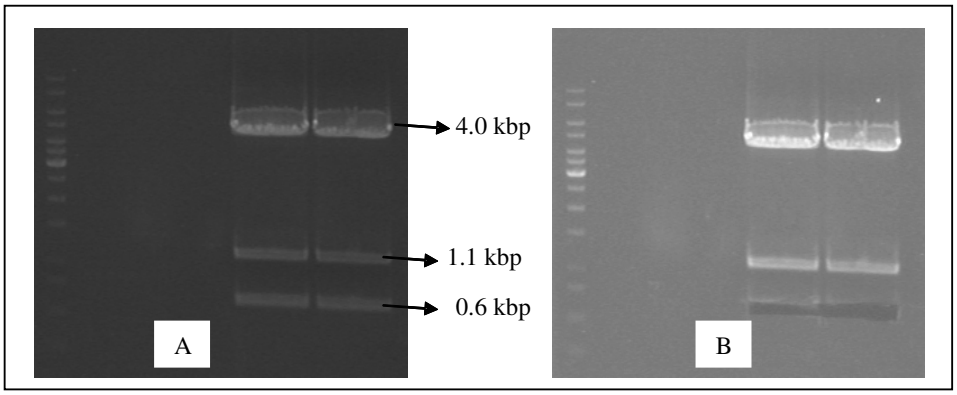

Figure 3.11: Isolation of 0.6 kbp fragment of *Bsa*AI digested pMOZIS333A. **A**. Separation of 4.0 kbp, 1.1 kbp and 0.6 kbp fragments of *Bsa*AI digested pMOZIS333A. **B**. Isolation of 0.6 kbp fragment from 1% agarose gel.

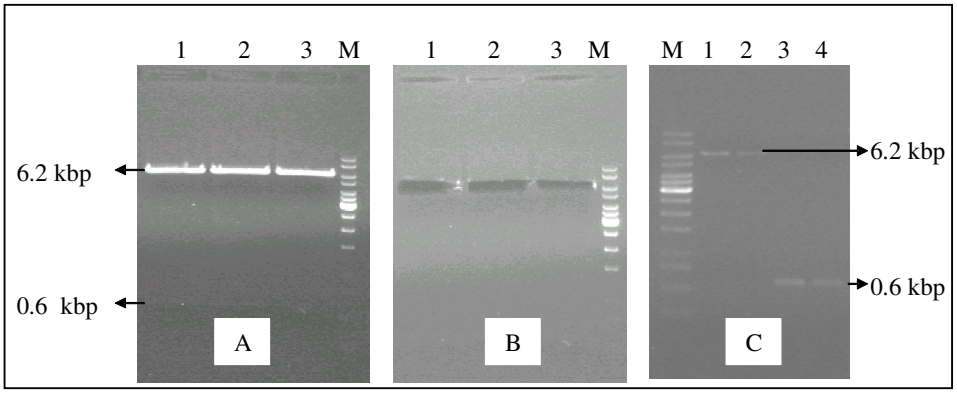

Figure 3.12: Isolation of the 6.2 kbp fragments of *Bsa*AI digested pMOZII DNA. **A**. It contains 6.2 kbp and 0.6 kbp fragments of *Xho*I digested pMOZII. **B** Isolation of the 6.2 kbp fragment of pMOZII from 1% agarose gel. **C;** Determination of the amount of the gel purified 6.2 kbp fragment from 1% agarose gel. Line 1 has 20ng/µl and line 2 contains 15 ng/µl dephosphorylated 6.2 kbp fragments. Line 3 and line 4 contains 15ng/µl DNA. M, marker.

Since insert and vector were digested with *Bsa*AI, 0.6 kbp fragment could be inserted into vector in two orientations during the ligation. To select the clone that have correct oriented insert, plasmid DNAs were isolated from three transformants and digested with *Sal*I which cuts once vector and once insert resulting 1.5 kbp and 5.3 kbp fragments if insert is correct oriented and 1.1 and 5.7 kbp fragments if insert is wrong oriented. After digestion of DNAs from three transformants, it was found that two of the three transformants DNA is correct oriented (Figure 3.13, line 3 and 4) and remaining is wrong oriented (Figure 3.13, line 5). The new clone that has correct oriented mutated insert was named as HB101/pMOZIIS333A and stored at -80 ºC.

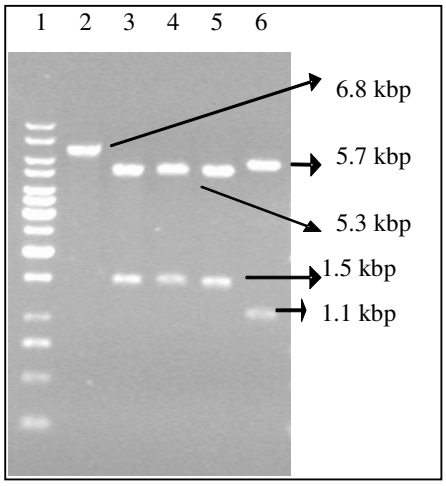

Figure 3.13: 0.6 kbp insert fragment orientation test by digestion of pMOZIIS333A with *Sal*I. Line 1: marker; line 2: 6.8 kbp linear pMOZII/*Cla*I digested DNA; Line 3: pMOZII/*Sal*I digested control DNA; line 4 and line 5: 5.3 kbp and 1.5 kbp fragment of pMOZIIS333-1 and pMOZIIS333-2/*Sal*I; line 6: 5.7 kbp and 1.1 kbp fragments of pMOZIIS333-3 DNA (wrong oriented insert).

3.4.3 Replacement of the 2.8 kbp *NO'* Fragment of pOX15 with the that of the pMOZIIS333A

To prepare 15.3 kbp pOX15S333A DNA, pMOZIIS333A and pOX15 plasmid DNAs were digested with *Xho*I restriction enzyme. The *Xho*I digested pOX15 DNA sample was dephosphorylated with CIAP to prevent to self ligation of 12.5 kbp vector. Digested samples were loaded on 1% agarose gel and electrophoresed at 70 V for 1 hour. The resulting fragments, 12.5 kbp and 2.8 kbp fragment from pOX15 (Figure 3.14.A) and, 2.8 kbp and 4.0 kbp fragments from pMOZIIS333A (Figure 3.15.A and B), were separated on 1 % agarose gel. Then, the 2.8 kbp fragment from pMOZIIS333A and the 12.5 kbp fragment from pOX15 DNA were isolated from the agarose gel. Amount of the 12.5 kbp and 2.8 kbp fragments were determined (40 ng/µl, 20 ng/µl and 20 ng/µl, respectively) by

loading 1 µl of DNA fragments on 1% agarose gel (Figure 3.14-B and Figure 3.15-C). Gel purified insert and vector ligated in 20 µl volume on ice overnight and 1 h at 22 ºC. Finally, 5 µl ligation mixes were transformed into 100 µl HB101 cells. Transformants were selected based on clone size, 15.3 kbp and new clone was named as HB101/ pOX15S333A and stored at -80 ºC.

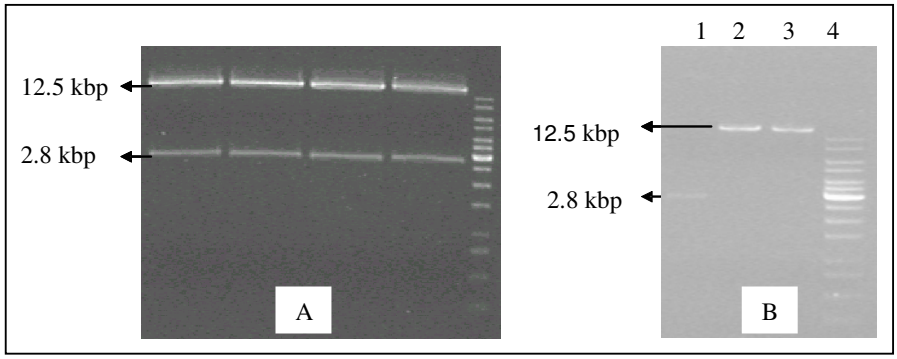

Figure 3.14: Isolation and determination of the amount of 12.5 kbp fragments of *Xho*I digested pOX15 vector DNA and 2.8 kbp insert DNA. **A**. Separation of 12.5 kbp and 2.8 kbp fragments of *Xho*I digested pOX15. **B**. Determination of the gel purified 12.5 kbp fragments from 1% agarose gel. Line 1: 2.8 kbp insert DNA (20 ng/µl); line 2 and line 3: dephosphorylated 12.5 kbp fragment of pOX15 vector DNA (40 ng/µl); line 4: marker.

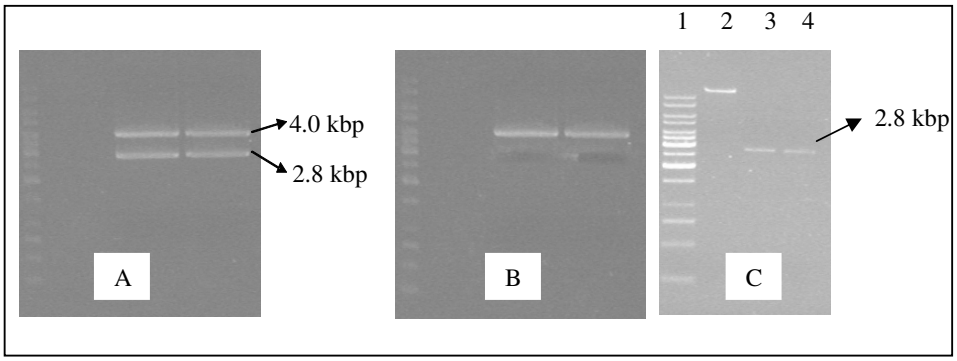

Figure 3.15: Isolation of the 2.8 kbp fragments of *Bsa*AI digested pMOZIIS333A. **A**. Separation of 4.0 kbp and 2.8 kbp *Xho*I digested pMOZIIS333A fragments on 1% agarose gel. **B**. Isolation of the 2.8 kbp fragments from 1 % agorose gel. **C**. Determination of the amount of the gel purified 2.8 kbp and 12.5 kbp fragments on 1% agarose gel. Line 2 has a 40 ng/µl 12.5 kbp dephosphorylated fragments and line 3 and 4 have a 20 ng/µl 2.8 kbp insert DNA.

Since insert and vector were digested with *Xho*I, 0.6 kbp fragment could be inserted into vector in two orientations. To select the clone that has correct oriented insert, plasmid DNAs were isolated from three transformants then they were digested with *Hind*III which cuts once vector and once insert resulting 3.6 kbp and 11.7 kbp fragments if insert is correct oriented, but 2.8 kbp and 12.5 kbp fragments appear if the insert is wrong oriented. After digestion of the DNAs from three transformants, it was found that one of them are correct oriented (Figure 3.16, line 5), and others are wrong oriented (Figure 3.16, line 3 and 4). The new clone that has correct oriented mutated insert was kept at -80 ºC and named as HB101/pOX15S333A.

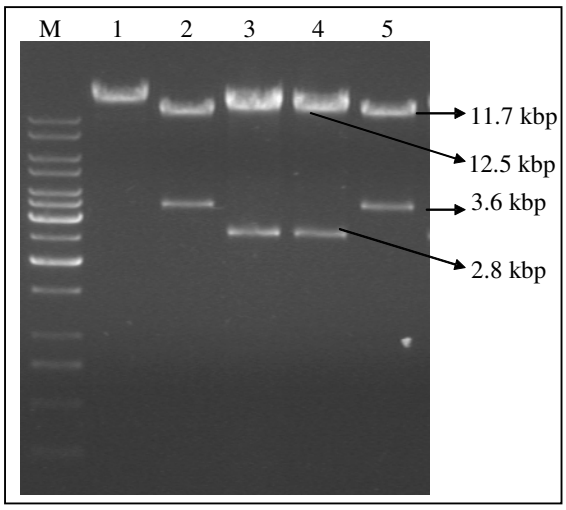

Figure 3.16: 2.8 kbp insert fragment orientation test by digesting of pOX15S333A DNA with *Hind*III. Line 1 contains *Cla*I digested 12.5 kbp liner DNA of pOX15. Line 2 contains *Hind*III digested pOX15 control DNA resulting 11.7 kbp and 3.6 kbp fragments. Line 3 and 4 have a wrong oriented *Hind*III digested pOX15S333-1 and pOX15S333-2 DNAs (12.5 kbp and 2.8 kbp fragments). Line 5 contains correct oriented *Hind*III digested pOX15S333-3 DNA resulting with 11.7 kbp and 3.6 kbp fragments.

3.4.4 Transformation of the pOX15S333A into *R. capsulatus*

The most efficient and generally applicable system for introducing plasmid DNA into *R. capsulatus* is conjugation. The *E. coli* donors contain chromosomal copies of the trans-acting elements that mobilize *oriT*-containing plasmids. The most commonly used vector system for complementation is those based on the RK2 replication. Plasmid pRK404 and pRK415 are used for such purposes in both *R. sphaeroides* and *R. capsulatus*. RK2 plasmids are stable in *R. capsulatus* as long as selective pressure is maintained.

The pOX15S333A plasmid DNA that is in HB101 strains of *E. coli* was transferred into GK32 strain of *R. capsulatus* Δ (*ccoNO::*kan) in the presence of HB101/pRK2013 helper cells. Transconjugants were selected based on tetracycline resistance. Transconjugants named as a GK32/pOX15S333A were selected and kept for further analysis at -80 ºC, to determine the cbb_3 oxidase respiratory phenotype by NADI test and subunit assembly of cbb_3 oxidase by SDS-TMBZ staining.

3.4.5 Testing of the cbb_3 Oxidase Phenotype of GK32/pOX15S333A

The presence of only one-type of cyt *c* oxidase in *R. capsulatus* allows efficient utilization of the NADI reaction (ά-Naphtol + Dimetyle-p- Phenilen Diamine (DMPD) + O_2 → Indophenol Blue + H_2O) to identify the mutation affecting cyt cbb_3 oxidase phenotype. Four transconjugants were tested with NADI staining for their oxidase phenotype by being overlaid a 1:1 (v/v) mixture of 35 mM ά-Naphtol in ethanol and 30 mM DMPD in H_2O [Keilin, 1966].

After NADI staining of the wild-type (MT1131), control mutant (GK32), complemented control mutant (GK32p/OX15) and generated mutant (pOX15S333A/GK32) colonies, we found that MT1131 and pOX15/GK32 were $NADI^{positive}$ and GK32 was $NADI^{negative}$ as expected, but the desired **GK32/pOX15S333A** mutants is **$NADI^{slow}$** (Figure 3. 17). GK32/pOX15S333A colonies turn blue very slowly compared with wild type which turns in blue within 30 seconds. NADI staining phenotype of this mutant indicates that the serine 333 is critical amino acid for enzyme activity.

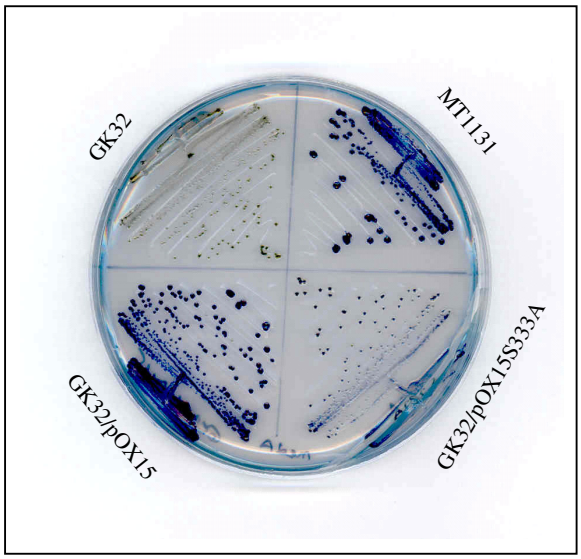

Figure 3.17: NADI-stained GK32/pOX15S333A plate. MT1131, wild-type (NADI^{positive}); GK32, control mutant (NADI^{negative}); GK32/pOX15, complemented control mutant (NADI^{positive}); and **GK32/pOX15S333A**, generated mutant (**NADI^{slow}**).

3.4.6 Analysis of the Cytochrome Profiles of GK32/pOX15S333A Mutant

The desired mutant GK32/pOX15S333A together with wild-type, MT1131; mutant, GK32; complemented mutant, GK32/pOX15 were analyzed for their *c*-type cyt content using TMBZ/SDS-PAGE analysis (Figure 3.18). Four distinct membrane-bound *c*-type cyts, with M_r of 32, 31, 29, and 28 kDa, are readly detected in chromotophore membranes of a wild type *R. capsulatus* strain like MT1131, grown semiaerobically in MPYE enriched medium. The 31-kDa protein is the cytochrome c_1 subunit of the cytochrome bc_1 complex [Jenney et al., 1994], the 29 kDa protein is the mmebrane-assosiated electron carrier cytochrome c_y [Jenny and Daldal, 1993]. The c_o, 32 Da, and c_p, 28 Da, subunits are the subunit

of the *cbb*$_3$ oxidase. This result ındicates that S333 is not important for cyt *cbb*$_3$-type oxidase assemly, but it seems to be significant for the activity of *cbb*$_3$-type cyt *c* oxidase.

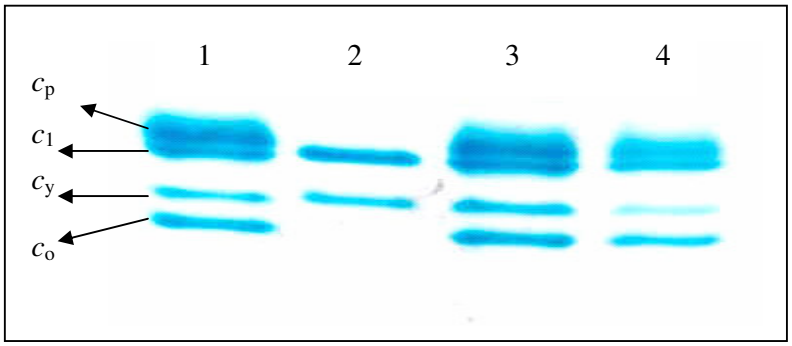

Figure 3.18. Cytochrome *c* profle of GK32/pOX15S333A mutant together with the wild type, MT1131; mutant, GK32; complemented mutant, GK32/pOX15 GK32/pOX15S333A. Cytochrome *c* profiles of chromatophore membranes of *R. capsulatus* strains grown in enriched MPYE medium under respiratory conditions. Aproximatelly 100 µg of protein was loaded in each lane of a 16.5% SDS-polyacrylamide gel. After electrophoresis, *c*-type cyts were detected by TMBZ staining. Lane 1, MT1131; lane 2, GK32; lane 3, GK32/pOX15; and line 4, **GK32/pOX15S333A** cyt c_p and c_o are the subunits II and III of cyt *cbb*$_3$ oxidase, and cyts c_1 and c_y correspond to the cyt c_1 subunit of the bc_1 complex and the membrane-attached electron carrier c_y, respectively.

3.5. Construction and Analysis of GK32/pOX15S340A Mutant

3.5.1 Sequencing of pMOZIS340-1 Mutant

One of the plasmid DNAs, pMOZ1S340-1, described in Table 1 was sequenced by using primer 578F 5' GGTGGCCTATCTGATCG 3' at MWG Biotech-FAQs custom sequencing services, Germany. When obtained sequence was compared with the nucleotide sequence of the cbb_3 oxidase from gene data bank, it was found that pMOZ1S340-1 plasmid DNA has a desired mutation (GCC) instead of TCC and it is long enough to see cloning restriction site, *Bsa*AI (Fig. 3.19, row 1 and 6), and there is no mutation other than desired one. The mutated codon (GCC) is underlined (Figure 3.19, row 4). The pMOZ1S340-1 clone having alanine amino acid instead of serine at site 340 was named as pMOZIS340A.

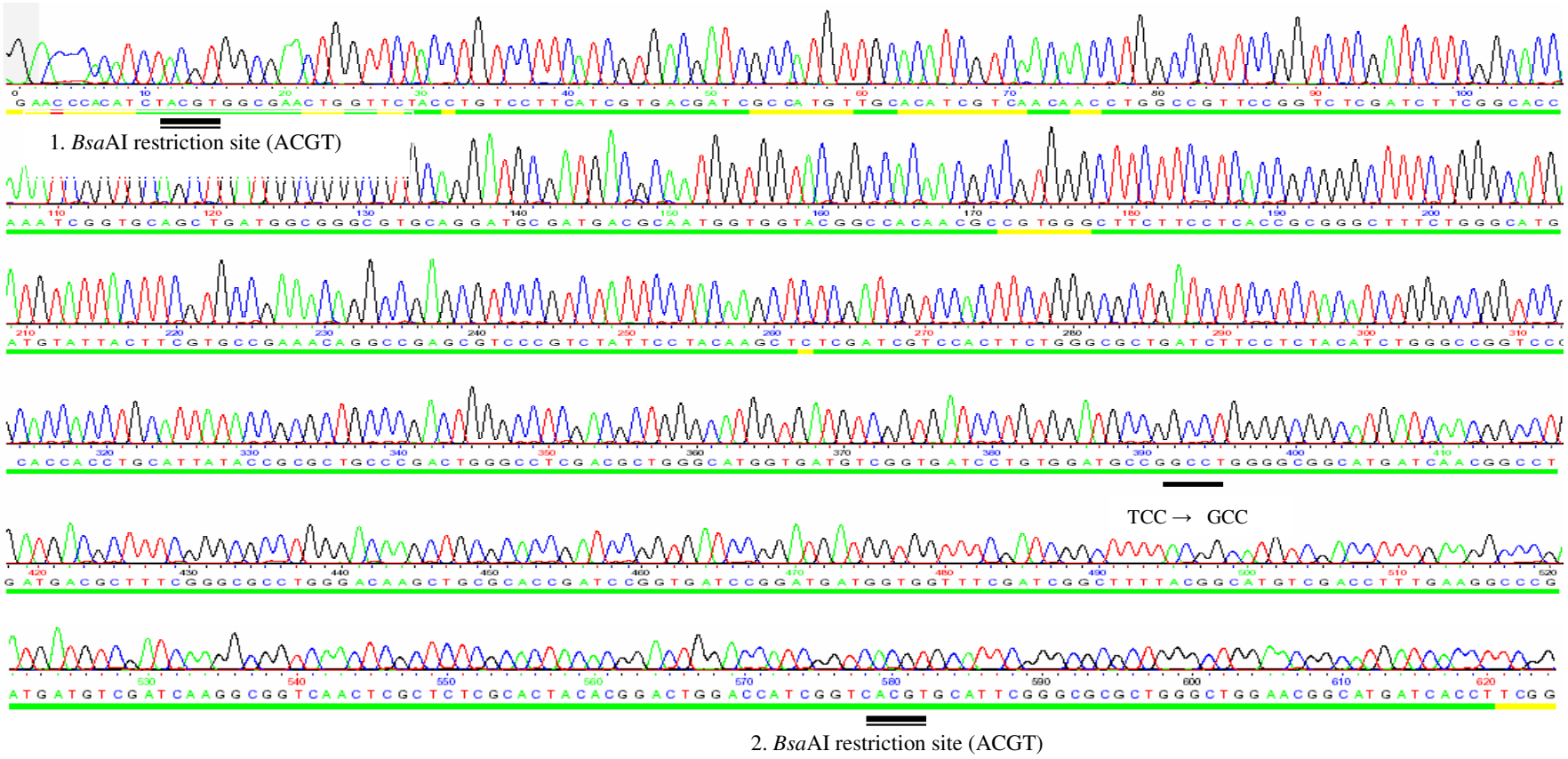

Figure 3.19: The partial sequence of pMOZIS340-1 transformant. The **TCC** codon was converted to **GCC** codon. *Bsa*AI restriction sites and mutation were underlined.

3.5.2 Replacement of the 0.6 kbp Fragment of pMOZII with that of the pMOZIS340A

To replace 0.6 kbp fragment of pMOZII with that of pMOZIS340A, pMOZIS340A DNA was digested with *Bsa*AI. The *Bsa*AI digested DNA sample was loaded on 1% agarose gel and resulting fragments, 0.6 kbp, 1.1 kbp and 4.0 kbp fragments were separated (Figure 3.20.A). Then 0.6 kbp insert fragments from pMOZIS333A were isolated from 1% agarose gel (Figure 3.20.B). Then amount of the gel purified 0.6 kbp fragments were determined (Figure 3.20.C). 0.6 kbp mutated fragment was inserted into 6.2 kbp vector by incubating at 22 ºC for two hours. 5 µl ligation mixtures were transformed into HB101 cells. Transformants were selected based on the size of the clone, 6.8 kbp in size.

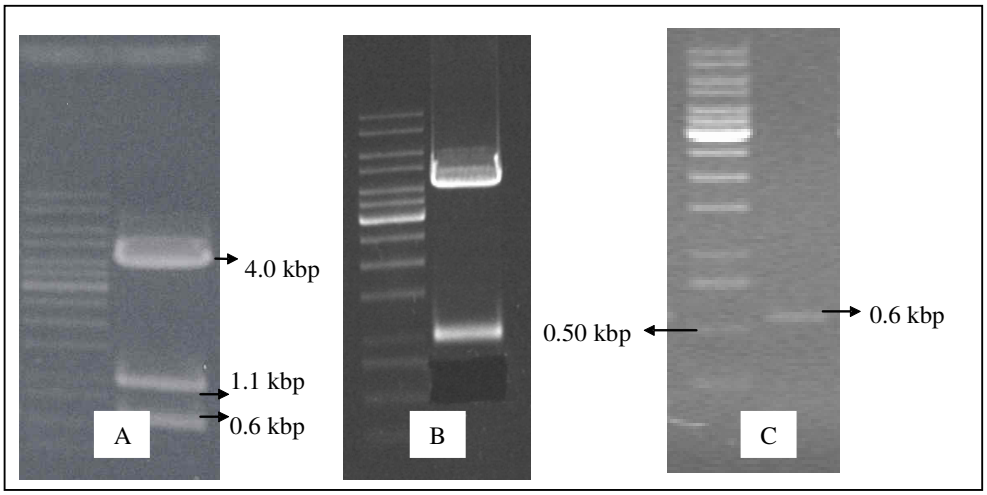

Figure 3.20: Isolation and purification of 0.6 kbp pMOZIS340-1. **A**. It contains 4.0 kbp, 1.1 kbp and 0.6 kbp fragments of *Bsa*AI digested pMOZIS340A. **B**. Isolation of 0.6 kbp fragment from agarose gel. **C**. Determination of gel purified 0.6 kbp fragment on 1% agarose gel, 15ng/µl.

To select the clone that have correct oriented insert, plasmid DNAs were isolated from three transformants and digested with *Sal*I. Among these transformats, *Sal*I digestion showed that one of the three transformant DNA is wrong oriented (Figure 3.21, line 4) and remaining are correct oriented (Figure 3.21, line 5 and 6). The new clone that has correct oriented mutated insert was named as HB101/pMOZIIS340A and they were kept at -80 ºC.

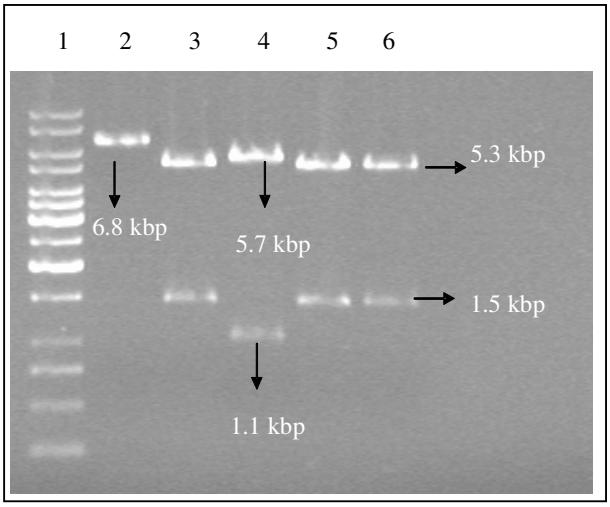

Figure 3.21: 0.6 kbp fragment orientation test by digestion of pMOZIIS340A with *Sal*I. Line 1: marker; Line 2 has a 6.8 kbp *Cla*I digested linear pMOZII DNA. Line 3 contains pMOZII/*Sal*I digested control DNA, 5.3 kbp and 1.5 kbp fragments. Line 4 has a 5.7 kbp and 1.1 kbp fragments of pMOZIIS340-1/ *Sal*I, and Line 5 and 6 have correct oriented pMOZIIS340-2 and pMOZIIS340-3 DNAs compared with that of pMOZII in line 2.

3.5.3 Replacement of the 2.8 kbp *NO'* Fragment of pOX15 with that of the pMOZIIS340A

To replace 2.8 kbp fragment of pOX15 vector with mutated one of the pMOZIIS340A, pMOZ2S340A and pOX15 plasmid DNAs were digested with *Xho*I restriction enzyme. Digested samples were loaded on 1% agarose gel. The resulting 2.8 kbp and 4.0 kbp fragments from pMOZIIS340A (Figure 3.22.A) and 12.5 kbp and 2.8 kbp fragments from pOX15 were separated on 1 % agarose gel. Then 2.8 kbp fragment from pMOZ2S340A (Figure 3.22.B) and 12.5 kbp fragments from pOX15 were isolated from the agarose gel and also amount of the DNAs were determined by loading of 1 µl DNA on 1% agarose gel (Figure 3.22.C). Gel purified insert and vector ligated in 20 µl volume at 4 ºC overnight (ON) and at 22 °C for half hours. Then 5 µl ligation mixes were transformed into 100 µl HB101 cells. Transformants were selected based on clone size, 15.3 kbp and tetracycline resistance.

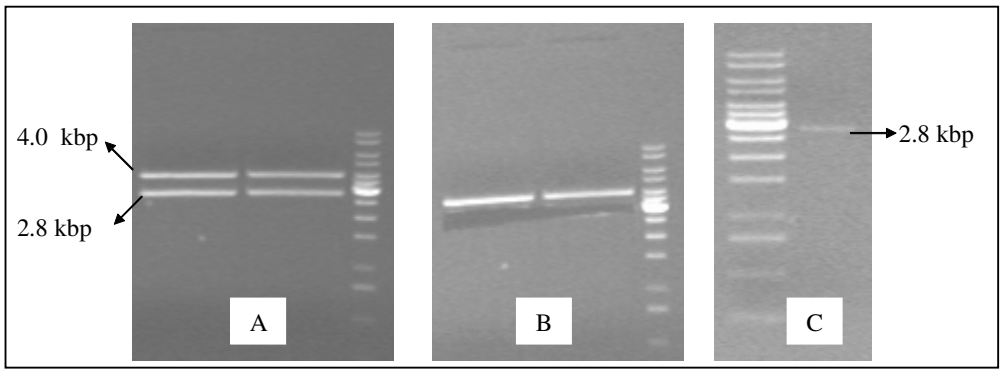

Figure 3.22: Isolation and purification of 4.0 kbp and 2.8 kbp fragments of *Xho*I digested pMOZIIS340A**. A**. Separation of 4.0 kbp and 2.8 kbp fragments of *Xho*I digested pMOZIIS340A. **B**. Isolation of the 2.8 kbp fragment from agorose gel. **C**. Determination of the amount of the gel purified 2.8 kbp fragments on 1% agarose gel, 15ng/µl.

To select the clone that have correct oriented insert, plasmid DNAs were isolated from three transformants then they were digested with *Hind*III which cuts once vector and once insert resulting 3.6 kbp and 11.7 kbp fragments if insert is correct oriented but 2.8 kbp and 12.5 kbp fragment appeared if the insert is wrong oriented. After digestion the DNAs from three transformants, It was found that two of them are correct oriented (Figure 3.23, line 2 and 4), and other is wrong oriented (Figure 3.23, line 3). The new clone that has correct oriented mutated insert was saved and named as HB101/pOX15S340A.

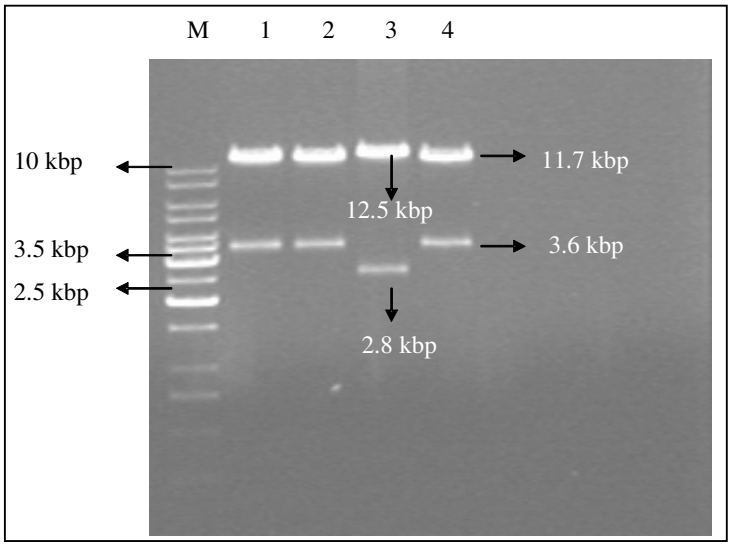

Figure 3.23: 2.8 kbp fragment orientation test by digesting of transformant DNAs with *Hind*III. Line1 contains pOX15/*Hind*III digested control DNA resulting 11.7 kbp and 3.6 kbp fragments. Line 2 and line 4 have a correct oriented pOX15S340-1/*Hind*III and pOX15S340-3/*Hind*III digested DNAs resulting with 11.7 kbp and 3.6 kbp fragments. Line 3 contains pOX15S340-2/*Hind*III digested DNA resulting with 12.5 kbp and 2.8 kbp fragments so, insert is wrong oriented. M, marker.

3.5.4 Transformation of the pOX15S340A into *R. capsulatus*

The pOX15S340A plasmid DNA was transferred into GK32 *R. capsulatus* strain by three parental mating in the presence of HB101/pRK2013 cells. Transconjugants were selected based on tetracycline resistance. Selected transconjugants were named as GK32/pOX15S340A and kept at -80 ºC for further analysis such as cbb_3 oxidase respiratory phenotype by NADI staining.

3.5.5 Testing of the cbb_3 Oxidase Phenotype of GK32/pOX15S340A Mutant

After NADI staining of the wild-type (MT1131), control mutant (GK32), complemented control mutant (GK32/pOX15) and generated mutant (GK32/pOX15S340A) colonies we found that MT1131, and GK32/pOX15 are $NADI^{positive}$, and GK32 is $NADI^{negative}$ as expected, but the desired **GK32/pOX15S340A** mutants is **$NADI^{positive}$** (Figure 3.24). The pOX15S340A/GK32 colonies turned blue compared with wild type which turns in blue within 30 seconds. NADI staining phenotype of this mutant indicates that the serine at position 340 is not critical amino acid for enzyme activity.

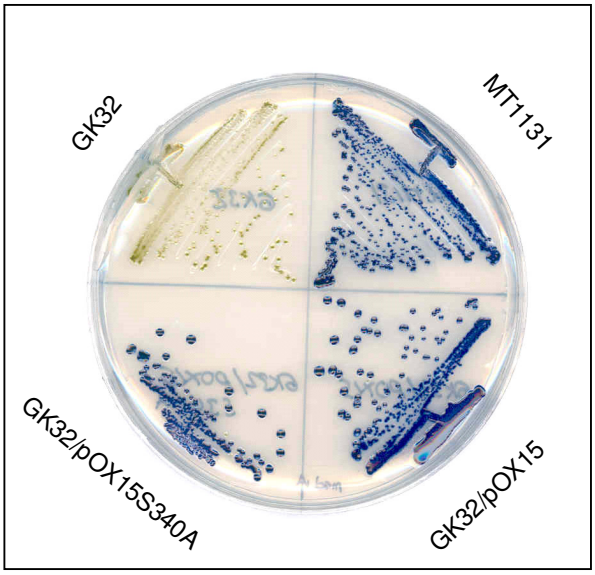

Figure 3.24: NADI-stained GK32/pOX15S340A plate. MT1131, wild type (NADI^{positiv}); GK32, control mutant (NADI^{negative}); GK32/pOX15, complemented control mutant (NADI^{positive}); and **GK32/pOX15S340**, generated mutant (**NADI^{positive}**).

3.5.6 Analysis of the Cytochrome Profiles of GK32/pOX15S340A Mutant

After TMBZ staining of the 100 µg MT1131, GK32, GK32/pOX15, GK32/pOX15S340A chromatophore loaded SDS-PAGE gel, it was found that subunits of the GK32/pOX15S340A mutant are almost the same with those of the controles, MT1131 and GK32/pOX15 (Figure 3.25). This profile showed that serine at position 340 is not signaficant for assemly of the *cyt* cbb_3-type oxidase.

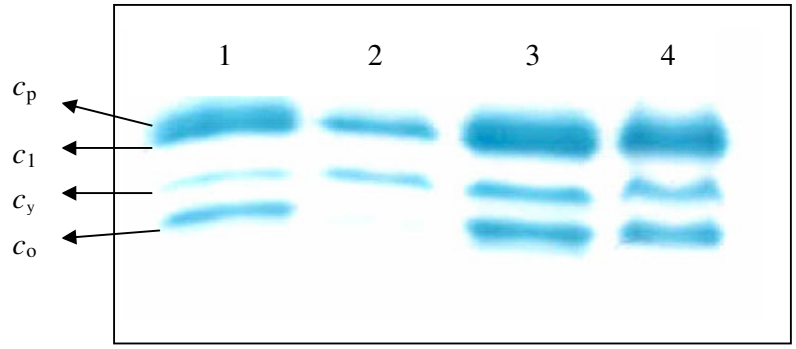

Figure 3.25: Cytochrome *c* profle of GK32/pOX15S340A. TMBZ/SDS-PAGE analysis of *c*-type cytochromes from various *R. capsulatus* strains obtained from cells grown on enriched MPYE medium (100 µg of membrane proteins were loaded per lane). Lane 1, MT1131; lane 2, GK32; lane 3, GK32/pOX15; and line 4, **GK32/pOX15S340A**. *Cyt* c_p and c_o are the subunits II and III of cyt cbb_3 oxidase, and cyts c_1 and c_y correspond to the cyt c_1 subunit of the bc_1 complex and the membrane-attached electron carrier c_y, respectively.

3.6 Construction and Analysis of GK32/pOX15ST350A Mutant

3.6.1 Sequencing of pMOZIT350-2 Mutant

The pMOZIT350-2 (Table 1) was sequenced with the 578F primer at Iontek Company, Istanbul. Obtained DNA sequence was compared with that of the wild-type strain, it was found that pMOZIT350-2 plasmid DNA has a desired alanine codon (GCG), which was underlined, instead of threonine codon (ACG) (Figure 3.26, row 5), and it is also long enough to see both cloning sites (Figure 3.26, row 1 and 6). However there is one more change on the 0.6 kbp obtained sequence. The ACG codon also has been substituted to ACA codon, highlighted and colored (Figure 3.26, row 2). Both of the codons code the threonine amino acid. Codon Usage Database shows that frequency of the ACA codon for *R. capsulatus* is 1.1 per thousand codons (http://www.kazusa.or.jp/codon).

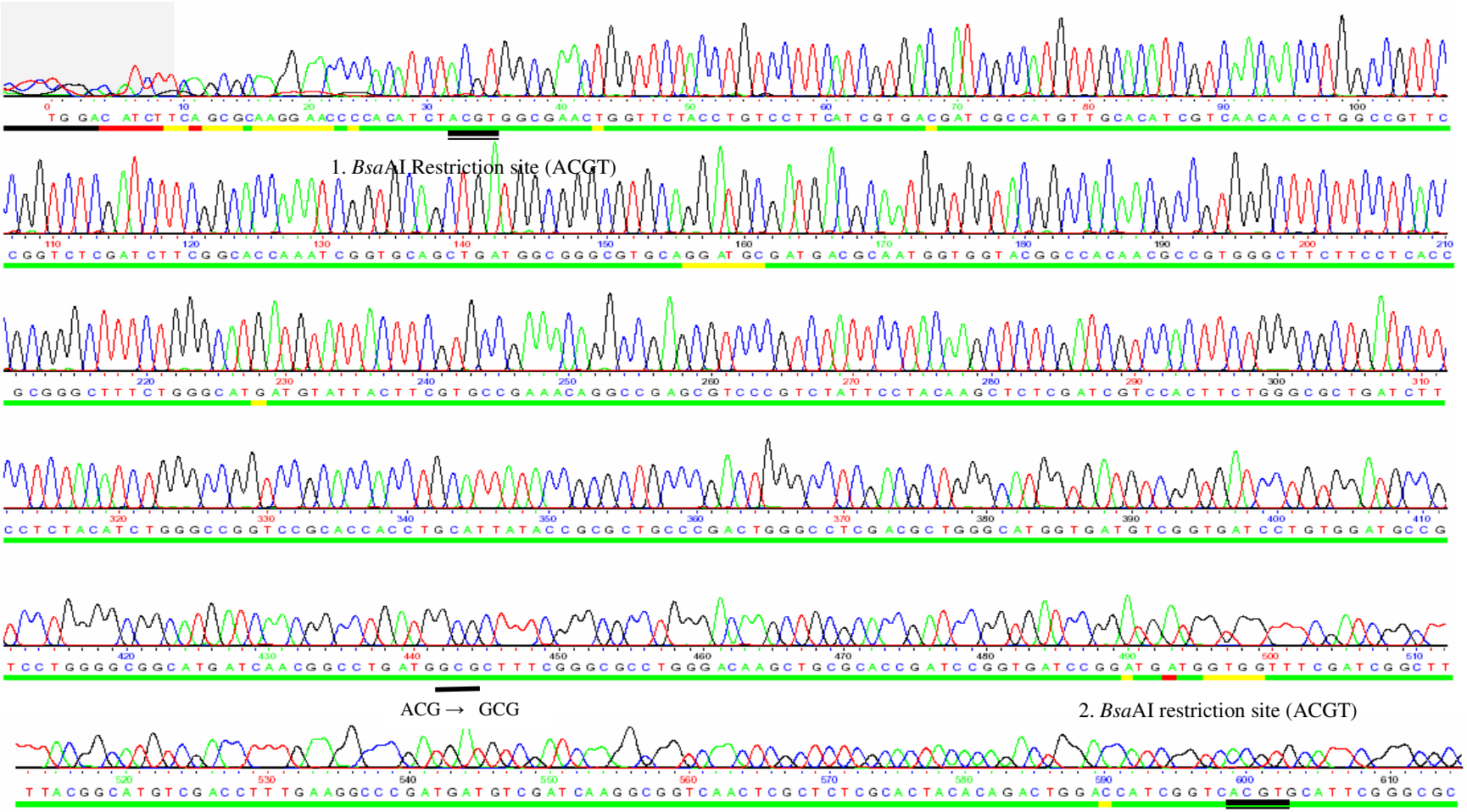

Figure 3.26: The partial sequence of pMOZIT350-2 transformant. The **ACG** codon was converted to **GCG** codon underlined at row 5.

3.6.2 Replacement of the 0.6 kbp Fragment of pMOZII with that of the pMOZIS350A

To replace 0.6 kbp fragment of pMOZII with that of pMOZIT350A, pMOZII and pMOZIT350A DNAs were digested with *Bsa*AI. Digested DNA samples were loaded on 1% agarose gel and resulting fragments, 0.6 kbp, 1.1 kbp and 4.0 kbp, was separated (Figure 3.27.A). Then 0.6 kbp insert fragments from pMOZIS333A were isolated from 1% agarose gel (Figure 3.27.B). Then 0.6 kbp mutated fragment was inserted into 6.2 kbp vector at 22 ºC for two hours. Finally 5 µl ligation mix was transformed into HB101 cells. Transformants were selected based on the size of the clone, 6.8 kbp in size.

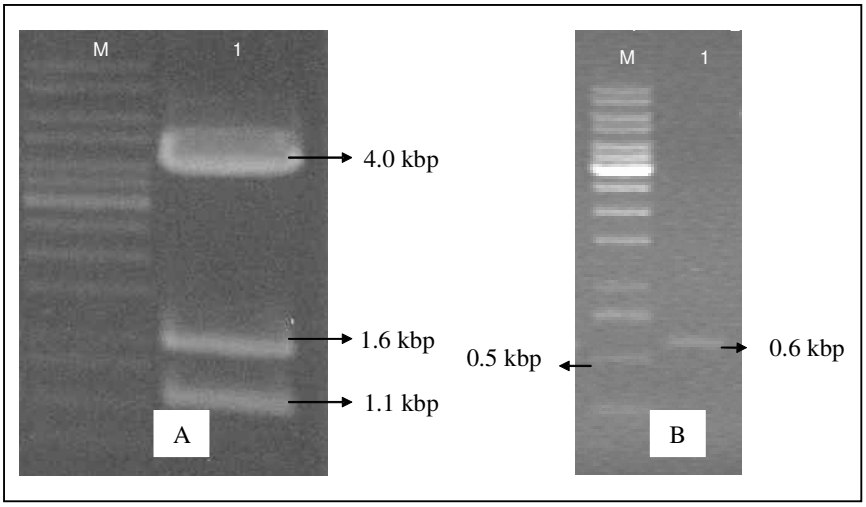

Figure 3.27: Isolation and purification of 0.6 kbp pMOZIT350A. **A)** Contains 4.0 kbp, 1.1 kbp and 0.6 kbp fragments of *Bsa*AI digested pMOZI350A. **B**) Determination of gel purified 0.6 kbp fragment on 1% agarose gel (15ng/µl).

To select the clone that have correct oriented insert, plasmid DNAs were isolated from three transformants and they were digested with *Sal*I. After digestion of transformant DNAs from three transformants, it was found that one of the three transformant DNA is correct oriented (Figure 3.28, line 6) and remaining are wrong oriented (Figure 3.28, line 4 and 5). The new clone that has correct oriented mutated insert was named as HB101/pMOZIIS350A and they were kept at -80 ºC.

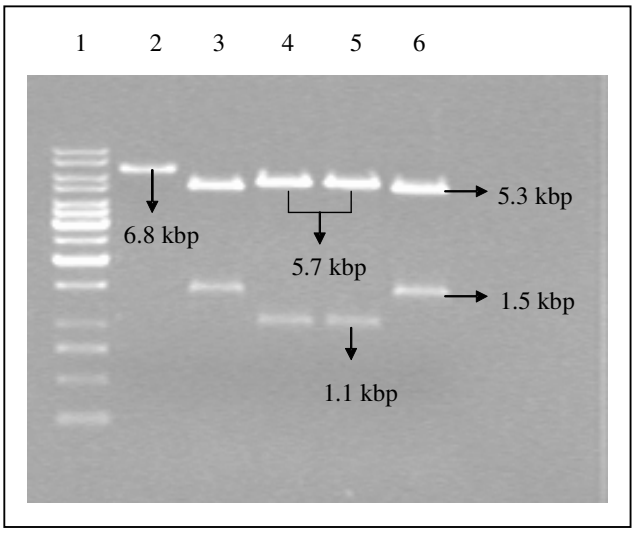

Figure 3.28: 0.6 kbp fragment orientation test by digestion of pMOZIIT350A with *Sal*I RE. Line 1: marker; line 2: 6.8 kbp linear pMOZII/*Sal*I digested DNA; line 3: contains pMOZII/*Sal*I digested control DNA; line 4 and line 5: 5.7 kbp and 1.1 kbp fragments of *Sal*I digested pMOZIIT350-1 and pMOZIIT350-2 DNAs (wrong oriented insert); line 6: 1.5 kbp and 5.3 kbp fragments of pMOZIIT350-3 (correct oriented insert).

3.6.3 Replacement of the 2.8 kbp *NO*' Fragments of pOX15 with that of the pMOZIIS350A

To replace 2.8 kbp fragment of pOX15 vector with that of the pMOZIIT350A, pMOZIIT350A and pOX15 plasmid DNAs were digested with *Xho*I restriction enzyme. Digested samples were loaded on 1% agarose gel and 2.8 kbp and 4.0 kbp fragments were separated on 1 % agarose gel (Figure 3.29.A). Then 2.8 kbp fragment was isolated from the agarose gel (Figure 3.29.B) and also amount of the DNA was determined by loading of 1 µl DNA on 1% agarose gel (Figure 3.29.C). Gel purified insert and vector ligated in 20 µl volume at 4 ºC overnight and at 22 °C for half hours. Then 5 µl ligation mixes were transformed into 100 µl HB101 cells. Transformants were selected based on clone size, 15.3 kbp and tetracycline resistance.

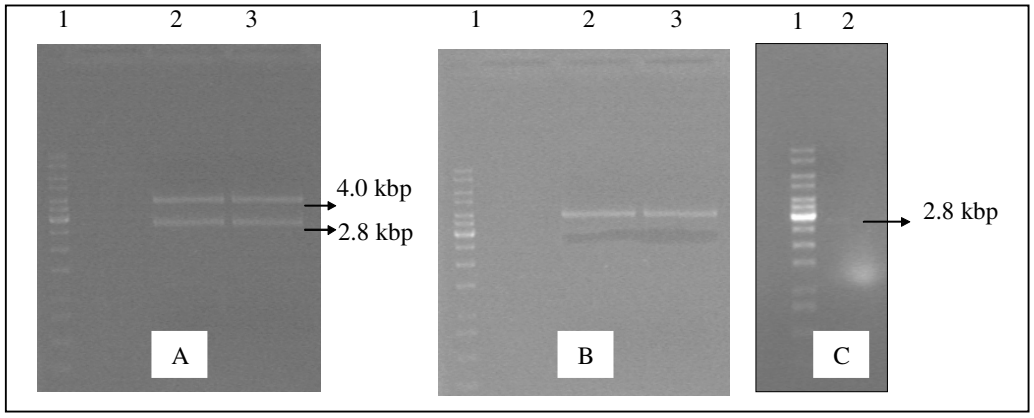

Figure 3.29: Isolation and purification of 4.0 kbp and 2.8 kbp fragments of *Xho*I digested pMOZIIT350A. **A**. Separation of 4.0 kbp and 2.8 kbp fragments of *Xho*I digested pMOZIIT350A. Line 1: marker; line 2 and line 3: *Xho*I digested pMOZIIT350A. **B**. Isolation of the 2.8 kbp fragments from agorose gel. **C**. Determination of gel purified 2.8 kbp fragments on 1% agarose gel. Line 1: marker; line 2 gel purified 2.8 kbp fragments from pMOZIIT350A, 15ng/µl.

To select the clone that have correct oriented insert, plasmid DNAs were isolated from three transformants then they were digested with *Hind*III which cuts once vector and once insert resulting 3.6 kbp and 11.7 kbp fragments if insert is correct oriented but 2.8 kbp and 12.5 kbp fragment appeared if the insert is wrong oriented. After digestion the DNAs from three transformants, It was found that one of them is correct oriented (Figure 3.30, line 5), other one is wrong oriented (Figure 3.30, line 3). One of the does not have any insert (Figure 3.30, line 4). The new clone that has correct oriented mutated insert was saved and designated as HB101/pOX15S350A.

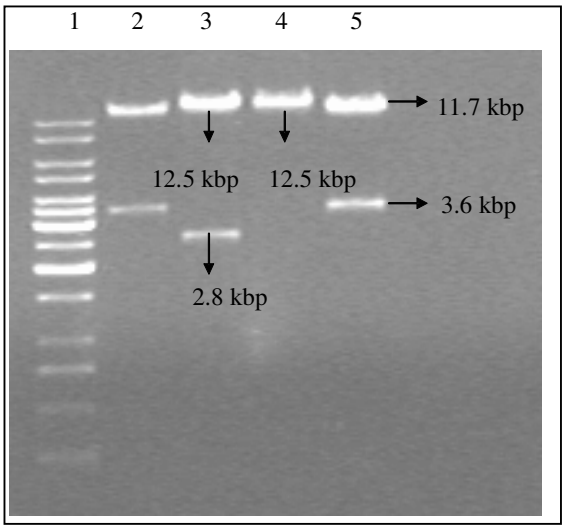

Figure 3.30: 2.8 kbp fragment orientation test by digesting of transformant DNAs with *Hind*III. Line 1: marker; Line 2 contains pOX15/*Hind*III digested control DNA. Line 3 contains 12.5 kbp and 2.8 kbp fragments of pOX15T350-1/*Hind*III. Line 4 does not contain insert. Line 5 has a correct oriented insert.

3.6.4 Transformation of the pOX15T350A into *R. capsulatus*

The pOX15T350A plasmid DNA was transferred into *R. capsulatus* strain (GK32) lacking *NO'* part of the *ccoNOQP* structural gene of cbb_3 oxidase, by three parental mating in the presence of HB101/pRK2013 cells. Transconjugants were selected based on tetracycline resistance. Selected transconjugants were named as GK32/pOX14S350A and kept at -80 ºC for further analysis such as cbb_3 oxidase respiratory phenotype by NADI staining.

3.6.5 Testing of the cbb_3 Oxidase Phenotype of GK32/pOX15T350A

After NADI staining of the wild-type (MT1131), control mutant (GK32), complemented control mutant (GK32/pOX15) and generated mutant (GK32/pOX15T350A) colonies it was found that MT1131, and GK32/pOX15 are $NADI^{positive}$, and GK32 is $NADI^{negative}$ as expected, but the desired **GK32/pOX15T350A** mutants is **$NADI^{positive}$** (Figure 3.31). The GK32/pOX15T350A colonies turned blue like wild type which turns in blue within 30 seconds. NADI staining phenotype of this mutant indicates that the threonine 350 is not critical amino acid for enzyme activity.

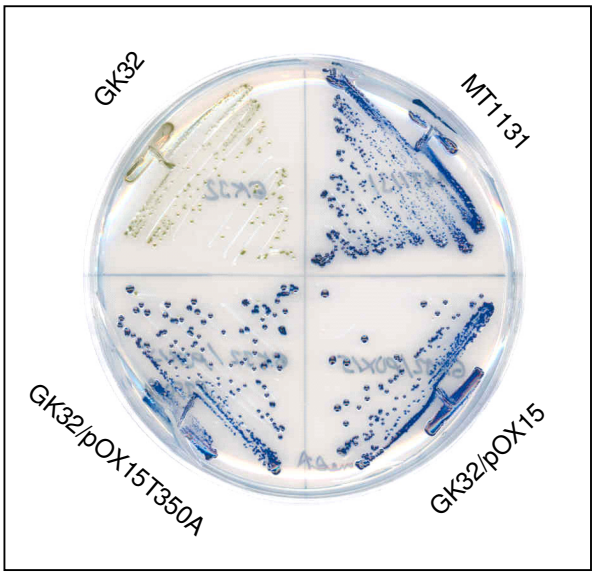

Figure 3.31 NADI stained GK32/pOX15T350A plate. MT1131, wild type (NADI^{positiv}); GK32, control mutant (NADI^{negative}); GK32/pOX15, complemented control mutant NADI^{positive}); and **GK32/pOX15T350A**, generated mutant (**NADI^{positive}**).

3.6.6 Analysis of the Cytochrome Profiles of GK32/pOX15S350A Mutant

After TMBZ staining of the SDS-PAGE gel on which 100 µg MT1131, GK32, GK32/pOX15 and GK32/pOX15S350A chromatophore samples were loaded, it was found that subunits of the GK32/pOX15T350A mutant are almost the same with those of the controles, MT1131 and GK32/pOX15 (Figure 3.32). Thus, it could be saıd that threonine at position 350 is not important for cyt *cbb*$_3$-type oxidase assemly.

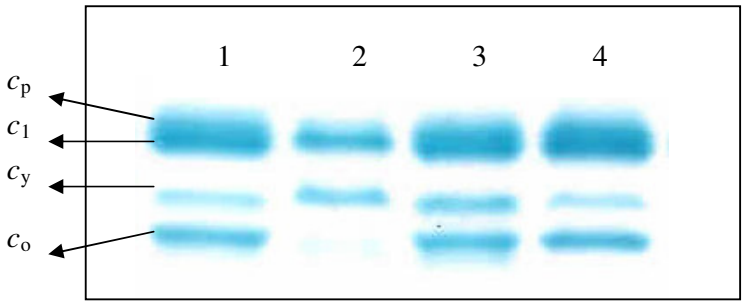

Figure 3.32. Cyt *c* profle of GK32/pOX15S350A. TMBZ/SDS-PAGE analysis of *c*-type cyts from various *R. capsulatus* strains obtained from cells grown on entiched MPYE medium (100 µg of membrane proteins were loaded per lane). Lane 1, MT1131; lane 2, GK32; lane 3, GK32/pOX15; and line 4, **GK32/pOX15T350A**. Cyt c_p and c_o are the subunits II and III of cyt cbb_3 oxidase, and cyts c_1 and c_y correspond to the cyt c_1 subunit of the bc_1 complex and the membrane-attched electron carrier c_y, respectively.

3.7 Construction and Analysis of GK32/pOX15N390A Mutant

3.7.1 Sequencing of MOZIN390-3 Mutant

One of the plasmid DNAs, pMOZIN390-3, described in Table 1 was sequenced by using primer 578F 5'-GGTGGCCTATCTGATCG-3' at MWG Biotech-FAQs custom sequencing services, Germany. When obtained sequence was compared with the nucleotide sequence of the cbb_3 oxidase from gene data bank, it was found that pMOZ1N390-3 plasmid DNA has a desired mutation (GCC) instead of AAC Asparagine codon and it is long enough to see cloning restriction site (Figure 3.33, row 1 and 6), *Bsa*AI, and there is no mutation other than desired one. The clone, pMOZ1N390-3 was named as pMOZIN390A.

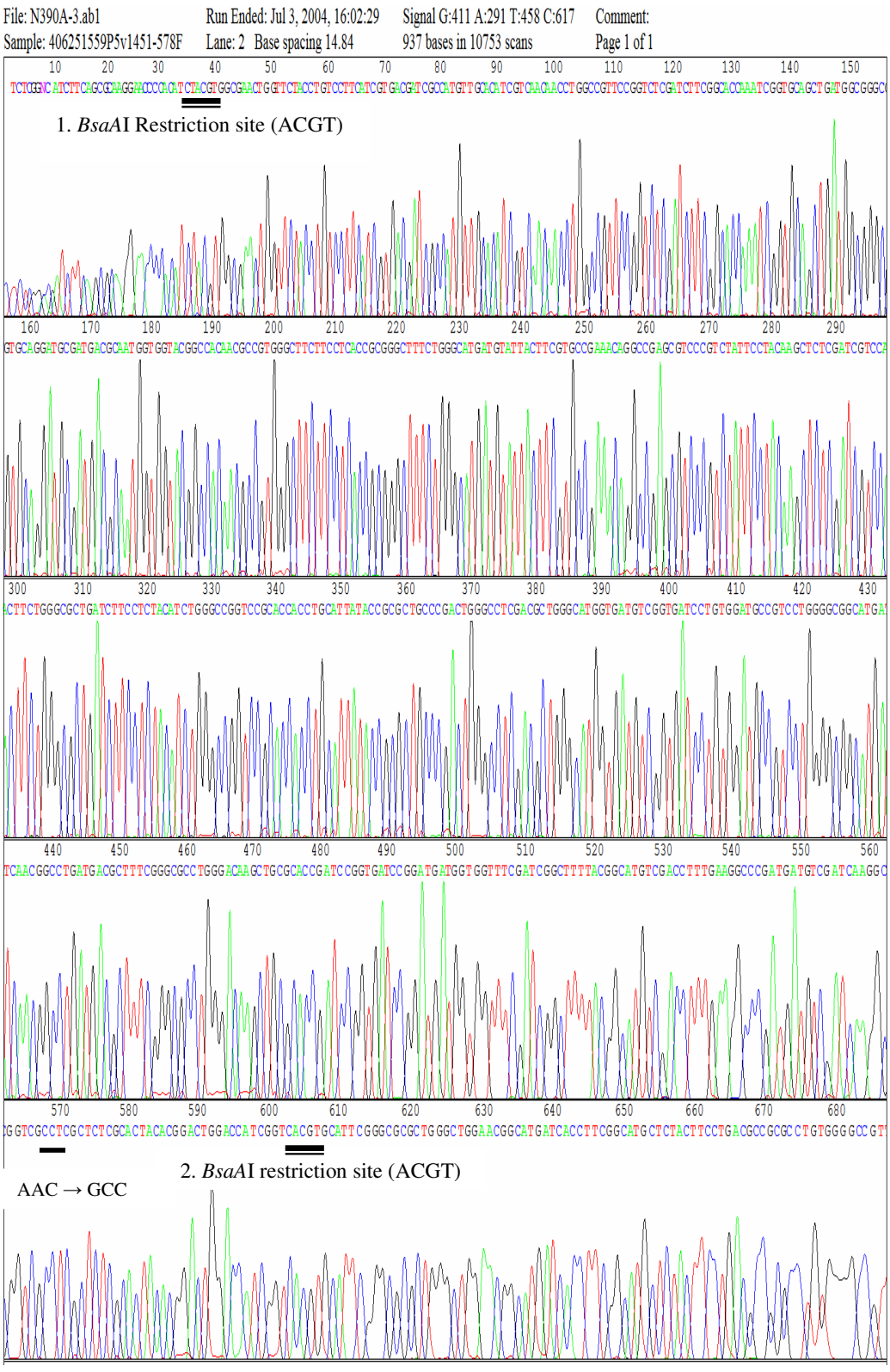

Figure 3.33 The partial sequence of pMOZIN390-3 transformant. The **AAC** codon was converted to **GCC** codon which is underlined at row 5.

3.7.2 Replacement of the 0.6 kbp Fragment of pMOZII with that of the pMOZIN390A

To replace 0.6 kbp fragment of pMOZII with that of pMOZIN390A, pMOZII and pMOZIN390A DNAs were digested with *Bsa*AI. To prevent self ligation of vector *Xho*I digested pMOZII sample was dephosphorylated with CIAP enzyme. Digested DNA samples were loaded on 1% agarose gel and resulting fragments, 0.6 kbp, 1.1 kbp and 4.0 kbp fragments were separated (Figure 3.34.A and B). Then 0.6 kbp insert fragments were isolated from 1% agarose gel (Figure 3.34.C). Then 0.6 kbp mutated fragment was inserted into 6.2 kbp vector at 22 ºC for two hours. Finally 5 µl ligation mix was transformed into HB101 cells. Transformants were selected based on the size of the clone, 6.8 kbp in size.

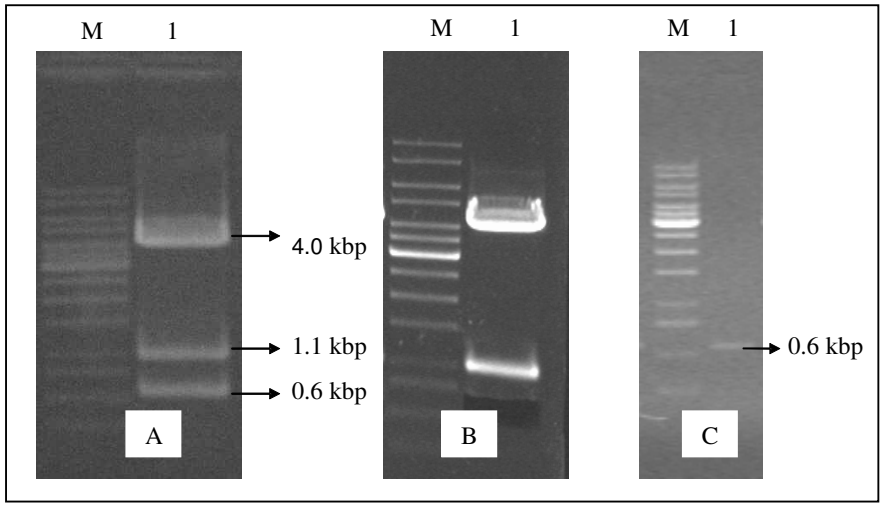

Figure 3.34: Isolation and purification of 0.6 kbp fragment of *Xho*I digested pMOZIN390-3. **A**. it contains 4.0 kbp, 1.1 kbp and 0.6 kbp fragments of *Bsa*AI digested pMOZIN390A. **B**. Isolation of 0.6 kbp fragment from agarose gel. **C**. Determination of gel purified 0.6 kbp fragment on 1% agarose gel (15ng/µl).

To select the clone that have correct oriented insert, plasmid DNAs were isolated from three transformants and digested with *Sal*I. The DNAs from three transformants were digested with *Sal*I and it was found that one of the three transformant DNA is wrong oriented (Figure 3.35, line 5) and remaining are correct oriented (Figure 3.35, line 3 and 4). The new clone that has correct oriented mutated insert was named as HB101/pMOZIIS390A and they were kept at -80 ºC.

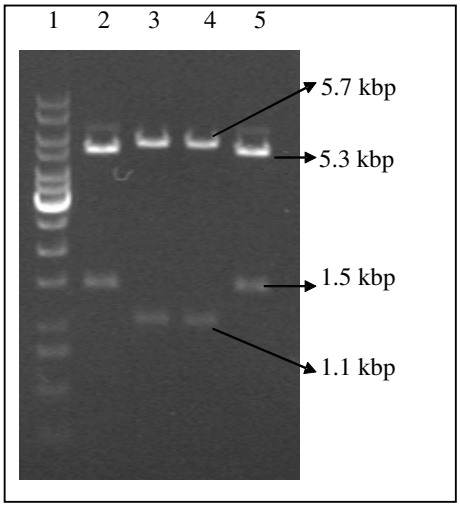

Figure 3.35: 0.6 kbp fragment orientation test by digestion of pMOZIIN390A with *Sal*I. Line1: marker; Line 2: pMOZII/*Sal*I digested control DNA; line 3 and line 4: 5.3 kbp and 1.5 kbp *Sal*I digested pMOZIIN390-1 and pMOZIIN390-2 DNA fragments (wrong oriented insert); line 5: 5.7 kbp and 1.1 kbp fragments of *Sal*I digested pMOZIIN390-3 DNA (correct oriented insert).

3.7.3 Replacement of the 2.8 kbp *NO'* Fragment of pOX15 with that of the pMOZIIN390A

To replace 2.8 kbp fragment of pOX15 vector with that of mutated one of the pMOZIIN390A, the pMOZIIN390A DNA was digested with *Xho*I restriction enzyme. *Xho*I digested samples were loaded on 1% agarose gel. The resulting 2.8 kbp and 4.0 kbp fragments were separated on 1 % agarose gel (Figure 3.36 A and B). Then 2.8 kbp fragment from pMOZIIN390A was isolated from the agarose gel and also amount of the DNAs were determined by loading of 1 µl DNA on 1% agarose gel (Figure 3,36C). Gel purified insert and vector were ligated in 20 µl volume at 4 ºC overnight and at 22 °C for half hours. Then 5 µl ligation mixes were transformed into 100 µl HB101 cells. Transformants were selected based on clone size, 15.3 kbp and tetracycline resistance.

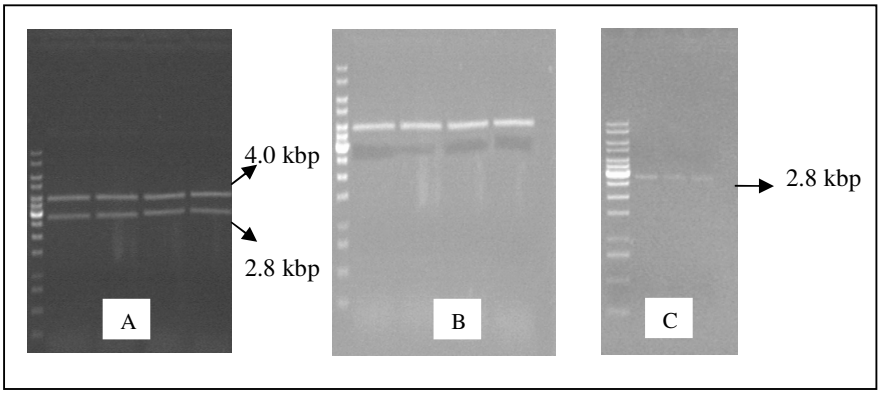

Figure 3.36: Isolation and purification of 4.0 kbp and 2.8 kbp fragments of *Xho*I digested pMOZIIN390A**. A**) Separation of 4.0 kbp and 2.8 kbp fragments of *Xho*I digested pMOZIIN390A. **B**) Isolation of 2.8 kbp fragment from agorose gel. **C**) Determination of gel purified 2.8 kbp fragments (15ng/µl).

To select the clone that have correct oriented insert, plasmid DNAs were isolated from three transformants then they were digested with H*ind*III. After digestion the DNAs from three transformants, It was found that one of them is correct oriented (Figure 3.37, line 5), and others are wrong oriented (Figure 3.37, line 4 and 6). The new clone that has correct oriented mutated insert was saved and named as HB101/pOX15N390A.

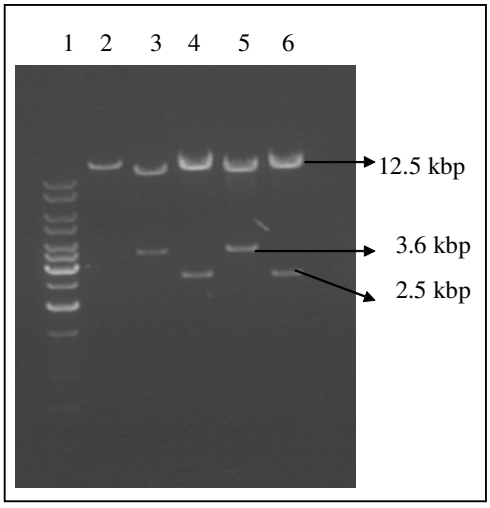

Figure 3.37: 2.8 kbp fragment orientation test of by digesting of transformant DNAs with *Hind*III. Line1: marker; line 2: uncut pOX15 DNA; line 3: pOX15/*Hind*III digested control DNA; line 4 and line 6: 12.5 kbp and 2.8 kbp fragments of pOX15-1/*Hind*III and pOX15-3/*Hind*III (wrong oriented insert); line 5: 3.6 kbp and 11.7 kbp fragments of pOX15-2/HindIII (correct oriented insert).

3.7.4 Transformation of the pOX15N390A into *R. capsulatus*

The pOX15N390A plasmid DNA was transferred into *R. capsulatus* strain, GK32 lacking *NO'* part of the *ccoNOQP* structural gene of cbb_3 oxidase, by three parental mating in the presence of HB101/pRK2013 cells. Transconjugants were selected based on tetracycline resistance. Four transconjugants were selected and kept at -80 ºC for further analysis such as cbb_3 oxidase respiratory phenotype by NADI staining.

3.7.5 Testing of the cbb_3 Oxidase Phenotype of GK32/pOX15N390A

After NADI staining of the wild-type (MT1131), control mutant (GK32), complemented control mutant (GK32/pOX15) and generated mutant (GK32/pOX15N390A) colonies we found that MT1131, and pOX15/GK32 are $NADI^{positive}$, and GK32 is $NADI^{negative}$ as expected, but the desired **GK32/pOX15N390A** mutants is **$NADI^{negative}$** (Figure 3.38). The GK32/pOX1N390A colonies did not turn blue compared with wild type which turns in blue within 30 seconds. NADI staining phenotype of this mutant indicates that the asparagine at position 390 must be critical amino acid for enzyme activity.

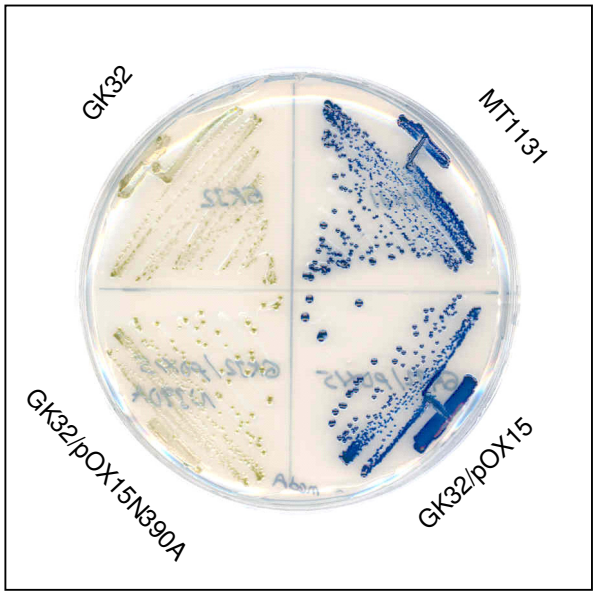

Figure 3.38: NADI-stainined GK32/pOX15N390A plate. MT1131, wild type (NADI^{positiv}); GK32, control mutant (NADI^{negative}); GK32/pOX15, complemented control mutant (NADI^{positive}); **GK32/pOX15N390A,** generated mutant (**NADI^{negative}**).

3.7.6 Analysis of the Cytochrome Profiles of GK32/pOX15N390A Mutant

The desired mutant GK32/pOX15N390A together with wild type, MT1131; mutant, GK32; complemented mutant, GK32/pOX15 were analyzed for their *c*-type cyt content using TMBZ/SDS-PAGE analysis. After TMBZ staining of the SDS-PAGE, it was found that subunits of the GK32/pOX15N390A mutant are almost the same with those of the controles, GK32, c_o and p_o subunits of the cbb_3 oxidase are absent (Fig. 3.39). It seems that asparagine at position 390 is important for cyt cbb_3-type oxidase assemly.

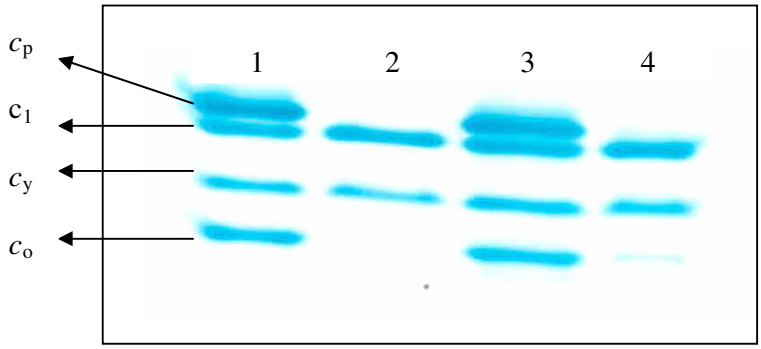

Figure 3.39: Cytochrome *c* profle of GK32/pOX15N390A mutant. TMBZ/SDS-PAGE analysis of *c*-type cyts from various *R. capsulatus* strains obtained from cells grown on entiched MPYE medium (100 µg of membrane proteins were loaded per lane). Lane 1, MT1131; lane 2, GK32; lane 3, GK32/pOX15; and line 4, **GK32/pOX15N390A**. Cyt c_p and c_o are the subunits II and III of cyt cbb_3 oxidase, and cyts c_1 and c_y correspond to the cyt c_1 subunit of the bc_1 complex and the membrane-attched electron carrier c_y, respectively.

3.8 Construction and Analysis of the GK32/pOX15T396A Mutant

3.8.1 Sequencing of the pMOZIT396-3 Mutant

The pMOZ1T396-3 was sequenced by using 578F primer at İontek Company, Istanbul. When obtained sequence was compared with the nucleotide sequence of the cbb_3 oxidase from gene data bank, it was found that pMOZ1T396-3 plasmid DNA has a desired mutation (ACG)instead of threonine codon (GCG) and it is long enough to see cloning restriction site (Figure 3.40, row 1 and 6), *Bsa*AI, and there is no mutation other than desired one. The mutated codon is underlined (Figure 40, row 5). The pMOZ1T396-3 clone having alanine amino acid instead of threonine at site 396 was named as pMOZIT396A and stored at -80 ºC.

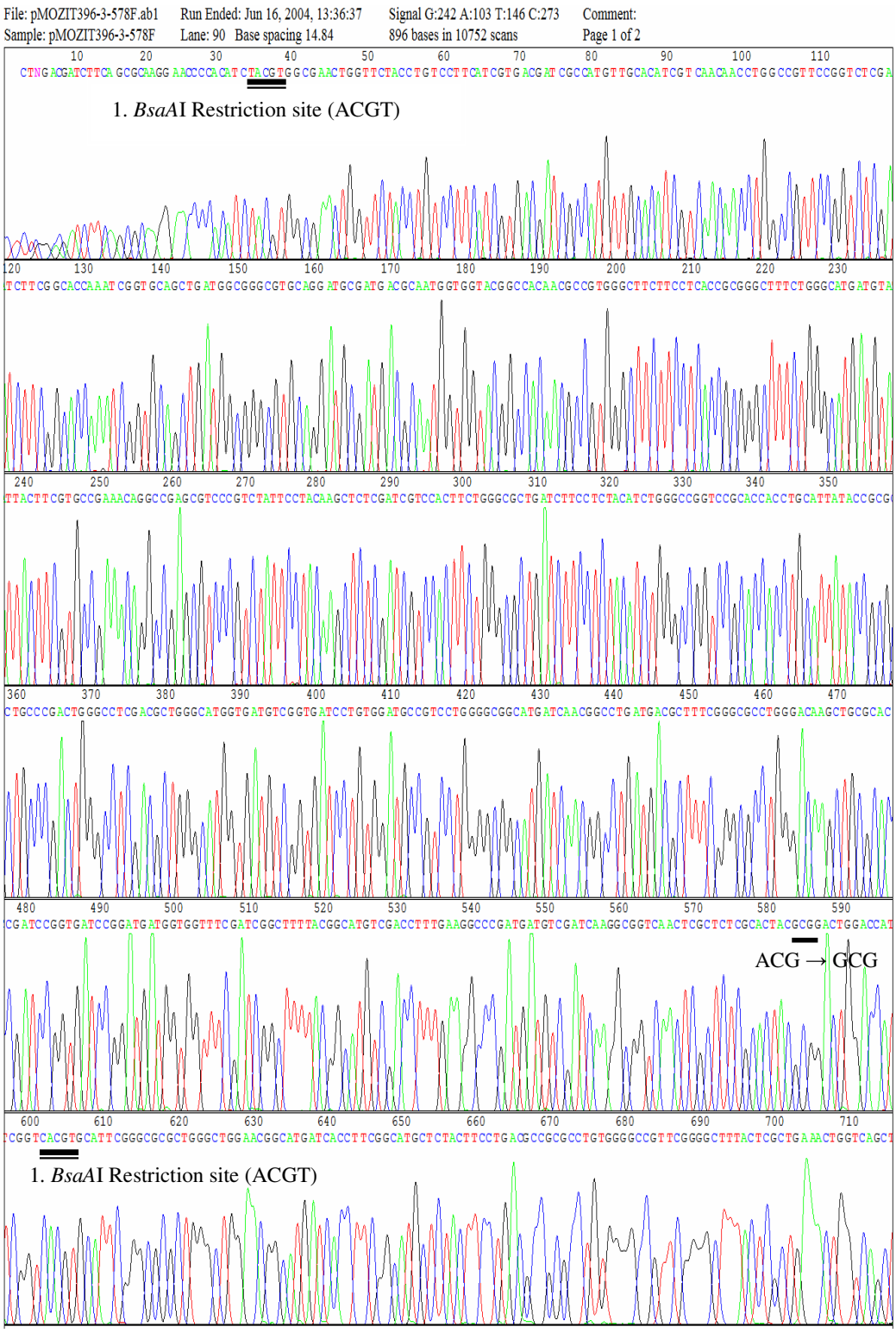

Figure 3.40: The partial sequence of pMOZIT396-3 transformant. The **ACG** codon was converted to **GCG** codon. Mutation and *Bsa*AI restriction sites were underlined.

3.8.2 Replacement of the 0.6 kbp Fragment of pMOZII with that of pMOZIT396A DNA

To replace 0.6 kbp fragment of pMOZII with that of pMOZIT396A, pMOZII and pMOZIT396A DNAs were digested with *Bsa*AI. The *Bsa*AI digested DNA samples were loaded on 1% agarose gel and resulting fragments, 0.6 kbp, 1.1 kbp and 4.0 kbp fragments were separated (Figure 3.41-A and B). Then 0.6 kbp insert fragments were isolated from 1% agarose gel (Figure 3.41.C). Then 0.6 kbp mutated fragment was inserted into 6.2 kbp vector at 22 ºC for two hours. Finally 5 µl ligation mix was transformed into HB101 cells. Transformants were selected based on the size of the clone, 6.8 kbp in size.

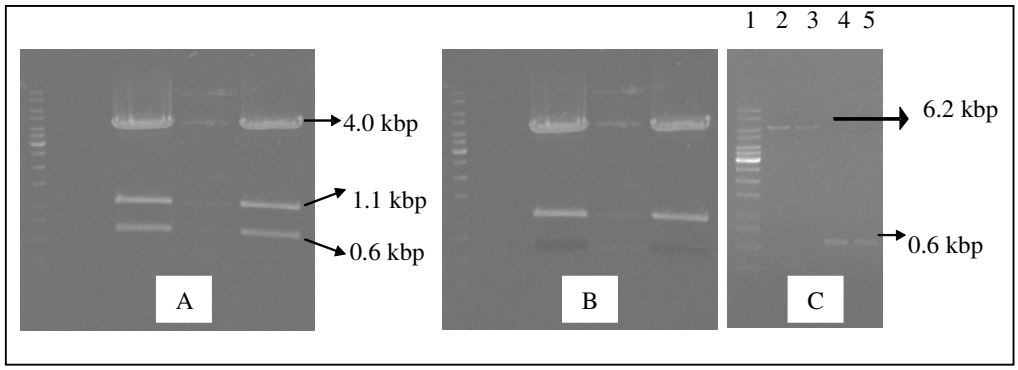

Figure 3.41: Isolation and purification of 0.6 kbp fragment of *Xho*I digested pMOZIT396-3. **A**. Separation of 4.0 kbp, 1.1 kbp and 0.6 kbp fragments of *Bsa*AI digested pMOZIT396A. **B**. Isolation of 0.6 kbp fragment from agarose gel. **C**. Determination of the amount of gel purified 0.6 kbp fragments isolated from pMOZIT396A/B*sa*AI DNA and 6.2 kbp fragments isolated from pMOZII DNA on 1% agarose gel. Line 1: marker; line 2 and line 3: 6.2 kbp vector (20ng/µl); line 4 and line 5: 0.6 kbp inserts (30ng/µl and 20ng/µl, respectively).

To select the clone that have correct oriented insert, plasmid DNAs were isolated from three transformants then they were digested with *Sal*I. After digestion the DNAs from three transformants, It was found that one of them is correct oriented (Figure 3.42, line 4), and others are wrong oriented (Figure 3.42, line 5 and 6). The new clone that has correct oriented mutated insert was saved and named as pMOZII/pOX15T396A.

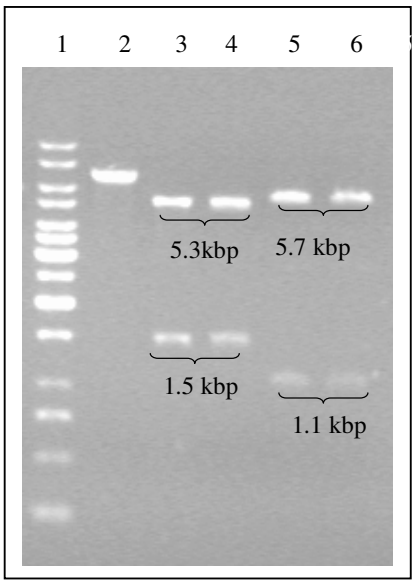

Figure 3.42: 0.6 kbp fragment orientation test by digestion of pMOZIIT396A with *Sal*I. Line 1: marker; Line 2: 6.8 kbp pMOZII/*Cla*I linear DNA as a control; line 3: pMOZII/*Sal*I control DNA; Line 4: 5.3 kbp and 1.5 kbp fragments of pMOZIIT396A-1/*Sal*I DNA (correct oriented insert); line 5 and line 6: 5.7 and 1.1 kbp fragments of pMOZIIT396-2/*Sal*I and pMOZIIT396-3/*Sal*I, respectively (wrong oriented inserts).

3.8.3 Replacement of the 2.8 kbp *NO'* Fragment of pOX15 with that of the pMOZIIT396A

To replace 2.8 kbp fragment of pOX15 vector with mutated one of the pMOZIIT396A, pMOZIIT396A with *Xho*I restriction enzyme. The *Xho*I digested samples were loaded on 1% agarose gel. The resulting 2.8 kbp and 4.0 kbp fragments were separated on 1 % agarose gel (Figure 3.43.A and B). Then 2.8 kbp fragment from pMOZIIT396A was isolated from the agarose gel and also amount of the DNAs were determined by loading of 1 µl DNA on 1% agarose gel (Figure 3.43.C). Gel purified insert and vector were ligated in 20 µl volume at 4 ºC overnight and at 22 °C for half hours. Then 5 µl ligation mixes were transformed into 100 µl HB101 cells. Transformants were selected based on clone size, 15.3 kbp and tetracycline resistance.

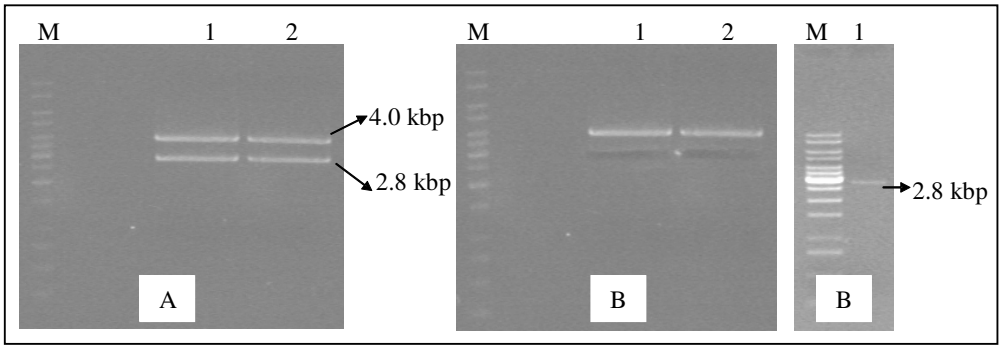

Figure 3.43: Isolation and purification of 4.0 kbp and 2.8 kbp fragments of *Xho*I digested pMOZIIT396A fragments (line 1 and 2)**. A**) Separation of 4.0 kbp and 2.8 kbp fragments of *Xho*I digested pMOZIIT396A. **B**) Isolation of the 2.8 kbp fragments from agorose gel. **C**) Determination of the gel purified 2.8 kbp fragments on 1% agarose gel. Line 1 has 20ng/µl 2.8 kbp insert DNA. M: marker.

To select the clone that have correct oriented insert, plasmid DNAs were isolated from three transformants then they were digested with *Hind*III. After digestion of the plasmid DNAs from these transformants, It was found that one of them are correct oriented (Fig. 3.44, line 4), and other is wrong oriented (Figure 3.44, line 5). The last one does not have any insert (line 6). The new clone that has correct oriented mutated insert was saved and named as HB101/pOX15T396A.

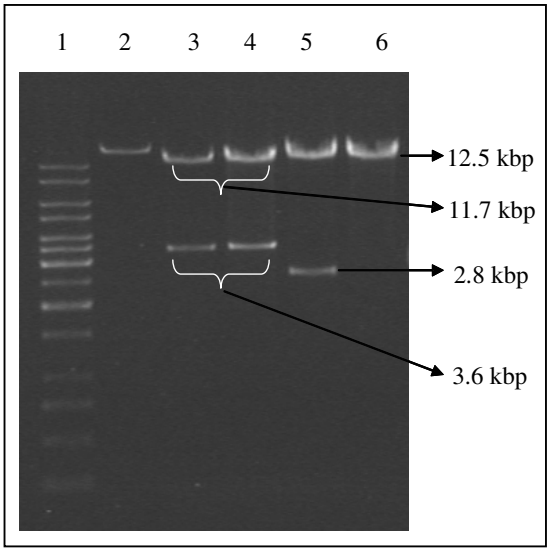

Figure 3.44. 2.8 kbp fragment orientation test by digestion of transformant DNAs with *Hind*III. Line 1: marker; line: linear pOX15/*Cla*I DNA. Line 3: 11.7 kbp and 3.6 kbp fragments of pOX15/*Hind*III control DNA; line 4: 11.7 kbp and 3.6 kbp pOX15T396-1/*Hind*III DNA fragments (correct oriented insert); line 5: 12.5 kbp and 2.8 kbp fragments of pX15T396-2/*Hind*III DNA fragments (wrong oriented insert); line 6: just 12.5 kbp pX15T396-3/*Hind*III DNA fragment (self ligation).

3.8.4 Transformation of the pOX15T396A into *R. capsulatus*

The pOX15T396A plasmid DNA was transferred into *R. capsulatus* strain, GK32 lacking *NO'* part of the *ccoNOQP* structural gene of cbb_3 oxidase, by three parental mating in the presence of HB101/pRK2013 cells. Transconjugants were selected based on tetracycline resistance. Four transconjugants were selected and kept at -80 ºC for further analysis such as cbb_3 oxidase respiratory phenotype by NADI staining.

3.8.5 Testing of the cbb_3 Oxidase Phenotype of GK32/pOX15T396A

After NADI staining of the wild-type (MT1131), control mutant (GK32), complemented control mutant (GK32/pOX15) and generated mutant (GK32/pOX15T96A) colonies we found that MT1131, and GK32/pOX15 are $NADI^{positive}$, and GK32 is $NADI^{negative}$ as expected, but the desired **GK32/ pOX15T396A** mutant is **$NADI^{positive}$** (Figure 3.45). The GK32/pOX15T396A colonies turned blue compared with wild type which turns in blue very quickly. NADI staining phenotype of this mutant indicates that the threonine at site 396 is not critical amino acid for cbb_3-type oxidase activity.

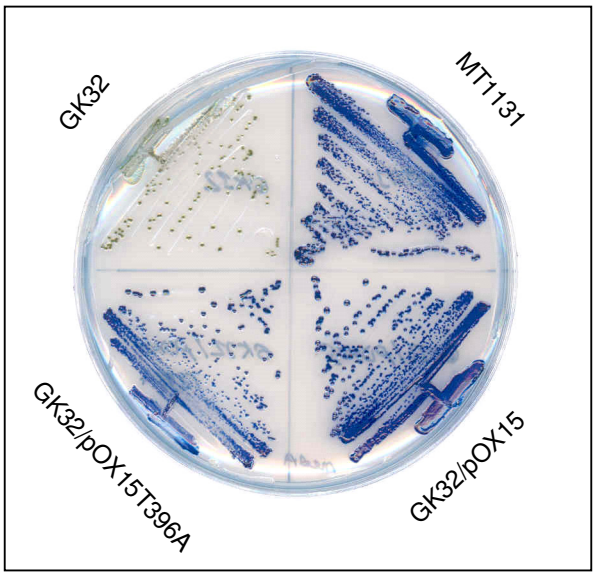

Figure 3.45: NADI-stainined GK32/pOX15N390A plate. MT1131, wild type (NADI^{positiv}); GK32, control mutant (NADI^{negative}); GK32/pOX15, complemented control mutant (NADI^{positive}); and **GK32/pOX15T396A,** generated mutant (**NADI^{positive}**).

3.8.6 Analysis of the Cytochrome Profiles of GK32/pOX15T396A Mutant

After TMBZ staining of the Shägger type SDS-PAGE gel on which 100 µg MT1131, GK32, GK32/pOX15, GK32/pOX15T396A chromatophore were loaded, it was found that subunits of the GK32/ pOX15T396A mutant are almost the same with those of the controles, MT1131 and GK32/pOX15 (Figure 3.46). This result indicates that threonine conserved amino acid at position 396 is not important for assemly of the cyt *cbb*$_3$-type oxidase.

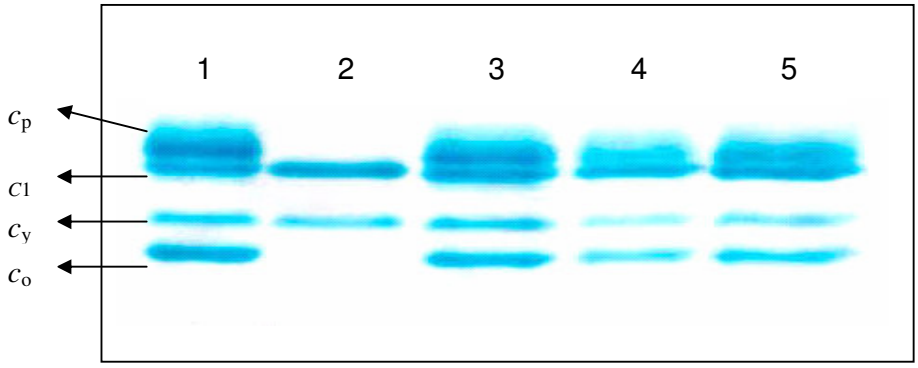

Figure 3.46: Cytochrome *c* profle of GK32/pOX15T396A mutant.TMBZ/SDS-PAGE analysis of *c*-type cytochromes from various *R. capsulatus* strains obtained from cells grown on enriched MPYE medium (100 µg of membrane proteins were loaded per lane). Lane 1, MT1131; lane 2, GK32; lane 3, pOX15/GK32; and line 4, **GK32/pOX15T396A** (80 µg sample was loaded)**;** lane 5 (100 µg) **GK32/pOX15T396A**. Cyt c_p and c_o are the subunits II and III of cyt cbb_3 oxidase, and cyts c_1 and c_y correspond to the cyt c_1 subunit of the bc_1 complex and the membrane-attched electron carrier c_y, respectively.

Phenotipic and genetic characterization of positive and negative controls MT1131, GK32 and GK2/pOX15, and targeted mutants, GK2/pOX15S333A, GK2/pOX15S340A, GK2/pOX15T350A, GK2/pOX15N390A and GK2/pOX15-T394A were summarized in table 5.1.

Table 5.1: Summary of the NADI staining and SDS-PAGE/TMBZ staining results of Wild type (MT1131), positive and negative control mutants (GK32, GK32/pOX15) and targeted mutants, GK32/pOX15S333A, GK32/pOX15S340A, GK32/pOX15T350A, GK32/pOX15N390A and GK32/pOX15T396A).

R. capsulatus strains	cbb_3 oxidase activity based on NADI staining	Cyt. *c* profile based on SDS-TMBZ staining c_p	c_o	Reference
MT1131	+	+	+	Koch et.al., (1998)
GK32	-	-	-	“
GK32/pOX15	+	+	+	This work
GK32/pOX15S333A	slow	+	+	“
GK32/pOX15S340A	+	+	+	“
GK32/pOX15T350A	+	+	+	“
GK32/pOX15N390A	-	-	small amount	“

DISCUSSION

The heme-copper oxidases, HCOs, are terminal respiratory oxidases. HCOs are represented in all three kingdoms of life and account for the reduction of more than 90% of the oxygen in the biosphere [Garcia et al., 1994]. These enzymes comprise a super family which utilizes different substrates (quinones, cyt *c*'s, or HiPIP Fe-S proteins) and includes members with different heme components such as hemes A, B, O, or C [Garcia et al., 1994*;* Ferguson et al., 1996]. One heme and the copper ion form a dinuclear center, the active site, where molecular oxygen is reduced to water.

Analysis of the subunit I amino acid sequences of HCO from twenty-six micro organisms including archea and bacterial suggested that these enzymes could be classified in three subfamilies [Pereira et al., 2001]. The *Type A* sub-family included the well-studied cytochromes aa_3 from *P. denitrificans* and *R. sphaeroides* and the quinol oxidase cyt bo_3 of *E. coli*. *Type B* enzymes are typified by the ba_3 type oxidase of *T. thermophilus*, while the *Type C* enzymes are a highly distinctive class of bacterial HCOs, the cyt cbb_3 oxidases that are found only in proteobacteria where they are presumed to play role in microaerobic respiration. That study also clearly revealed that especially sixteen amino acids in subunit I of bacterial HCOs are highly conserved [Pereira et al., 2001].

All of these HCO are all pumps proton, and it is this aspect which has motivated good research interest on these enzymes. For example, X-ray structures of several heme-copper oxidases have been determined [Soulimane et al., 2000; Yoshikawa et al., 2000]. Although reported structures of them have propelled research forward, still some fundamental questions are left such as how the proton pump works and how it is coupled with the reduction of O_2 to H_2O remain still a mystery [Michel, S., 1999]. Three putative proton-conducting input pathways have been identified in the X-ray structures [Yoshikava et al., 1998; Gennis, R. B., 1998]. These are called the K-channel, D-channel and the H-channel. The names are derived from conserved amino acid residues within each of the putative channels. The H-channel is proposed to be important for conveying pumped protons across the membrane, but only for the oxidases of animals [Yoshikava et al., 1998]. The K-channel and the D-channel, on the other hand, are observed in both the prokaryotic and eukaryotic oxidase structures [Tsukihara et al., 1996; Yoshikava et al., 1998; Ostermier et al., 1997], and the importance of these two channels in proton input to the enzyme is supported by extensive functional analysis of mutants.

The D-channel is defined by an aspartic acid (D132) near the protein surface (bacterial cytoplasm) and a glutamic acid (E286) about 25 Å away from D132 and 12 Å from the heme-copper center. Between these two acidic residues it is a chain of water molecules that presumably provides a pathway to facilitate proton transfer. The K-channel, so-called because of a critical lysine residue (K362) in its center, begins at a glutamic acid residue in subunit II (E101) on the cytoplasmic surface of the enzyme and terminates at a tyrosine (Y288) at the

heme-copper oxygen reduction site [Pawate et al., 2002]. This channel includes threonines (T352) and (T359), and leads to the hydroxyl group of tyorosine (Y288) at the active site. Since Y288 (cross-linked to H284, see above) is in a position to be a direct proton or hydrogen donor to the active site, it is reasonable to consider this is a proton pathway for the delivery of at least one of the substrate protons [Pawate et al., 2002]. Mutations within the K-channel result in greatly reduced steady-state cyt *c* oxidase activity. The K362M mutant is virtually inactive (<0.05% turnover). Those mutants with residual activity (e.g., T352A, T359A) pump protons with the same stoichiometry as does the wild-type enzyme on *bo*-type quinol oxidase in *E. coli* [Fetter et al., 1995]. More interesting, perhaps, is that none of the canonical residues of the D-channel is present in all cbb_3 oxidases. K-channel is much more conserved than the D-channel, especially the residues equivalent to threonine (T351) and serine (S291) [Piearare et al., 2001].

In the absence of either a three-dimensional structure of a cbb_3-type oxidase or experiments that inform on the roles of conserved residues in CcoN, it is not yet possible to conclude whether cytochrome cbb_3 oxidases have independently evolved a distinctive method for coupling oxygen reduction to proton translocation. Alternatively, the mechanism of energy transduction might be functionally conserved in the cbb_3-type oxidases, even though key residues of the D- and K-channels are apparently missing [Pereira et al., 2001].

In the *R capsulatus* cbb_3 oxidase, two potential K-channel residues in TM helix VIII, serine (S333) and threonine (T350), are absolutely conserved while

threonine/serine represents a third potential K-channel residue serine (S340) in almost all other oxidases. Substitution of the threonine residues, (T352) and (T359) which are equivalent to serine (S333) and threonine (S340) respectively, by alanine in *R. sphaeroides* cyt aa_3, indicates the importance of these residues for the (re-) reduction of the active site of the oxidase during turnover [Hosler et al., 1996]. The role of threonine (T350) is not known. Two other residues in the periplasmic loop between TM helices IX and X, asparagine (N390) and threonine (T396), are also functionally conserved and, in the case of the type A HCO (*R. sphaeroides*), have been proposed to play role in the exit of pumped protons and capping the active site respectively [Qian et al., 1997].

Serine mutation (S333A): It has already been pointed out that helix VIII of bo_3-type quinol oxidase of *E. coli has* a highly conserved face containing several polar residues which could play a role in facilitating proton and/or water movement during turnover of the oxidase. Mutations of highly conserved polar residue in helix VIII of the *E. coli*, threonine (T352) (homologous to serine (S333) of cbb_3 oxidase in *R. capsulatus*), was found to eliminate oxidase activity [Jefferey et al., 1993]. Replacement of serine (S333) of cbb_3-type oxidase in *R. capsulatus* with alanine decreased the activity of the enzyme, but it did not affect the cbb_3 oxidase assembly.

Serine mutation (S340A): The threonine (T351) in *P. denitrificans* which is homologous to serine (S340) indicates that it is only part of the alternative K-channel. The K-pathway seems to be essential for the reduction of heme a_3 in *P.*

denitrificans [Michel et al., 1998], but the reduction of Cu_B upon the first electron transfer is still possible [Junemann et al., 1997]. It would transfer the proton via threonine (T351), the hydroxy group of the side chain of heme a_3 to tyrosine (Y280), which is located very close the active site in *P. Denitrificans* [Michel et al., 1998-1999]. Substitution of the equivalent residues threonines, (T352) and (T359), which are homologous to serine (S333) and threonine (T340) in *R .capsulatus*, with alanine in *R. sphaeroides* cytochrome aa_3 indicated to the importance of these residues for the (re-)reduction of the active site of the oxidase during turnover. Threonine (T352) might be involved direct proton donation to an oxygenated intermediate during catalysis. Threonine (T352) in particular, may be indirect contact with the binding pocket encompassing the heme-copper binuclear center [Jefferey et al., 1993]. Our results indicated that serine at position 340 does not effect enzyme activity.

Asparagine mutation (N390A): The asparagine (N399) is located in the loop region between the transmembrane helices IX and X, near the periplasmic interfaces between subunits I and II of the complex of *P. denitrificans* aa_3-type oxidase. Replacements at this position have been studied: both the glutamate and the asparagine result in a moderate reduction of the turnover rate (residual activity between 40% and 60%), without any major effect on the stoichiometry of protons pumped in the reconstituted enzyme [Qian et al., 1997]. The asparagines (N399) residue on aa_3 type oxidase of *P. denitrificans* plays an essential role at the subunit I/II interface on the periplasmic side [Pfitzner et al., 2000]. Previously asparagines (N399) had been assumed to play a role at the potential exit site [Iwata et al., 1995; Thomas et al., 1993; Behr et al., 1998]. However, the data

obtained from *P. denitrificans* enzyme do not agree with the recent conclusion [Qian et al., 1997], which excluded any role for this residue in the *R. sphaeroides*. *P. denitrificans* cyt *c* oxidase in terms of the N and E substitutions, showed that a hydrophobic residue in this position may cause a structural change, possibly altering the H-bonding pattern around the propionate of heme a_3 [Behr et al., 2000]. Asparagine (N390A) mutation in *R. capsulatus* has lack of stability.

Threonine mutations (T350A and T396A): At T350 and T396 position of subunit I of cbb_3-type oxidase in *R. capsulatus*, there are threonine or serine residue in all oxidases; however, there are no mutagenesis data reported so far on these residues of any type of cyt *c* oxidase. Substitution of these two threonines by alanine did not change the cbb_3-type oxidase activity and assembly.

Of the five mutations that were constructed in the present work, four did not affect enzyme stability or assembly. The lack of stability of the asparagines (N390A) mutant was a surprise given that a mutation of the equivalent residue in the type A oxidase from *R. sphaeroides* was benign [Qian et al., 1997]. Of the four complexes that assembled normally, three showed normal activity in a NADI plate assay, although it is important to note that this method would not necessarily reveal changes in catalytic activity. A mutation serine (S333A) showed impaired oxidase activity that could be commensurate with impaired proton movements.

CONCLUSION AND FUTURE OUTLOOK

Our results showed that the asparagine (N390A) residue on the periplasmic side of subunit I of *cbb*$_3$-type oxidase plays an essential role for enzyme activity and assembly. One further position, serine (S333A) located at helix VIII, showed almost complete loss of enzyme activity. Even though serine (S340) and threonine (T350) at position VIII and threonine (T396) on the loop between helix IX and X of *cbb*$_3$-type oxidase in *R. capsulatus* conserved in all type of heme-copper oxidases, our data clearly demonstrated that exchange of these amino acids with alanine have not altered the activity and assembly of *cbb*$_3$ oxidase (Table 5.1).

Two *cbb*$_3$ oxidases containing the serine (S333A) and asparagine (N390A) mutants were considered to be good candidates for purification and further analysis for understanding structural changes in the catalytic center. To further determine the functions of the asparagine (N390) and serine (S333), biochemical, spectroscopic and crystallographic studies are necessary. To determine if the amino acid substitutions have any previously undetermined effects on catalytic activity, possibly due to either perturbation of the proton uptake pathways or changes in the properties of the redox centers. Membrane vesicle proteins from mutants could be used in the future experiments for characterization of the effects of these mutations on the *cbb*$_3$ oxidase activity.

1. Effect of mutations on the steady state reduction of oxygen

Both the soluble cytochrome c_2 and the membrane associated cytochrome c_y can serve as an electron donor to cytochrome cbb_3 oxidase in *R. capsulatus* [Daldal et al., 2001]. The rate of oxygen reduction by mutants will be assessed in palaeographic assays using ascorbate and cytochrome c_2 as a specific and immediate electron donor. This experiment is not only anticipated to confirm the reduced activity of the S333A revealed by the NADI plate assay but also will indicate any smaller changes in catalytic activity of other mutations, S340A, T350A and T396A.

2. Low temperature UV/visible spectroscopy

Using ascorbate/TMPD as electron donors in the presence of myxothiazol (a specific inhibitor of the bc_1 complex); it is possible to specifically reduce the cytochrome cbb_3 oxidase. Consequently it is possible to determine reduced *minus* oxidised and reduced-CO *minus* reduced spectra of both the wild-type cytochrome cbb_3 oxidase and of the mutants. Recording these spectra at low temperature (77K) markedly improves the signal to noise ratio and can reveal considerable spectroscopic detail. These difference spectra will indicate any perturbations in the environments of the hemes *b* and b_3 in subunit I that result from of any of the mutations.

3. CO-recombination kinetics to the binuclear centre

The integrity of the active site in the mutant forms of the *cbb*$_3$ oxidase can be further probed by studying the kinetics of CO recombination to the reduced dinuclear centre. Briefly cytochrome *cbb*$_3$ will be specifically reduced in the membranes and exposed to carbon monoxide. The Fe (II)-CO will be broken by transient illumination with a laser and the kinetics of combination monitored at an appropriate wavelength [Pitcher et al., 2003]. Changes in the kinetics of recombination due to mutations will reflect perturbations to the environment of the active site (dinuclear centre).

4. Effect of mutations on proton movements

Membrane potential ($\Delta\psi$) can be determined in membrane vesicles isolated from *Rhodobacter* species by measuring the electrochromic response of the endogenous carotenoid pigments at either 528-511 nm (or at 503-487 nm in the case of "green mutants" such as MT1131) [Jackson et al. 1971]. A membrane potential should be established in response to pumping of protons by the *cbb*$_3$ oxidase when electrons are supplied to correctly orientated vesicles by ascorbate/cytochrome c_2 in the presence of myxothiazol [Bell et al. 1992]. Changes in the kinetics of the electrochromic response in the mutants compared with wild-type cytochrome *cbb*$_3$, either the rate at which $\Delta\psi$ is established or its magnitude, will indicate any perturbations in proton uptake pathways.

REFERENCES

Amesz, J., Knafff, D.B. (1988). Molecular Mechanisms of Bacterial Photosynthesis, Jhon Wiley & Sons, Chapter 3.

Aygün, S. (1999). *Rhodobacter capsulatus* Bakterisinde Sitokrom *c* Oksidaz Mutantlarının Eldesi ve Karakterizasyonu, Master Thesis.

Babcock, G.T., and Wikstrom, M. (1992). Oxygen activation and the conservation of energy in cell respiration, *Nature*, 356: 301-309.

Baccarini-Melandri, A., Zannoni, D., and Melandri, B.A. (1973). Energy transduction in photosynthetic bacteria. IV. Respiratory sites and energy conservation in membranes from dark-grown cells of *Rhodopseudomonas capsulata*. *Biochim. Biophys. Acta,* 314: 298-313.

Batut, J., Daveran-Mingot, M.L., David, M., Jacobs, J., Garnerone, A.M., Kah, D. (1989). *fixK*, a gene homologous with *fnr* and *crp* from *Escherichia coli*, regulates nitrogen fixation genes both positively and negatively in *Rhizobium meliloti*. EMBO J., 8: 1279-1286.

Behr, J., Michel, H., Mantele, W., Hellwig, P. (2000). Functional Properties of the Heme Propionates in Cytochrome *c* Oxidase from *Paracoccus denitrificans.* Evidence from FTIR Difference Spectroscopy and Site-Directed Mutagenesis. *Biochemistry*, 39: 1356-1363.

Bell, L.C., Richardson, D.J., and Ferguson, S.J. (1992) *J. Gen. Microbiol.,* 138: 437-443

Bosna, G., Braster, M., Stouthamer, A.H. and Verseveld, H.W. (1987). Sub fractionation and characterization of soluble *c*-type cytochromes from

Paracoccus denitrificans cultured under various limiting conditions in the chemostat. *Eur. J. Biochem*., 165: 665-670.

Brander, P.J. Mc Evan, A. G. Kaplan, S. J. (1989). Expression of the *Rhodobacter sphaeroides* cytochrome c_2 structural gene. *J. Bacteriol*., 171, 360-368.

Caffrey, M.S. (1994). Strategies for the study of cytochrome *c* structure and function. *Biochimie,* 76: 622-630.

Caffrey, M.S. Cusanovich, M. A. (1994). Site-specific mutagenesis studies of cytochromes *c*. *Biochimica et Biophysica Acta*, 1187: 277-288.

Castresana, J., Lubben, M., Saraste, M., and Higgins, D.G. (1994). Evolution of cytochrome oxidase, an enzyme older than atmospheric oxygen, *EMBO J*., 13: 2516-2525.

Cusanovich, M., Meyer, T. and Tollin, G. (1988). In Adv. Inorganic Biochemistry, Vol. 7. Heme Proteins (Eichorn, G. and Marzilli, L., eds.), pp. 37-91, Elsevier, New York.

Daldal, F., Cheng, S., Applebaum, J., Davidson, E., and Prince, R.C. (1986). Cytochrome c_2 is not essential for photosynthetic growth of *Rhodopseudomonas capsulata*. *Proc. Natl. Acad. Sci.* USA, 83: 2012-2016.

Daldal, F., Mandaci, S., Winterstein, C., Myllykallio, H., Duyck, K., & Zannoni, D. (2001) *J Bacteriol* **183**, 2013-2024

Daldal, F., Davidson, E., and Cheng, S. (1987). Isolation of the structural genes for the Rieske Fe-S protein, cytochrome *b* and cytochrome c_1, all components of the ubiquinol: cytochrome *c* oxidoreductase complex of *Rhodopseudomonas capsulata*. *J. Mol. Biol*., 195: 1-12.

Davis, J. Donohue, T.J. Kaplan, S. (1988). Construction, characterization, and complementation of a Puf- mutant of *Rhodobacter sphaeroides*. J. *Bacteriol*., 170; 320-329.

Debus R.J., Feher G., and Okamara, N.Y. (1985). Complex of Reaction Center from *Rhodopseudomonas virdi*. R.26: Characterization and Reconstitution with H subunit, *Biochemistry*, 24: 2488-2500.

de Gier, J.-W., Lübben, M., Reijnders, N.M., Tipker, C.A., Slotboom, D.J., van Spanning, R.J.M., Stouthammer, A.H., and van der Oost, J. (1994). The terminal oxidases of *Paracoccus denitrificans*. *Mol. Microbiol*., 13: 183-196.

de Gier, J.-W.L., Schepper, M., Reijnders, W.N.M., van Dyck, S.J., Slotboom, D.J., Warne, A., Saraste, M., Krab, K., Finel, M., Stouthamer, A.H., van Spanning, J.R.J., van der Oost, M. (1996). Structural and functional analysis of aa_3-type and cbb_3-type cytochrome c oxidases of *Paracoccus denitrificans* reveals significant differences in proton pump design, *Mol. Microbiol*., 20:1247-1260.

Ditta, G. Schimidhauser, E. Yakopsen, P., Lu, X.W. Liang, D.R. Guiney, D. and Helinsky, D. (1985). Plasmids related to the broad host range vector, pRK290, useful for gene cloning and for monitoring gene expression. *Plasmid,* 13: 149-153.

D'Mello, R., Hill, S. and Poole, R.K. (1995). The oxygen affinity of cytochrome *b*o in Escherichia coli determined by the deoxygenation of oxyleghemoglobin and oxymyoglobin: Km values for oxygen are in the submicromolar range*, J. Bacteriol*., 177: 867-870.

Donohue, T.J., McEwan A.G., Van Doren, S., Crofts, A.R., and Kaplan, S. (1988). Phenotypic and genetic characterization of cytochrome c_2 deficient mutants of *Rhodobacter sphaeroides*. *Biochemistry*, 27: 1918-1925. Methods in Enzymology vol. 204: 459-485.

Donohue, T. J. Kaplan, S. (1991). Genetic techniques in *Rhodospirillaceae. Methods Enzymol*, 204: 459-485.

Eraso, J.A. and Kaplan, S. (2000). From Redox Flow to Gene Regulation: Role of the PrrC Protein of *Rhodobacter sphaeroides* 2.4.1. *Biochemistry*, 39: 2052-2062.

Ferguson-Miller, S., Babcock, G.T. (1996). Heme/cupper terminal oxidases. *Chem. Rev*., 96: 2889-907.

Fetter, R.J., Qian, J., Shapleigh, J., Thomas, J.W., Gargia-Horsman, A., Schmidt, E., Hosler, J., Babcock, T.G., Gennis, R.B., and Ferguson-Miller, S. (1995) Possible proton relay pathways in cytochrome *c* oxidase. *Prot.Natl. Acad. Sci.* USA192: 1604-1608.

Fischer, H.M. (1996). Environmental regulation of rhizobial symbiotic nitrogen fixation. *Trends Microbiol,* 4: 317-320.

Florens, L., Schmidt, B., McCracken, J. and Ferguson-Miller, S. (2001). Fast Deuterium Access to the Buried Magnesium/Manganese Site in Cytochrome *c* Oxidase. *Biochemistry*, 40: 7491-7497.

Garcia-Horsman, J.A., Barquera, B., Rumbley, J., Ma, J. and Gennis, R.B. (1994). The super family of heme-copper respiratory oxidases, *J. Bacteriol,* 176: 5587-6000.

Garcia-Horsman, J.A., Berry, E., Shapleigh, J.P., Alben, J.O., and Gennis, R.B. (1994). A novel cytochrome *c* oxidase from *Rhodobacter sphaeroides* that lacks Cu_A. *Biochemistry*, 33: 3113-3119.

Gennis, R.B. (1998). Multiple proton-conducting pathways in cytochrome oxidase and a proposed role for the active-site tyrosine. *Biochim. Biophys. Acta*, 1365: 241-248.

Gennis, R.B., Barquera, B., Hacker, B., Van, D.S.R, Arnaud, S., Crofts, A.R., Davidson, E., Gray, K.A., and Daldal, F. (1993). Journal of *Bioenergetics and Biomembranes*, 25: 195-209.

Gray, K.A., Grooms, M., Myllykallio, H., Moomaw, C., Slaughter, C., and Daldal, F. (1994). *Rhodobacter capsulatus* contains a novel *cb*-type cytochrome *c* oxidase without a Cu_A center. *Biochemistry*, 33: 3120-3127.

Gomes C.M, Backgren. C., Teixeira, M., Puustinen, A., Verkhovskaya, M.L., Wikstrom, M., Verkhovsky, M.I. (2001). Heme-copper oxidases with

modified D- and K-pathways are yet efficient proton pumps. FEBS Lett., 25: 159-64.

Gray, K.A., Daldal, F. (1995). Mutational Studies of the Cytochrome bc_1 Complexes. Kluwer Acadenmic Publishers, Netherlands. *Anoxigenic photosynthetic Bacteria*, 747-774.

Heidelberg, J.F., Eisen, J.A., Nelson, W.C., Clayton, R.A., Giwinn, M.L., Dodson, M.J., Haft, D.H., Hickey, E.K., Peterson, J.D., Umayam, L., Gill, S.R., Nelson, K.E., Read, T.D., Ettelin, H., Richardson, D., Ermoleava, M.D., Vamathevan, J., Bass, S., Qin, H., Dragoi, I., Sellers, P., McDonald, L., Utterback, T., Fleishmann, R.D., Nierman, W.C., and White, O. (2000). DNA sequence of both chromosomes of the cholera pathogen *Vibrio cholerae*. *Nature*, 406: 477-83.

Hosler, J. P., Fetter, J., Tecklenburg, M. M., Espe, M., Lerma, C., and Ferguson-Miller, S. (1992). Cytochrome aa_3 of *Rhodobacter sphaeroides* as a model for mitochondrial cytochrome *c* oxidase. Purification, kinetics, proton pumping and spectral properties. *J. Biol. Chem.,* 267: 24264-24272.

Iwata, S., Ostermeier, C., Ludwig, B., Michel, H. (1995). Structure at 2.8 Å resolution of cytochrome *c* oxidase from *Paracoccus denitrificans*. *Nature*, 376: 660-669.

Jenney, F.E., and Daldal, F. (1993). A novel membrane-associated *c*-type cytochrome, cyt c_y can mediate the photosynthetic growth of *Rhodobacter capsulatus* and *Rhodobacter sphaeroides*. *EMBO J*. 12:1283-1292.

Junnemann, S., Meunier, B., Gennis, R.B. (1997). Effects of Mutation of the Conserved Lysine-362 in Cytochrome *c* Oxidase from *Rhodobacter sphaeroides. Biochemistry,* 36: 14456-14464.

Kahn, D., David, M., Domergue, O., Daveran, M.L., Ghai, J., Hirsch, P.R., Batut, J. (1989). *Rhizobium meliloti fixGHIS* sequence predicts involvement of a specific action pump in symbiotic nitrogen fixation, *J. Bacteriol*., 171: 929-939.

Karpefors, M., Adelroth, P. and Brzezinski, P. (2000). Localized Control of Proton Transfer through the D-Pathway in Cytochrome *c* Oxidase: Application of the Proton-Inventory Technique. *Biochemistry*, 39: 6950-6856.

Keen, N. T. Tmaki, S. Kobayashi, D. and Trollinger, D. (1988). Improved broad-host-range plasmids for DNA cloning in Gram-negative bacteria. *Gene*, 70: 191-197.

Koch, H.G., Hwang, O., and Daldal, F. (1998). Isolation and characterization of *Rhodobacter capsulatus* mutants affected in cytochrome cbb_3 oxidase activity. *J. Bacteriol*., 180: 969-978.

Koch, H.G., Winterstein, C., Saribas, A.S., Alben, J.O., Daldal, F. (2000). Roles of the *ccoGHIS* gene products in the biogenesis of the cbb_3- type cytochrome *c* oxidase. *J. Mol. Biol.,* 297: 49-65.

Konstantinov, A.A., Siletsky, S., Mitchell, D., Kaulen, A. and Gennis, R.B. (1997). The roles of the two proton input channels in cytochrome *c* oxidase from *Rhodobacter sphaeroides* probed by the effects of site-directed mutations on time-resolved electrogenic intraprotein proton transfer. *Proc. Natl. Acad. Sci.* USA, 94: 9085-9090.

Lubben, M., Morand, K. (1994). Novel prenylated hemes as cofactors of cytochrome oxidases. Archaea have modified hemes A and O. *J. Biol. Chem.,* 269: 21473-21479.

Madigan, M.T., Martinko, J.M., Parker, Prentice Hall, J. (1997). Biology of Microorganisms, Prentice Hall, Upper Saddle River, NJ, 07458.

Mandon, K., Kaminski, P.A., Elmerich, C. (1994). Functional analysis of the *fixNOQP* region of *Azorhizobium caulinodans*. *J. Bacteriol.*, 176: 2560- 2568.

Meyer, T.E., and Donohue, T.J. (1995). Cytochromes, iron-sulfur, and copper proteins mediating electron transfer from the cyt bc_1 complex to photosynthetic reaction center complexes, p. 725. In R. E. Blankenship, M. T.

Madigan, and C. E. Bauer (ed.), Anoxygenic photosynthetic bacteria. *Kluwer Academic Publishers*, Dordrecht, Netherlands.

Michel, H., Behr, J., Harrenga, A., Kannt, A. (1998). Cytochrome *c* oxidase: Structure and Spectroscopy, Annu. Rev. Biophys. *Biomol. Struct*, 27: 329-56.

Michel, H. (1999). Cytochrome *c* Oxidase: Catalytic Cycle and Mechanisms of Proton Pumping-A Discussion. *Biochemistry*, 38: 15129-15140.

Moore G, Peltigrew G. (1990). In: Cytochromes *c: Erobaionary. Structural and Physiological Aspects.* Springer-Verlag, Berlin

Myllykallio., Koch, H.G., Daldal, F. (1999). Membrane-Associated *c*-type cytochromes of *Rhodobacter capsulatus* involved in photosynthesis and Respiration, Plenum Publishers, New York.

Myllykallio, H., Zannoni, D., and Daldal, F. (1999). *Rhodobacter sphaeroides* cyt c_y is a membrane-attached electron carrier that is deficient in photosynthesis but proficient in respiration. *Proc. Natl. Acad. Sci.* USA, 96: 4348-4353.

Myllykallio, H., Liebl, U. (2000). Dual role for cytochrome cbb_3 oxidase in clinically relevant Proteobacteria. *Trends Microbiol*., 8: 542-543.

Namslauer, A., Pawate, A.S., Gennis, R.B., Brzezinski, P. (2003). Redox-coupling proton translocation in biological systems: Proton shuttling in cytochrome *c* oxidase, *PNAS,* 100: 15543-47.

Nitschke, W. and Dracheva, S.M. (1995). Reaction center associated cytochromes in: Anoxygenic Photosynthetic Bacteria Blankenship, R.E., Madigan, M.T. and Bauer, C.E., eds., Kluwer Academic Publ., Dordrecht, Chapter 36, pp. 775-805.

Oh, J. and Kaplan, S. (1999). The cbb_3 Terminal Oxidase of *Rhodobacter sphaeroides* 2.4.1: Structural and Functional Implications for the Regulation of Spectral Complex Formation. *Biochemistry*, 38: 2688-5666.

Oh, J. Kaplan, S. (2002). Oxygen Adaptation. *The Journal of Biological Chemistry*, 277: 16220-16228.

Ostermier, O., Iwata, S., Michel, H. (1996). Cytochrome *c* oxidase, *Current Opinion in Structural Biology*, 6; 460-466.

Ostermeier, C., Harrenga, A., Ermler, U., Michel, H. (1997). Structure at 2.7 A resolution of the *Paracoccus denitrificans* two-subunit cytochrome oxidase complexed with an antibody Fv fragment, *Proc. Natl. Acad. Sci.* USA, 94: 10547-10553.

Pawate, A.S., Morgan, J., Namslauer, A., Mills, D., Brzezinski, P., Ferguson-Miller, S., and Gennis, R.B. (2002). A Mutation in Subunit I of Cytochrome Oxidase from *Rhodobacter sphaeroides* Results in an Increase in Steady-State Activity but Completely Eliminates Proton Pumping. *Biochemistry,* 41: 13417 -13423.

Pereira, M.M., Santana, M., Tixeira, M. (2001). A novel scenario for the evolution of heme-copper oxygen reductases. *Biochimica at Biophysica Acta,* 1505: 185-208.

Pettigrew, G., Moore, G.M. (1987). *In Cytochromes c: Biological Aspects.* Springer-Verlag, Berlin.

Pfitzner, U., Hoffmeier, K., Harrenga., Kannt, A., Hartmut, M., Bamberg, E., Oliver, M., Richter, H., Ludwig, B. (2000). Tracing the D-Pathway in Reconstituted Site-Directed Mutants of Cytochrome *c* Oxidase from *Paracoccus denitrificans*. *Biochemistry*, 39: 6756-6762.

Pielak, G., Mauk, G., Smith, M. (1985). Site-directed mutagenesis of cytochrome *c* shows that an invariant Phe is not essential for function. *Nature*, 313: 152-154.

Pitcher, R.S., Brittain, T., Watmough, N.J. (2002). Cytochrome cbb_3 oxidase and bacterial microaerobic metabolism, *Biochem. Soc. Trans.*, 30: 653-658.

Pitcher, R.S., Watmough, N.J. (2003). The bacterial cytochrome cbb_3 oxidases *Biochimica et Biophysica Acta,* 1655: 388-399.

Preisig, O., Anthamatten, D., Hennecke, H. (1993). Genes for a micro aerobically induced oxidase complex in *Bradyrhizobium japonicum* are essential for a nitrogen-fixing endosymbiosis, *Proc. Natl. Acad. Sci*., USA, 90: 3309- 3313.

Preisig, O., Zufferey, R., Hennecke, H. (1996). The *Bradyrhizobium japonicum fixGHIS* genes are required for the formation of the high affinity cbb_3-type cytochrome oxidase, *Arch. Microbiol*., 165: 297-305.

Preisig, O., Zufferey, R., Thony-Meyer, L., Appleby, C.A., Hennecke, H. (1996). A high affinity cbb_3-type cytochrome oxidase terminates the symbiosis specific respiratory chain of *Bradyrhizobium japonicum*, *J. Bacteriol*., 178: 1532-1538.

Prince, R.C. (1990). Bacterial photosynthesis: From Photons to Δp The Bacteria, Vol. XII. Chapter: 5.

Puistinen, A. and Wikstrom, M. (1999). Proton exit from the heme-copper oxidase of *Escherichia coli***.** *Proc. Natl. Acad. Sci*., USA, 96: 35-37.

Qian, J., Shi, W., Pressler, M., Hoganson, C., Mills, D., Babcock, G.T., and Ferguson-Miller, S. (1997). Aspartate-407 in *Rhodobacter sphaeroides* Cytochrome *c* Oxidase Is Not Required for Proton Pumping or Manganese Binding. *Biochemistry*, 36: 2539 – 2543.

Rich, P.R. (1995). Towards an Understanding of the Chemistry of Oxygen Reduction. *Aust. J. Plant Physiol*., 22: 479-486.

Richter, O.M., H.Ludwig, B. (2003). Cytochrome *c* oxidase – structure, function, and physiology of a redox-driven molecular machine *Rev Physiol Biochem Pharmacol.*, 147: 47-74.

Riistama, A., Puustinen, A., Verkhovsky, M.I., Morgan, J.E., Wikstrom, M. (2000). Binding of O_2 and Its Reduction Are Both Retarded by Replacement

of Valine 279 by Isoleucine in Cytochrome *c* Oxidase from *Paracoccus denitrificans*. *Biochemistry,* 39: 6365-6372.

Ruitenberg, M., Kannt, A., Bamberg, E., Fendler, K., and Michel, H. (2002). Reduction of cytochrome *c* oxidase by a second electron leads to proton translocation. *Nature*, 417: 99–102.

Saraste, M. (1990). Structural features of cytochrome oxidase, Q. *Rev. Biophys.,* 23: 331-366.

Sarıbaş, A.S., Mandacı S., and Daldal, F. (1999). An Engineered Cytochrome b_6 c_1 Complex with a Split Cytochrome B is able to Support Photosynthetic Growth of *Rhodobacter capsulatus*. *Journal of Bacteriology*, 181: 5365-5372.

Sasaki, T., Notokawa, Y., and Kikuchi, G. (1970). Occurrence of both *a*-type and *o*-type cytochromes as the functional terminal oxidases in *Rhodopseudomonas sphaeroides*. *Biochim. Biophys. Acta,* 197: 284-291

Saunders, V.A. (1992). Genetics of the photosynthetic prokaryotes. New York.

Shapleigh, J.P., Hill, J.J., Alben, J.O. and Gennis, R.B. (1992). Spectroscopic and genetic evidence for two heme-Cu-containing oxidases in *Rhodobacter sphaeroides*. *J. Bacteriol*., 174: 2338-2343.

Simon, R., Priefer, U. and Puhler, A. (1983). *Biol technology*, 1: 784

Sistrom W.R., Macaluso, A. and Pledger, R. (1984). Mutants of *Rhodopseudomonas sphaeroides* useful in genetic analysis. *Arch Microbiol*., 138: 161-165.

Soulimane, T. Buse, G. Bourenkov, H.D. Bartunik, R. Huber, R. Than, M.E. (2000). Structure and mechanism of the aberrant ba_3-cytochrome *c* oxidase from *Thermus thermophilus. EMBO J*, 19: 1766-1776.

Soupène, E., Foussard M., Boistard P., Truchet G., Batut J. (1995). Oxygen as a key developmental regulator of *Rhizobium meliloti* N2-fixation gene expression within the alfalfa root nodule. *Proc. Natl. Acad. Sc.,* USA, 923: 759-3763.

Stackebrandt, E., Murray, R.G.E., and Trüper, H.G. (1988). Proteobacteria classis nov., anme for the phylogenetic taxon that includes the "Purple bacteria and their relatives." Int. J. Syst. Bacteriol.

Stover, C. K. Pham, X. Q., Erwin, A. L., Mizoguchi, s. D., Warrener, P., Hickey, M.J., Brimkman, F.S., Hufnagle, W.O., Kowalik, D.J., Lagrou, M., Garber, R.L., Goltry, L., Tolentino, E., Westbrock-Wadman, S., Yuan, Y., Brody, L.L., Coulter, S.N., Folger, K.R., Kas, A.,Lrbig, K., Lim, R., Smith, K., Spencer, D., Wong, G.K., Wu, Z. and Paulsen, I.T. (2000). Complete genome sequence of *Pseudomonas aeruginosa* PAO1, an opportunistic pathogen. *Nature*, 406: 959-964.

Thomas, J.W., Lemieux, L.j., Alben, J.O., and Gennis, R.B. (1993). Site-directed mutagenesis of highly conserved residues in helix VIII of subunit I of the cytochrome bo ubiquinol oxidase from *Escherichia coli*: An amphipathic transmembrane helix that may be important in conveying protons to the binuclear center. *Biochemistry*, 32: 1173-11180.

Thöny-Meyer, L., Beck, C., Preisig, O., Hennecke, H. (1994). The *ccoNOQP* gene cluster codes for a *cb*-type cytochrome oxidase that functions in aerobic respiration of *Rhodobacter capsulatus*, *Mol. Microbiol.*, 14: 705-716.

Thöny-Meyer, L. (1997). Biogenesis of respiratory cytochromes in bacteria. *Microbiol. Mol. Biol. Rev.*, 61: 337-376.

Tomb, J.F., White, O., Kerlavage, A.R., Clayton, R.A., Sutton, G.G., Fleischmann, R.D., Ketchum, K.A., Klenk, H.P., Gill, S., Dougherty, B.A., Nelson, K., Quackenbush, J., Zhou, L., Kirkness, E.F., Peterson, S., Loftus, B., Richardson, D., Dodson, R., Khalak, H.G., Glodek, A., McKenney, K., Fitzegerald, L.M., Lee, N., Adams, M.D., Venter, J.C. (1997). The complete genome sequence of the gastric pathogen Helicobacter pylori, *Nature,* 388: 539-547.

Tsukihara, T., Aoyama, H., Yamashita, E., Tomizaki, T., Yamaguchi, H., Shinzawa-Itoh, K., Nakashima, R., Yaono, R. and Yoshikawa, S. (1996). The whole

structure of the 13-subunit oxidized cytochrome c oxidase at 2.8 A. *Science*, 272: 1136-1144.

Urbani, A., Gemeinhardt, S., Warne, A. and Saraste, M. (2001). Properties of the detergent solubilised cytochrome *c* oxidase (cytochrome cbb_3) purified from *Pseudomonas stutzeri*. *FEBS Lett*., 508: 29-35.

van der Oost, J., de Boer, A.P.N., de Gier, J.-W.L., Zumft, W.G., Stouthamer, A.H., van Spanning, R.J.M. (1994). The heme-copper oxidase family consists of three distinct types of terminal oxidases and is related to nitric oxide reductase, *FEMS Microbiol Lett.,* 121: 1-9.

van Spanning, R.J.M., de Boer, A.P.N.,W. Reijnders, N.M., Westerhoff, H.V., Stouthammer, A.H., and van der Oost, J. (1997). FnrP and NNR of *Paracoccus denitrificans* are both members of the FNR family of transcriptional activators but have distinct roles in respiratory adaptation in response to oxygen limitation. *Mol. Microbiol.,* 23: 893-907.

Varotsis, C.A., Babcock, G.T., Garcia-Horsman, J.A., Gennis, R.B. (1995). Resonance Raman spectroscopy of the heme groups of cytochrome cbb_3 in *Rhodobacter sphaeroides*, *J. Phys. Chem.,* 99:16817-16820.

Wang, J., Gray, K.A., Daldal, F., and Rousseau, D.L. (1995). The cbb_3-type cytochrome *c* oxidase from *Rhodobacter capsulatus* contains a unique active site. J. *Am. Chem. Soc.,* 117: 9363-9364.

Weiner, M.P., Gackstetter T., Costa, G.L., Bauer, J.C., Kretz, K.A. From *Molecular Biology: Current Innovations and Future Trends.* Eds. Griffin, A.M. and Griffin, H.G. ISBN 1-898486-01-8 (1995). Horizon Scientific Press, PO Box 1, Wymondham, Norfolk, U.K.

Wikstrom, M. (1989). Identification of the electron transfers in cytochrome oxidase that are coupled to proton-pumping. *Nature*, 338: 776-778.

Wikstrom, M. (2000). Mechanism of proton translocation by cytochrome *c* oxidase: a new four-stroke histidine cycle. *Biochim. Biophys. Acta,* 1458: 188-198.

Williams, J., Steiner, L., and Feher, G. (1986). Primary structure of the reaction center from *Rhodopseudomonas sphaeroides. Proteins,* 11: 312-325.

Yen, H.C., and Marrs, B.L. (1977). Growth of *Rhodopseudomonas capsulata* under anaerobic dark conditions with dimethyl sulphoxide. *Arch. Biochem. Biophys*, 181: 411-418.

Yhosikawa, S., Shinzawa-Itoh, K., Nakashima, R., Yaono, R., Yamashita, E., Inoue, N., Yao, M., Fei, M.J., Libeu, C.P., Mizushima, T., Yamaaguchi, H., Tomizaki, T., and Tshukihara, T. (1998). *Science,* 280: 1723-1729.

Yhosikawa, S., Shinzawa-Itoh, K., and Tshukihara, T. (2000). X-ray structure and the reaction mechanism of bovine heart cytochrome *c* oxidase**.** *J. Inorg.Biochem.* 82: 1-7.

Youvan, D., Bylina, E., Alberti, M., Begusch, H., and Hearst, J. (1984). Nucleotide and deduced polypeptide sequences of the photosynthetic reaction-center, B870 antenna, and flanking polypeptides from *Rhodopseudomonas capsulata*. *Cell,* 37: 949-957.

Youvan, D.C. and Byline Edward J. (1989). Photosynthesis in *Rhodospirillace*. Chapter: 5.

Yu, P.L. Cullum, J. Drews, G. (1981). Conjugational transfer systems of *Rhodopseudomonas capsulate* mediated by R plasmids. *Arch Microbiol*, 128: 390-393.

Zannoni, D., Melandr, B.A., and Baccarini-Melandri, A. (1976). Composition and function of the branched oxidase system in wild-type and respiratory mutants of *Rhodopseudomonas capsulata*. *Biochim. Biophys. Acta,* 423: 413-430.

Zannoni, D. (1995). Aerobic and anaerobic electron transport chains in anoxygenic phototrophic bacteria, p. 949-971, in R. E. Blankenship, M. T. Madigan, and C. E. Bauer (ed.), Anoxygenic photosynthetic bacteria. Kluwer Academic Publishers, Dordrecht, the Netherlands.

Zeilstra-Ryalls, J.H., and Kaplan, S. (1995). Aerobic and anaerobic regulation in *Rhodobacter sphaeroides* 2.4.1: the role of the *fnrL* gene. *J. Bacteriol.,* 177: 6422-6431.

Zeilstra-Ryalls, J.H., and Kaplan, S. (1996). Control of *hemA* expression in *Rhodobacter sphaeroides* 2.4.1: regulation through alterations in the cellular redox state. *J. Bacteriol.,* 178: 985-993.

Zufferey, R., Preisig, O., Hennecke, H., and Thony-Meyer, L. (1996). Assembly and function of the cytochrome cbb_3 oxidase subunits in *Bradyrhizobium japonicum*, *J. Biol. Chem.*, 271: 9114-9119.

Zufferey, R. Arslan, E. Toney-Mayer, L. Hennecke, H. (1998). How Replacements of the 12 Conserved Histidines of Subunit I Affect Assembly, Cofactor Binding, and Enzymatic Activity of the *Bradyrhizobium japonicum* cbb_3-type Oxidase. J. *Biol. Chem*., 273: 6452-6459.

APENDIX A

BACTERIAL GROWTH MEDIA

Liquid LB Medium (Luria Broth)

	For 1 lt
Bacto tryptone	10 g
Yeast extracts	5 g
NaCl	10 g

These are dissolved in 800 ml dH_2O. pH is adjusted to 7.5 with NaOH. The volume is completed to 1 lt with dH_2O and autoclaved.

LB Plate

For 1 lt liquid LB medium, 15 g agar (1.5 %) (Difco-Bacto agar) is added and autoclaved.

Liquid MPYE-Medium (Enriched Medium)

	For 1 lt
Bacto peptone (0.3%)	3 g
Yeast extract (0.3%)	3 g
$CaCl_2$ (1 mM)	1 ml
$MgCl_2$ (1.6 mM)	1 ml

These are dissolved in 800 ml dH_2O and volume completed to 1 lt. pH is adjusted with NaOH to 7 and autoclaved.

MPYE Plate

For 1 lt liquid MPYE medium, 15 g agar (1.5%, Difco-Bacto agar) is added.

Sistrom's Minimal Medium (Med A)

	For 1 lt
NaCl [10%]	5 ml
$(NH_4)_2SO_4$ [10%]	5 ml
Sodium (or Potassium) Succinate [10%]	20 ml
L-Aspartic acid [2%, pH: 7]	2 ml
L-Glutamic acid [5%, pH: 7]	2 ml
Potassium phosphate [1M, pH: 6.8]	20 ml
Macroelement solution	20 ml

These are complemented up to 1 lt and autoclaved. Sterile 10 ml 100X vitamin and appropriate antibiotics were added and mixed when the temperature is 50-55 ºC.

Med A Plate	For 1 lt
L-Aspartic acid [2%, pH: 7]	2 ml
NaCl [10%]	5 ml
L-Glutamic acid [5%, pH: 7]	2 ml
Sodium (or Potassium) Succinate [10%]	20 ml
$(NH_4)_2SO_4$ [10%]	5 ml

These are complemented with 920 ml dH_2O. 15 g agar [1.5%] is added, and autoclaved. Sterile 20 ml macroelement solution, 20 ml potassium phosphate [1M, pH: 6.8], and 10 ml 100X vitamin are added and mixed when the temperature of the medium is 50-55 ºC.

Stock Solution of Med A

A) Microelements Solution

	For 1 lt
$ZnSO_4.7H_2O$	10.00 g
EDTA	2.50 g
$FeSO_4.7H_2O$	5.00 g
H_3BO_3	1.14 g
$MnSO_4.H_2O$	1.54 g
$CuSO_45H_2O$	3.92 g
$Co(NO_3)_2.6H_2O$	2.50 g

These were dissolved in 1lt dH_2O, autoclaved and stored.

B) Macro elements Solution (Solution C)

	For 1 lt
Nitrilotriacetic acid	10.0 g
$MgSO_4.7H_2O$	29.5 g
$CaCl_2.2H_2O$	3.3 g
$FeSO_4.7H_2O$	9.9 g
Microelements solution	50.0 ml

These are dissolved in 800 ml dH_2O. pH is adjusted with KOH to 6.8-7. The volume is completed to 1 lt with dH_2O and autoclaved.

C) Vitamins (100X)

	For 1 lt
Nicotinic acid	100.0 mg
Thiamin HCl	25.0 mg
Biotin (40 µg/ml stock)	12.5 ml

These are dissolved in 1 lt H_2O, sterilized with 0.22 µm filter, and stored at 4 ºC.

*Growth mediums, solutions and buffers are sterilized by autoclaving at 121ºC for 25 min.

APPENDIX B

SOLUTIONS AND ANTIBIOTICS

10% Ammonium persulfate (APS)

0.1 g Ammonium persulfate (APS) was dissolved in 1ml of dH_2O

EDTA (Ethylenediamine-tetraacetic acid) (0.5 M)

For 250 ml EDTA solution, 46.5 g EDTA is dissolved in 150 ml dH_2O, and pH is adjusted with NaOH to 8,00. The volume is completed to 250 ml with H_2O and autoclaved.

10% SDS Solution

0.1 g Sodium Dodecyl Sulphate (SDS) was dissolved in 1ml of ddH_2O

0.25 M Na-Acetate (pH: 5)

17.01 g Na-Acetate (MW: 136.08) was dissolved in 400 ml water and pH was adjusted to 5.0 using Glacial Acetic Acid.

49.5% Acrylamide-Bis Acrylamide Mixture (49.5%T, 3%)

Acrylamide 48.0 g

Bis-acrylamide 1.5 g

They were dissolved in 60 ml ddH_2O and filtered using Whatman filter paper than volume was tap to 100 ml. It was stored in RT in bottle wrapped with aluminum foil.

MOPS/KCl Solution (50 mM MOPS/1 mM KCl)

11.56 g MOPS was dissolved in 700 ml H_2O. pH was adjusted to 8,0 with H_2O. Than 74 mg KCl was added and final volume was tap to 1 lt. After it was autoclaved it was kept at 4 ºC.

Solutions Used for Lowry Method to Determine Amount of the Protein

Solution A: 2 g Na_2CO_3 is dissolved in 0.1 N NaOH than volume completed to 100 ml with ddH_2O.

Solution B: 1 g $CuSO_4$. H_2O is dissolved in 1000 ml ddH_2O.

Solution C: 2 g Sodium potassium tartarate are dissolved in ddH_2O

Solution D: Solution B and C are mixed (1/1 ratio) (It is daily prepared).

Solution E: 1 ml solution D was added in 50 ml solution A (It is prepared just before used).

Ampicillin

For 10 ml 100 mg/ml stock solution; 1 g Ampicillin is dissolved in 10 ml dH_2O, sterilized with 0.22 μm filter, and stored at -20ºC.

Kanamycin

For 10 ml 50 mg/ml stock solution; 500 mg kanamycin is dissolved in 10 ml dH_2O, sterilized with 0.22 μm filter, and stored at -20ºC.

Tetracycline

For 100 ml 1.25 mg/ml stock solution; 125 mg tetracycline is dissolved in 100 ml 50 % (v/v) ethanol/dH_2O, sterilized with 0.22 μm filter, and stored in dark at -20 ºC.

APPENDIX C

BUFFERS

PAGE Buffer	For 100 ml
Tris	36.33 g
SDS	0.30 g

They were dissolved in 100 ml dH_2O and pH adjusted to 8.45 with HCl.

10X Anode Buffer

24.22 g Tris was dissolved in 100 ml ddH_2O and pH was adjusted to 8.9 with HCl.

10X Cathode Buffer	For 200 ml
Tris	24.20 g
Tricine	35.84 g
SDS	0.60 g

They were dissolved in 200 ml ddH_2O and pH was not adjusted which was around 8.25.

TAE Buffer (50X)

	For 1 lt
Tris Base	242 g
Acetic acid (Glacial)	57.1 ml
EDTA.2H_2O (0.5 M, pH: 8)	100 ml

The volume is completed to 1 ml with H_2O, and sterilized by autoclaving.

TE

	For 100 ml
Tris Base (1M, pH: 7.50)	1 ml
EDTA.2H_2O (0.5 M, pH: 8)	200 µl

The volume was completed to 100 ml with ddH_2O, and sterilized by autoclaving.

DNA Loading Dye

	For 1 lt
Bromphenol blue	0.025 g
Glycerol (100%)	5 ml
EDTA.2H_2O (0.5 M, pH: 8)	200 µl
TBE (10X)	5 ml

Loading Dye for SDS-PAGE

ddH2O	340 µl
10 % SDS	400 µl (4%)
100% Glycerol	120 µl (12%)
0.5 M Tris/HCl (pH; 6.8)	100 µl (50%)
0.5 % Bromophenol Blue	40 µl (0.01%)
Total volume:	1 ml

APPENDIX D

CHEMICALS

Acetic acid (Merck, 100056)

Acrylamide (J.T..Baker 79-06-1)

Agar (Difco, 0140-01)

Agarose (Research organics 1170A) cat number 9012-36-6

Ammonium persulfate [APS] (Sigma, A-9164)

Ampicillin (Sigma, A-0166)

L-Aspartic acid (Sigma, A,-9256)

Bacto peptone (Difco, 0118-17-0)

Bacto tryptone (Difco, 0123-17-3)

BSA [Bovine Serum Albumin] (Sigma, A-9647)

DMPD [N, N-Dimethyl –p-Phenylene –Diamine] (Sigma, D-5004)

N, N'-Metylene-bis-Acrylamide (Sigma, M-7256)

EtBr [Ethidium Bromide] (Sigma, E-8751)

Glycerol, cell culture tested (Sigma, G-2025)

Glycerol, Electrophoresis grade (Sigma G-8773)

L-Glutamic acid (Sigma, G-1251)

Hydrogen peroxide [(H_2O_2), 30%] (Aldrich, Chemical Co., 21, 676.3)

Kanamycin (Sigma, K-4378)

2-Mercaptoetanol (Electrophoresis Regent, Sigma, M-7154)

Methanol (Carlo Erba reagent, 309203)

MOPS [3- (N-Morpholino) propanesulfonic acid] (Sigma, M-9381)

α-Naphthol (Sigma, N-1000)

Phenol (Sigma, P-4557)

Phenol (Merck, 100995)

SDS (Lauryl sulfate) (Sigma, L-5750)

Sigmacote® (Sigma, SL-2)

Sodium acetate (Merck, 6268.1000)

Succinic acid [Disodium Salt Hexahydrate] (Sigma, S-9637)

TEMED (Sigma, T-7024)

Tetracycline Hydrochloride, Crystalline (Sigma, T-33839

Tris Base (Trizma base, J.T.Baker 77-86-1)

Tricine (Electrophoresis Grade) Sigma T-7911

TMBZ (Aldrich Chemical Co., 86, 033-6)

Yeast Extract (Difco, 0127-17-9).

APPENDIX E

ENZYMES

RESTRICTION ENDONUCLEASES

*Bsa*AI (New England Biolabs): cat. # R0531S

*Sac*I (MBI): cat. # ER1131

*Bsu*151 *(Cla*I) (MBI): cat. # ER0141

*Dpn*I (MBI): cat. # ER1701

*Hind*III (MBI): cat. # ER0501

*Sal*I (MBI): cat. # ER0641

X*ho*I (MBI): cat. # ER0691

POLYMERASES

Pfu DNA polymerase (MBI): cat. # EP0501

LIGASES

T4 DNA Ligase (MBI): cat. # EL0331

PHOSPHATASES

Calf Intestine Alkaline Phosphatase (CIAP) (MBI): cat. # ER EF0341

dNTP Set

dNTP (MBI): cat. # R0181

APPENDIX F

EQUIPMENTS USED IN THIS STUDY

PCR, Eppendorf, Mastercycler gradient

34 ºC and 37 ºC Etuve (Nuve EN 500)

34 ºC and 37 ºC shaker-incubator (Nuve SL 350)

4 ºC- 99 ºC Incubator, Memmert

Anaerobic jar (Oxoid)

Gas Generating Kit (BR038B)

Anaerobic catalyst (BR55)

Electrophoresis Systems

Miniprotein II Biorad

Sigma-Aldrich Techware Protein Electrophoresis System

DNA Electrophoresis System

Power supplies

Biorad Model 200/2.0 Power supply

Biolab, PS 9009 TX, Apelex, Power supply

Heat Blocks

Dry Bloc (Techne DB 2A, Dry-Block)

Shaker-heater (IKA RCT basic)

Autoclave (V/O Medoxport rk-100-2)

pH meter (Metrohm 744)

Micropipettes, Pipetman®, Gilson

0-20, 0-200 and 100-1000 µl pipettes

Centrifuges

Desktop centrifuges (Biofuge fresco Heraeus instruments)

Micro 20 centrifuge, Hettich

Megafuge 2.0R Heraeus sepatech)

Sorval RC5C-Santrifuge

Sorval RC 28S

Sorvall Ultracentrifuges OTD75B

Coolers

+4 ºC Refrigerators

+4 ºC Room

-20 ºC deepfreeze, Bosh

-85 ºC deepfreeze, Nuaire -85 ultraslow freezer

French® Pressure Cell Press, SIM-AMINCO

Spectrophotometer (Biorad, SmartSpect™ 3000)

Scales

UV Transalluminator

Vortex (IKA MSI Minishaker)

APPENDIX G

COMMERCIAL PLASMID VECTORS USED IN THIS STUDY

Map of the pBluescript SK+ Vector (Stratagene)

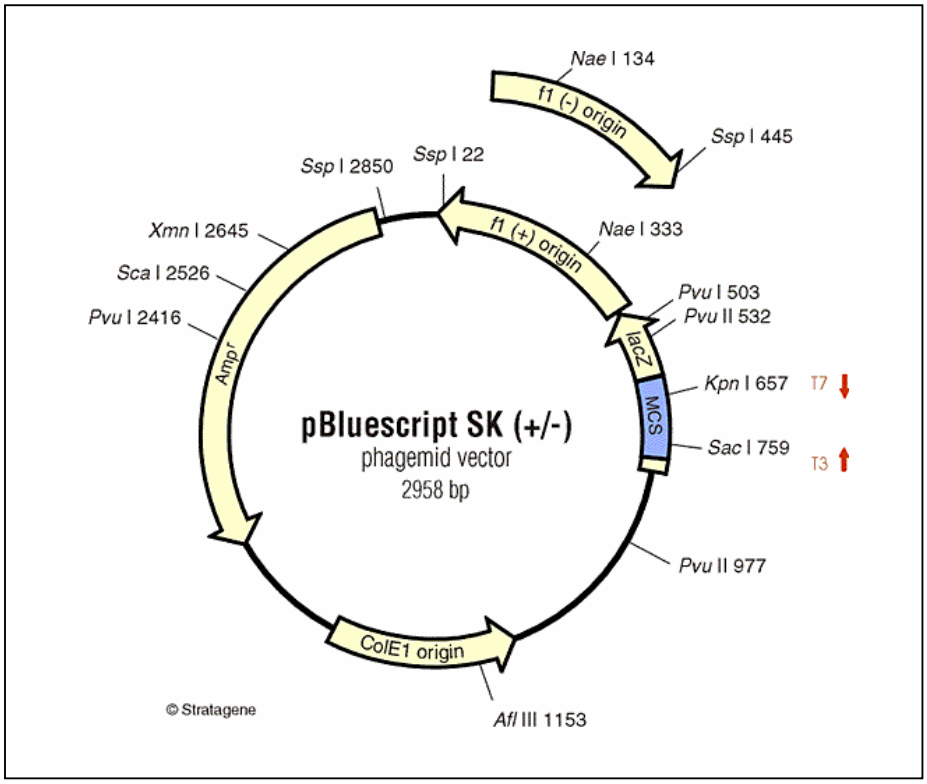

Map of the pACYC177 vector (New England Biolabs)

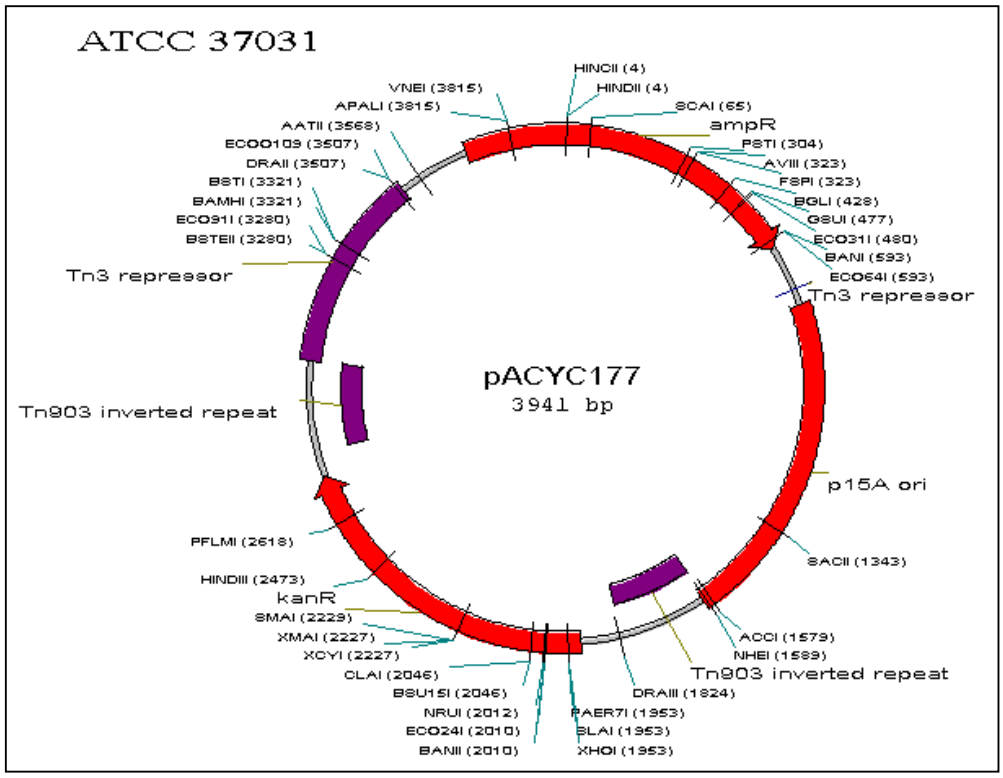

CURRICULUM VITAE

Name **:** Mehmet ÖZTÜRK
Permanent Address **:** Oruç Reis mahallesi 4. sokak, No: 2
46040, K. Maraş.
Degree and date to be conferred: Ph.D., 2005
Place, date of birth **:** K. Maraş, 04.03.1967

Collegiate institutions attended	**Dates**	**Degree**	**Date of degree**
Hacettepe University, Biology	1985-1989	BS	12.06.1989
Murray State University, Biology	1996-1998	MSc	08.25.1998
Abant Izzet Baysal University, Biology	2001-2005	Ph.D.	16.12.2005

Publications:

1. Zimmerer, E. J., Carneal, J., Robertson, J. B., Öztürk, M., Cardiff, S., & Luo, M. (2000). Genome Organization and Phylogenetic Distribution of a Novel Family of Ancient Murine Endogenous Proviruses with Evidence for Transposition-Modified Proliferation. *Biochemical Genetics*, 39, 246-258.

2. Öztürk, M., Aygün, S., Gürel, E., Mandacı, S. (2003). Characterization of *R. capsulatus* Mutants Mutated with EMS. XII. Biotechnology Congress, 25-29 August, Çanakkale, Turkey.

3. Moleküler Biyoloji ve Yönlendirilmiş Mutagenez: Temel Bilgiler ve Deneysel Uygulamalar, S. Mandacı, S. Aygün ve (2003). Chp. 8, DNA Dizi Analizi. M. Öztürk ISBN 975-403-293-9 TUBITAK.

4. Öztürk, M., Gürel, E., Mandacı, S. (2005). Effects of the Replacement of Some of the Highly Conserved Amino Acids of Cytochrome cbb_3 Oxidase. Turk J of Biochem, 30 (1):1-172. 19th National Biochemistry Congress, 22-25 April 2005, Kemer-Antalya, Turkey.

5. Öztürk, M., Gürel, E., Mandacı, S. (2005). Sitokrom cbb_3 Oksidaz Enziminin I. Alt Ünitesinde Korunmuş Amino Asitlerin Mutasyonu ve Enzimin İşlevine Etkileri, 14. Biyoteknoloji kongresi.

Research Activities:

1) Characterization of a New Eβ Endogenous Retrovirus Family in *Mus musculus caroli*: Sequence Analysis.
2) Molecular structure and functions of cbb_3-type oxidase in *R. capsulatus.*

Scolarship/Fellowship:

1) Turkish Ministry of Education full scholarship for MSc, 1996-1998.
2) European Molecular Biology Organization (EMBO) short-term fellowship, Julay-October, 2005.

Positions held:

1989-1994 : Teaching Biology and Science at High Schools in Afyon and K. Maraş.

1998-Present: Teaching Assistant at Abant Izzet Baysal University, Biology Department, 1998-present.